UNIVERSITY OF MILAN

GRADUATE SCHOOL IN PHARMACOLOGICAL SCIENCES

Department of Pharmacological and Biomolecular Sciences

PhD course in Pharmacological Sciences (XXVI cycle)

Sector of study: BIO/14

Eukaryotic Elongation Factor 2 Kinase Downregulates Vesicle Release and GABAergic Transmission by Translation Control of a Subset of Proteins

Tutor:
Dr. Carlo Sala

Doctoral Thesis of:
Christopher Heise

Registration number
("Matricola"):
R09362

Coordinator:
Prof. Alberto Panerai

Academic year 2012/2013

Table of Contents

1 Introduction

1.1 eEF2K

Eukaryotic elongation factor 2 kinase (eEF2K) is a ubiquitous, well conserved protein involved in the control of protein translation, whose catalytic activity is Ca^{2+}-dependent and is therefore also known as Ca^{2+}/Calmodulin-dependent kinase III (CaMKIII). Upon activation, eEF2K phosphorylates and inhibits eukaryotic elongation factor 2 (eEF2), its only known substrate. This leads to a halt of protein synthesis at the level of elongation (Ryazanov et al., 1988; Diggle et al., 1999; Pavur et al., 2000; Browne and Proud, 2002; Ryazanov, 2002; Pigott et al., 2012).

1.1.1 Structure of eEF2K

In terms of sequence similarity, eEF2K is not related to the superfamilies of conventional protein kinases but instead belongs to a heterogenous small group of kinases called α-kinases, which have a high degree of similarity in their catalytic region. However, the three-dimensional structure of α-kinases and the sequence of their functionally relevant motifs may be very similar to that of conventional protein kinases, indicating that they may serve similar functions in the cell and probably have a mutual evolutionary origin (Pavur et al., 2000; Drennan and Ryazanov, 2004).

eEF2K is a middle sized protein (length: 725 aa for human eEF2K) which is well-conserved between mammals (Ryazanov et al., 1997). It consists of an N-terminal catalytic domain which includes the adenosine triphosphate (ATP)-binding site, a C-terminal domain that is necessary for eEF2 binding, and an interposed unorganized linker region. Even further N-terminally there is the Calmodulin (CaM) binding region (Ryazanov et al., 1997; Diggle et al., 1999; Pavur et al., 2000). Several upstream kinases such as AMP-activated protein kinase (AMPK), P70S6 kinase (p70S6K), and p90 ribosomal S6 kinase (p90RSK1) phosphorylate and regulate eEF2K by acting on the linker region, (see paragraph 1.1.2) (Pigott et al., 2012).

eEF2K point-mutated at Ser366 renders eEF2K constituitively active. This mutated version of eEF2K is described in literature and is known as “eEF2Kca” (eEF2K constituitively active) (Verpelli et al., 2010). Instead, there are also several described versions of eEF2K with point mutations which render the kinase catalytically inactive, one example of which is “K170M” (point mutation at position 170; substitution of Lys with Met) (Pigott et al., 2012). Both of these constructs were extensively used in the course of this study (see results section 3.1 and onwards).

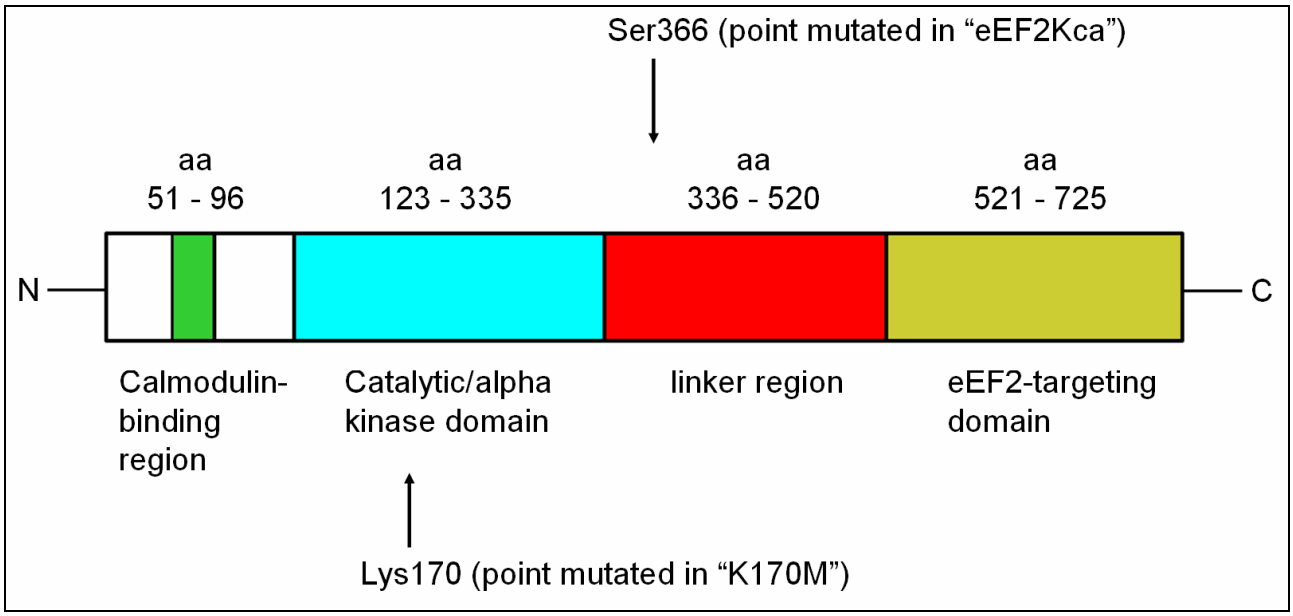

Figure 1: Basic structure of human eEF2K and point mutations of the eEF2Kca and K170M constructs. eEF2K is a well-conserved Ca^{2+}/CaM-dependent kinase (also known as Ca^{2+}/CaM-dependent kinase III) (Ryazanov et al., 1997) and is a middle sized protein (length: 725 aa for human eEF2K). It consists of an N-terminal catalytic domain (aa 123-335; in turquoise) where the ATP-binding site resides and an even further N-terminally located CaM binding region (aa 51-96; in green). A mutation in the catalytic domain at Lys170 renders eEF2K catalytically inactive and leads to a version of eEF2K called “K170M” (indicated by arrow). C-terminally, there is a domain that is necessary for eEF2 binding (eEF2-targeting domain; aa 521-725; in yellow). More precisely, only the very C-terminal tip of eEF2K (aa 706-725) is necessary for eEF2 binding (Diggle et al., 1999). Lastly, there is an interposed unorganized linker region (aa 336-520; in red) which is the target of several upstream regulating kinases such as AMPK, p70S6K, and p90RSK1 (see paragraph 1.1.2) (Pigott et al., 2012). A mutation in the linker region at Ser366 renders eEF2K constituitively active and leads to a version of eEF2K called “eEF2Kca” (indicated by arrow).

1.1.2 Regulation of eEF2K

Since eEF2K downregulates translation at the elongation level, it is well positioned as an element to be regulated by various basic cellular events since protein synthesis is an ATP-dependent process which must therefore be tightly controlled by any organism. Even though most researchers agree that protein translation is mainly regulated at the initiation level (Browne and Proud, 2002; Sonenberg and Hinnebusch, 2009; Gildish et al., 2012), it has been shown eEF2K is strongly influenced by upstream cellular events and associated kinases which execute the control of eEF2K activity (Browne and Proud, 2002) (Fig. 2).

eEF2K activity is increased by both low pH and low energy (i.e. a low availability of aa) in the mammalian cell (low energy in cells leads to activation of AMPK, which in turn activates eEF2K by phosphorylating it on Ser398). This has been explained by the fact that under tissue acidosis (which may take place under conditions like hypoxia and ischemia) or under conditions where energy is sparse, protein translation must be inhibited to conserve energy in order to react properly to these forms of cell stress (Dorovkov et al., 2002; Browne et al., 2004). Also, eEF2K activity is increased by elevated levels of the second messenger Ca^{2+} and the Ca^{2+}-dependent protein CaM (Nairn et al., 1985; Mitsui et al., 1993; Dorovkov et al., 2002) which represents a rather unspecific

way of changing eEF2K activity since Ca^{2+} is a very broadly employed signalling element (Clapham, 2007; Chuderland and Seger, 2008; Fortin et al., 2013). However, there are also examples of changes in intracellular Ca^{2+} in response to specific signalling pathways which subsequently change eEF2K activity. For example, in the context of neuronal cells, Ca^{2+} influx after N-methyl-D-aspartate receptor (NMDAR) activation appears to be strongly related to eEF2K activation and subsequent neuronal events which depend on the regulation of protein translation (Scheetz et al., 1997, 2000; Nosyreva et al., 2013) (see paragraph 1.3). Interestingly, Ca^{2+}/CaM is also necessary for autophosphorylation of eEF2K, which tends to activate eEF2K further (e.g. autophosphorylation on Thr348) and appears to render eEF2K activity independent of Ca^{2+}/CaM (Pyr Dit Ruys et al., 2012; Tavares et al., 2012). Lastly, it has also been shown that eEF2K activity can be increased by the activation of metabotropic glutamate receptors (mGluRs), possibly since mGluR activation liberates eEF2K from its inhibiting interaction with the receptor itself (Park et al., 2008) (see paragraph 1.3).

On the contrary, eEF2 activity is reduced by mammalian target of rapamycin (mTOR) signalling which triggers p70S6K-dependent phosphorylation of eEF2K on Ser366, a major phosphorylation site that is associated with inhibition of eEF2K (Wang et al., 2001). Since mTor activity is increased by insulin and the availability of aa or energy in the cell (Browne and Proud, 2002), it may play the biological counterpart to eEF2K activation by AMPK which serves to activate protein translation when the circumstances allow for cell growth and other ATP-dependent processes in the cell that depend on protein synthesis. Another well-described signalling cascade that inactivates eEF2K is mitogen-activated protein/extracellular signal-regulated kinase (MEK/ERK) signalling which leads to eEF2K phosphorylation on Ser366 by employing $p90^{RSK1}$ as a mediator (Wang et al., 2001; Browne and Proud, 2002).

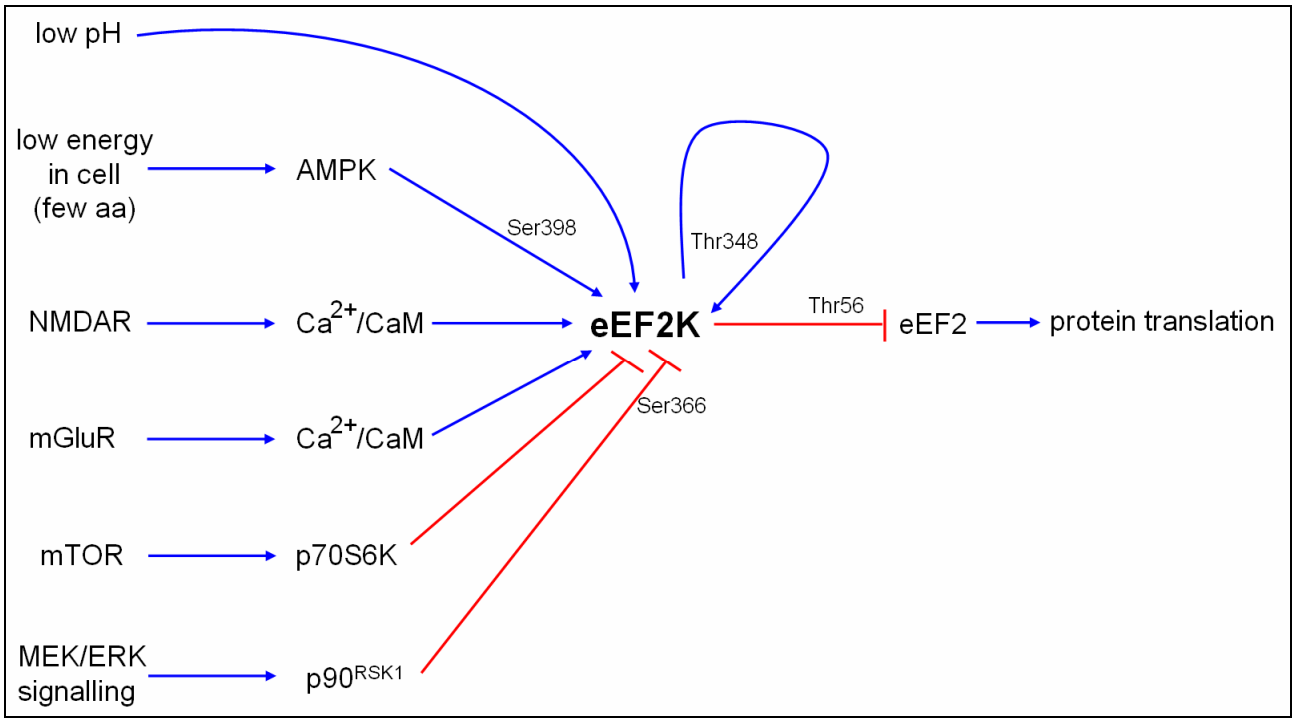

Figure 2: Regulation of eEF2K activity by upstream events have an effect on protein translation. Activation is indicated by blue arrows, inhibition is indicated by red T-bars. Since eEF2K activity leads to a downregulation of peptide chain elongation, it is a good target of signalling events enabling proper cellular responses to stimuli which demand changes in protein translation. Notably, changes in cellular pH and availability of aa have a strong influence on eEF2K activity. E.g. when there are few aa, AMPK is activated which subsequently activates eEF2K, thereby reducing protein translation which is a sensible response to few aa since the available energy in the cell is probably sparse and protein translation must therefore be reduced to a minimum. Conversely, an abundance of aa activates mTOR signalling which, in turn, inactivates eEF2K. Moreover, eEF2K activity is dynamically altered by specific signalling events, such as NMDAR-mediated influx of Ca^{2+} into neurons or MEK/ERK signalling. Interestingly, eEF2K activity is also increased by Ca^{2+}/CaM-dependent autophosphorylation which, in turn, renders eEF2K activity independent of Ca^{2+}/CaM.

1.1.3 eEF2K/eEF2 pathway

As mentioned, eEF2K downregulates protein synthesis, since its activity leads to a phosphorylation of eEF2 on Thr56 (henceforth referred to as peEF2 or phosphorylated eEF2). More specifically, peEF2 is not able to bind to the ribosomes and can therefore not catalyze the peptidyl-Transfer RNA (tRNA) translocation from the acceptor region to the peptidyl region, effectively rendering eEF2 catalytically inactive and halting peptide chain elongation/protein translation at the elongation level (Diggle et al., 1999; Pigott et al., 2012). Importantly, there are also phosphatases acting on peEF2, reconverting it into eEF2, thereby restoring peptide chain elongation. One of these phosphatases is protein phosphatase 2A (Browne and Proud, 2002; Hong-Brown et al., 2007; Kaul et al., 2011). The regulation of eEF2 activity and peptide chain elongation is therefore controlled by an array of phosphatases and a single kinase (namely eEF2K) since eEF2 is the only known substrate of eEF2K and increases in eEF2 phosphorylation have only been convincingly linked to eEF2K (Browne and Proud, 2002; Dorovkov et al., 2002; Ryazanov, 2002; Nosyreva et al., 2013).

It is important to emphasize that the eEF2K/eEF2 pathway exists in every mammalian cell and is highly conserved (Kaul et al., 2011). It has been linked to cellular processes as diverse as cancer,

cytokine production, milk lactation, and synaptic processes in neurons (Chen et al., 2011; Kaul et al., 2011; Gonzalez-Teran et al., 2012; Leprivier et al., 2013; Taha et al., 2013). In this context it seems rather surprising that eEF2K-knockout (eEF2K-KO) mice do not show any obvious phenotypes since they are fertile, viabile, and do not show any behavioural abnormalities under physiological conditions (Ryazanov, 2002; Nosyreva et al., 2013).

1.2 Synapses

Synapses are highly specialized cell junctions where transduction of electrical signals takes place between neural cells- typically between two neurons, though the participitation of glial cells in synaptic processes has become increasingly obvious over the past years (Perea et al., 2009). The exchange of these electrical signals (of this "information") can be viewed as a "communication" between neural cells that *in vivo* serves information processing which is crucial for an organism to respond adequately to changes in the surrounding and within the organism itself (Haydon, 2000; Breedlove et al., 2007). Based on the nature of signal transduction and the biochemical buildup, one can differentiate between two types of synapses- namely chemical and electrical ones. Chemical synapses are far more abundant than electrical ones and represent a much more complex subcellular compartment where the signal transduction can be heavily modified. Importantly, chemical synapses convey the electrical signals indirectly via biochemical agents (known as neurotransmitters) whereas electrical synapses convey the electrical signal directly via channels (known as gap junctions). As a result, signal transduction occurs faster at electrical synapses but is much less modifiable and therefore is not so versatilely employable for information processing in neural networks. For the present study, the relevant synapse is the chemical one so all of the following information refers to this type of synapse.

1.2.1 Signal transduction at the chemical synapse: pre- and postsynapse

In the classical view, the chemical synapse consists of a pre- and postsynaptic compartment, devided by an extracellular space called the synaptic cleft. Each compartment pertains to an individual neuron, one which (from an information processing persepective) is upstream of the synapse (called presynaptic neuron, contributes the presynaptic compartment) and one which is downstream (called postsynaptic neuron, contributes the postsynaptic compartment).

When an action potential is generated at the axon hillock (compartment of neuronal soma with high concentration of voltage gated ion channels) of the presynaptic neuron, it is actively propogated

along the axon by voltage gated Na^+ and K^+ channels. It then induces the influx of Ca^{2+} via voltage-dependent Ca^{2+} channels at the presynaptic compartment of the synapse. This, subsequently, triggers Ca^{2+}-dependent events that eventually lead to the fusion of synaptic vesicles (SVs), which contain the neurotransmitters, with the cell membrane. After fusion of the SVs with the cell membrane, the neurotransmitters diffuse across the synaptic cleft and bind to receptors present at the cell surface of the postsynaptic compartment. For ionotropic receptors, this binding causes the receptor to allow for the entry of ions into the postsynaptic neuron which changes the probability for the generation of an axon potential at the axon hillock of this cell. Instead, activation of metabotropic receptors by neurotransmitters leads to a variety of cellular events one which is the induction of indirect entry of ions into the postsynaptic cell via the activation of second messengers (Kandel et al., 2000; Breedlove et al., 2007).

The presynaptic compartment is highly organized to allow for the fusion of SVs and the release of neurotransmitters in response to Ca^{2+} influx and presents a complex protein machinery to do so (Frank et al., 2010). SVs consist of a lipid membrane with interspersed proteins that can enable Ca^{2+}-dependent responses for the release of neurotransmitters into the synaptic cleft. Among other things, SVs must be trafficked to the presynapse, loaded with neurotransmitters, and docked at the site of release before fusion with the cell membrane. After the fusion with the cell membrane, SVs must then be endocytosed to allow for the refilling with neurotransmitters and so another cycle of neurotransmitter delivery via SVs ("SV cycle") can begin (Sudhof, 2004). Some of the proteins involved in this SV cycle/ in SV dynamics are Glutamate decarboxylase-65 (GAD65), vesicular glutamate transporter (VGLUT), vesicular gamma-Aminobutyric acid (GABA) transporter (VGAT), Synapsin (Syn), Synaptotagmin (SYT), Synaptophysin (Syp) and Cask. For example, GAD65 is involved in the (local) synaptic synthesis of GABA, whereas VGLUT and VGAT are involved in the loading of SVs. Instead, Syns are involved in the anchoring of SVs to the presynaptic scaffold, as well as the Ca^{2+}-dependent release of SVs from the scaffold, Syp appears to be relevant for the endocytosis of SVs, and adaptor proteins like Cask are indirectly involved in the anchoring SVs at the presynaptic release site (Kanaani et al., 2002; Tabuchi et al., 2002; Kwon and Chapman, 2011; Sudhof and Rizo, 2011).

Instead, the postsynaptic compartment is highly organized to enable a response to neurotransmitter binding which includes (but is not limited to) a neurotransmitter-dependent influx of ions and a neurotransmitter-dependent induction of signalling cascades. For example, the postsynapse harbors neurotransmitter receptors like the α-amino-3-hydroxy-5-methyl-4-isoxazolepropionic acid receptor (AMPAR), an ionotropic GluR, or the $GABA_A$ receptor ($GABA_AR$) which represents the main ionotropic GABA receptor (GABAR). These ionotropic GluRs and GABARs are probably

heterotetra- and heteropentamers, respectively, consisting of such subunits as GluR1 (subunit 1 of the AMPAR) and $GABA_AR\alpha1$ ($\alpha1$ subunit of the $GABA_AR$) (Dingledine et al., 1999; Sarto et al., 2002). The postsynapse also harbors metabotropic neurotransmitter receptors like mGluRs or $GABA_B$ receptors which diversify the response of the postsynapse to neurotransmitters. Additionally, the postsynapse exhibits an extensive scaffold which links neurotransmitters with the cytoscelleton and signalling machinery; some prominent members of this scaffold include Postsynaptic Density protein 95 (PSD95) or Homer1. There are also cell adhesion molecules like neuroligin-1 (NLGN1), which are linked to presynaptically located cell adhesion molecules like neurexins and, finally, the postsynaptic compartment also exhibits many proteins which are related to synaptic and synapto-nuclear signalling like Ca^{2+}/Calmodulin-dependent kinase II (CaMKII), neuronal nitric oxide synthases, or cyclic adenosine monophosphate response element-binding protein 2 (Sala et al., 2001; Iida et al., 2004; Arancibia-Carcamo and Moss, 2006; Fainzilber et al., 2011; Sheng and Kim, 2011; Luo et al., 2012).

Lastly, it is also noteworthy that the functionality of the chemical synapse does not only depend on the pre- and postsynaptic neuron but instead is also determined by astrocytes and other glia cells (Perea et al., 2009). Glia cells, which ensheath neurons and synapse, do not only function in stabilizing neurons and serving their metabolic processes but instead take an active role in signalling at the synapse despite their inability to generate action potentials. For example, astrocytes have been shown to change their activity in response to synaptically released neurotransmitters and can communicate between each other using Ca^{2+} as a second messenge. Conversely, changes in astrocyte activity can have an effect on neuronal activity. One striking example of this is that astrocytes have been shown to release D-serine in dependency of neuronal activity which, in turn, influences postsynaptic GluR-activation since D-serine is a co-agonist for the GluR called NMDAR (Panatier et al., 2006; Perea et al., 2009).

1.2.2 Chemical Synapse: Excitatory and inhibitory synapse

One can differentiate three classes of chemical synapses: excitatory synapses, inhibitory synapses, and complex/modulatory synapses. These synapses differ in biochemical buildup and in the neurotransmitters that are principally used. In the brain, excitatory synapses usually employ glutamate, inhibitory synapses usually employ GABA, and modulatory synapses can use a variety of neurotransmitters, such as melatonion, serotonin or dopamine.

Simplified, activation of the excitatory synapse causes the release of glutamate from the presynaptic compartment and, in turn, leads to the activation of ionotropic GluRs which allow for the flux of

Na^+, K^+, and sometimes Ca^{2+}. Due to the ionic concentrations of the extracellular and intracellular space, this causes a net influx of Na^+ and outflux of K^+ which depolarizes the postsynaptic neuron and thereby increases the probability of the generation of an action potential at its axon hillock. With other words, activating excitatory synapses leads to the generation of an excitatory postsynaptic current (EPSC). Instead, activation of the inhibitory synapse causes the release of GABA from the presynaptic compartment and, subsequently, leads to the activation of ionotropic GABARs which allow for the flux of Cl^-. Due to the ionic concentrations of the extracellular and intracellular space, this causes an influx of Cl^- which hyperpolarizes the postsynaptic neuron and thereby decreases the probability of the generation of an action potential at its axon hillock. With other words, activating inhibitory synapses leads to the generation of an inhibitory postsynaptic current (IPSC) (Junge, 1981). Activation of complex/modulatory synapses can lead to either an EPSC or IPSC at the postsynaptic neuron but is not of relevance in the context of this study. It is important to note that postsynaptic currents (PSCs) are not solely induced when the presynaptic compartment is activated as a consequence of presynaptically generated action potentials. Instead, PSCs can also be the consequence of spontaneous fusion of individual SVs which occurs largely independently of action potentials (Fatt and Katz, 1952). Since these spontaneous events lead to much smaller PSCs than those evoked by presynaptically generated action potentials, they are called miniature postsynaptic currents (mPSCs). mPSCs can occur at excitatory synapses where they cause miniature excitatory postsynaptic currents (mEPSCs) or they can occur at inhibitory synapses where they cause miniature inhibitory postsynaptic currents (mIPSCs). Importantly, mPSCs contain important information about the amount of functional synapses and can give an indication of the efficacy and dynamics of the pre- and postsynaptic compartment (see also paragraph 3.1.5).

Morphologically, one can differentiate excitatory and inhibitory synapses by electron microscopy because the latter has a symmetric structure whereas the former has an asymmteric structure with a prominent postsynaptic structure called the postsynaptic density (the part of the postsynapse that is in near vicinity to the synaptic cleft is enriched in proteins and is therefore electron-dense). Additionally, the excitatory synapse usually exhibits (postsynaptic) dendritic protrusions called “spines”, whereas inhibitory synapses are positioned on the dendritic shaft [dendrites represent “the branched projections of a neuron that receive synaptic inputs conveyed by axons from other neurons” (Sheng and Kim, 2011)]. In addition, various structural and biochemical differences exist between excitatory and inhibitory synpapses. For example, excitatory synapses employ scaffolding proteins like PSD95 or Synapse-associated protein (SAP) 97 which contain PDZ domains to enable the (indirect) interaction with other scaffolding proteins like those of the ProSAP/Shank family

(Sheng and Kim, 2011). Instead, the scaffold of the inhibitory synapse employs proteins like Gephyrin or Profilin (Giesemann et al., 2003).

1.3 eEF2K/eEF2 pathway and the chemical synapse

Even though eEF2K and eEF2 are ubiquitously expressed and eEF2 phosphorylation is generally associated with reduced protein translation, it is likely that the eEF2K/eEF2 pathway regulates protein translation in a particular manner in neurons and possibly also in other cells. For example, it has been found that even though eEF2 phosphorylation is related with a decrease in general protein translation at synapses, it is actually associated with an increased expression of certain proteins in the vicinity of the synapse, though the mechanism by which this happens is poorly understood (Scheetz et al., 1997, 2000). This indicates that the eEF2K/eEF2 pathway can regulate protein translation not only in a cell-type specific manner but also in a fashion that is specific for subcellular compartments. In the context of neuroscience, particular attention has been paid to eEF2K and the eEF2K/eEF2 pathway not least because the activity of eEF2K is Ca^{2+}-dependent and many synaptic processes involve Ca^{2+} (Breedlove et al., 2007; Sutton et al., 2007), which may suggest a link between these processes and eEF2K activity.

In fact, there is a multitude of publications showing that certain synaptic functions involving GluRs like synaptic signal-transduction and synaptic plasticity (change of synaptic structure/strength in response to changes in synaptic activity) depend on eEF2K activity and vice versa (Taha et al., 2013). For example, Davidkova and Carroll demonstrated that mGluR activation causes an eEF2K-dependent upregulation of Microtubule-associated protein 1B (MAP1b) which, in turn, leads to the endocytosis of AMPARs. Our own group has shown that prolonged mGluR-mediated activation of eEF2K can increase the expression of Brain-derived neurotrophic factor (BDNF), which is essential for the proper morphology of dendritic spines (Verpelli et al., 2010). Interestingly, it has also been shown that a certain form of synaptic plasticity called mGluR-dependent-Long Term Depression (mGluR-LTD) depends on eEF2K activity as this form of synaptic plasticity is absent in eEF2K-KO mice (Park et al., 2008). mGluR-LTD involves the reduction of synaptic strength in response to mGluR activation. This reduction in synaptic strenght can be the result of different cellular events, for example the endocytosis of GluRs (Citri and Malenka, 2008). Park et al. show that mGluR-activation detaches eEF2K from the receptor itself which liberates eEF2K activity. eEF2K then phosphorylates eEF2 which for not well-understood reasons leads to the upregulation of activity-regulated cytoskeletal-associated protein (Arc). Arc then leads to the endocytosis AMPARs, thereby

completing the process of mGluR-LTD since a reduction in surface AMPARs drastically decreases synaptic strength.

Importantly, since eEF2K is a Ca^{2+}-dependent kinase, a significant amount of research on eEF2K at the synapse has focused on the NMDAR, which can allow for the entry of Ca^{2+} into neurons (Dingledine et al., 1999). For example, brief activation of NMDARs triggers synaptic eEF2 phosphorylation which leads to a local downregulation of general protein synthesis but curiously leads to an upregulation of the α subunit of CaMKII ("local" in this context means at or in the vicinity of the synapse) (Scheetz et al., 1997, 2000). Interestingly, several studies have also linked mEPSCs with eEF2K. Sutton et al. were the first to show that synaptic eEF2K activity and the associated decrease in general protein translation is increased in response to NMDAR-mediated Ca^{2+}-influx triggered by mEPSCs. On the contrary, action potentials appear to reduce eEF2K activity, leading to an increase of protein translation. This result suggests that the eEF2K/eEF2 pathway could represent a postsynaptic decoder of spontaneous (mPSC-mediated) and evoked (action potential-mediated) neurotransmission. In line with this result, other groups have found that blocking the mEPSC-triggered NMDAR activation with the NMDAR antagonist ketamin decreases eEF2K activity. This, in turn, leads to the upregulation of BDNF and AMPARs, which appears to be the molecular basis for the rapid antidepressive effect of ketamin (Autry et al., 2011; Nosyreva et al., 2013). The fact that eEF2K activity can be negatively or positively associated with the translation rate of one and the same protein (such as BDNF) shows that the eEF2K-dependent regulation of the synaptic proteome is complex and depends on the specific signalling pathway involved.

It is worthy to note that all of these publications demonstrate an involvement of the eEF2K/eEF2 pathway exclusively at the excitatory postsynapse, mostly in response to acute stimulation of GluRs (see Fig. 3). This raises the question whether eEF2K is localized only to the subcellular compartment of excitatory synapses and primarily changes its activity in response to acute changes of GluR activity or whether simply further research is needed to have a more comprehensive view of the eEF2K/eEF2 pathway at the synapse. For example, is eEF2K also important for the functionality of the GABAergic postsynapse and is the eEF2K/eEF2 pathway also located in the presynaptic compartment or is its synaptic localization limited to the postsynaptic compartment? What about somatically localized eEF2K activity, does it affect the pre- and postsynaptic compartment? And does a chronic change in eEF2K activity (as opposed to an acute change in eEF2K activity) have implications for the functionality of the synapse, as well? To the best of our knowledge, there are no publications focusing on these and other important questions which are

relevant to address in order to have a more complete understanding of what the eEF2K/eEF2 pathway does at the synapse.

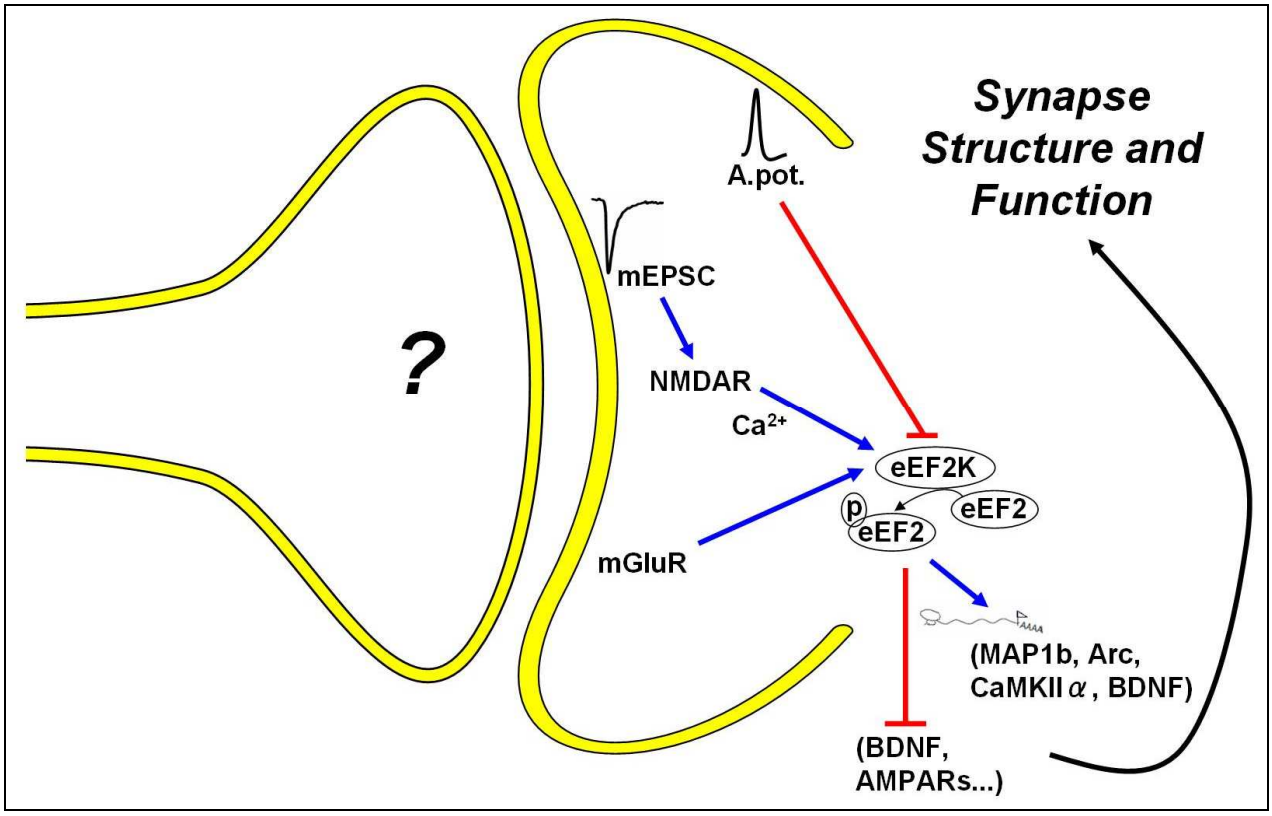

Figure 3: The eEF2K/eEF2 pathway at the excitatory postsynapse can be actively modulated by GluR signalling. NMDAR or mGluR activation induces an increase in eEF2K activity which is associated with proteomic changes that, subsequently, lead to changes in synaptic structure and function. For example, mEPSC-mediated activation of NMDARs leads to an influx of Ca^{2+} and an increase in eEF2K activity which then induces a downregulation of BDNF and (surface) AMPAR levels. Consequently, AMPAR-mediated currents are reduced. It is important to note that even though activation of eEF2K leads to a downregulation of global protein translation, at the chemical synapse eEF2K activity is positively correlated with a subset of proteins such as MAP1b and Arc. Curiously, it is not known whether eEF2K activity is also presynaptically localized or whether it has an effect on presynaptic functions such as SV release.

1.4 Aim of the study

As mentioned in the previous section, the effect that eEF2K activity has on the synapse is probably underestimated since most research has focused on changes in eEF2K activity at the excitatory postsynapse in response to acute alterations in GluR activation. However, since synapses are crucial signalling-elements in neurons and neural networks and because many synaptic events depend on protein translation, it is important to have a better understanding of what the eEF2K/eEF2 pathway does at the synapse.

Importantly, even though acute changes in eEF2K activity have been addressed, there is an incomplete view of what kind of effect chronic changes in eEF2K activity have on synapses, neurons, and neural networks. Accordingly, we decided to analyze what kind of functional and

proteomic effects chronic alteration and chronic absence of eEF2K activity have on neuronal and network processes, synapses, and synaptic events such as signal transmission at the chemical synapse. This analysis was mainly carried out by employing an *in vitro* eEF2K-gain-of-function design (primary neuronal cultures) and an *in vivo* loss-of-function design (eEF2K-KO mice).

2. Materials and methods

2.1 Materials

2.1.1 Animals

To prepare primary neuronal rat cultures, pregnant female rats (Rattus norvegicus) of the phylum Wistar were purchased from Charles River (Charles River Laboratories, Calco, Italy). eEF2K-KO and Syn I, II, III triple knock-out (TKO) mice were re-derived on a C57BL/6 background (Charles River Laboratories, Calco, Italy). Mice and rats were housed under constant temperature (22 ± 1°C) and humidity (50%) conditions with a 12 h light/dark cycle, and were provided with food and water ad libitum. For proteomic and electrophysiological analysis of eEF2K-KO mice, male littermates between postnatal day (P) 30-42 were used, whereas for electroencephalography (EEG) and behavioural analysis 3-4-month-old male mice were used.

All experiments involving animals followed protocols in accordance with the guidelines established by the European Communities Council and the Italian Ministry of Health (Rome, Italy). Experimental procedures of EEG and behavioural analysis followed the guidelines established by the Italian Council on Animal Care and were approved by the Italian Government decree No. 17/2013. Animal experiments involving TKO mice were approved by the Institutional Animal Care and Use Committee of the San Raffaele Scientific Institute (Milan, Italy; IACUC permission no. 565). All efforts were made to minimize the number of subjects used and their suffering.

2.1.2 Biochemical substances, chemical substances, and equipment

Biochemical substances, chemical substances, and equipment were purchased from the manufacturer initially listed. When not stated otherwise, chemicals were aquired from Sigma-Aldrich.

2.1.3 Antibodies

Primary antibodies:

Antibody	Origin, immunogen	Dilution	Manufacturer
anti (β-)actin	slightly modified β-cytoplasmic actin N-terminal peptide, Ac-Asp-Asp-Asp-Ile-Ala-Ala-Leu-Val-Ile-Asp-Asn-Gly-Ser-Gly-Lys, conjugated to KLH	WB: 1: 1,000	Sigma-Aldrich

anti Caspase-3	rabbit, synthetic peptide which corresponds to residues around the cleavage site of human caspase-3	WB: 1: 1,000	Cell Signalling
anti eEF2	rabbit, synthetic peptide which corresponds to residues N-terminally of human eEF2	WB: 1: 400	Cell Signalling
anti eEF2K	rabbit, synthetic peptide which corresponds to residues at the N-terminus of human eEF2k	WB: 1: 400	Cell Signalling
anti eEF2K	rabbit, synthetic peptide which corresponds to residues at the N-terminus of human eEF2k	IF: 1:50	Thermo Scientific
anti $GABA_AR\alpha1$	mouse, aa 355-394 of mouse $GABA_AR\alpha1$	WB: 1: 1,000 IF: 1: 500	NeuroMab
anti GAD65	mouse, synthetic peptide which corresponds to aa 4-22 of human GAD65	IF: 1: 500	Abcam
anti GAPDH	rabbit, synthetic peptide which corresponds to residues at the N-terminus of mouse GAPDH, aa 314-333	WB: 1: 2,000	Sigma-Aldrich
anti GFP	mouse, partially purified recombinant Aequorea victoria GFP	WB: 1: 1,000	Roche
anti GluR1	rabbit, KLH-conjugated linear peptide which corresponds to human GluR1 at the C-terminus	WB: 1: 1,000 IF: 1: 200	Millipore
anti MAP1b	rabbit, MAP1B fusion protein ag16255	WB: 1: 1,500	Proteintech
anti MAP2	mouse, bovine MAP2	IF: 1: 400	Abcam
anti NLGN1	mouse, fusion protein with aa 551-640 of human NLGN1	WB: 1: 10,000	NeuroMab
anti peEF2	rabbit, synthetic phosphopeptide which corresponds to residues around Thr56 of human eEF2	WB: 1: 500	Cell Signalling
anti PSD95	mouse, aa 77-299 of human PSD95	WB: 1: 5,000 IF: 1: 400	NeuroMab
anti Syp	mouse, rat retina synaptosome	WB: 1: 200	Sigma-Aldrich
anti Syn	mouse, partially purified Syn2b from N-terminal region	WB: 1: 1,000	home made antibody (Vaccaro et al., 1997)
anti Syn1/2	rabbit, synthetic peptide which corresponds to aa 2-28 in rat Syn	IF: 1: 400	Synaptic Systems
anti Syn2	mouse, partially purified Syn2b from N-terminal region	WB: 1: 1,000	home made antibody

			(Vaccaro et al., 1997)
anti TRIM3	rabbit, synthetic peptide from N-terminal residues of human TRIM3	WB: 1: 200	Abcam
anti (α-)tubulin	Sarkosyl-resistant filaments from Strongylocentrotus purpuratus (sea urchin) sperm axonemes	WB: 1: 1,000	Sigma-Aldrich
anti VGAT	rabbit, synthetic peptide which corresponds to aa 75-87 in rat VGAT	IF: 1: 200	Synaptic Systems
anti VGLUT	rabbit, fusion protein containing rat VGLUT, aa 456-560	IF: 1: 200	Synaptic Systems

Secondary antibodies:

Antibody	**Origin**	**Dilution**	**Manufacturer**
anti mouse IgG, peroxidase-conjugated	goat	WB 1: 5,000	Jackson ImmunoResearch Laboratories
anti mouse IgG, 680RD	goat	WB: 1: 15,000	LI-COR
anti mouse IgG, FITC		IF: 1: 100	Jackson ImmunoResearch Laboratories
anti mouse IgG, Cy3	goat	IF: 1: 200	Jackson ImmunoResearch Laboratories
anti mouse IgG, Cy5	goat	IF: 1: 100	Jackson ImmunoResearch Laboratories
anti rabbit IgG, peroxidase-conjugated	goat	WB 1: 5,000	Jackson ImmunoResearch Laboratories
anti rabbit IgG, 800RD	goat	WB: 1: 15,000	LI-COR
anti rabbit IgG, FITC		IF: 1: 100	Jackson ImmunoResearch Laboratories
anti rabbit IgG, Cy3	goat	IF: 1: 200	Jackson ImmunoResearch Laboratories
anti rabbit IgG, Cy5	goat	IF: 1: 100	Jackson ImmunoResearch Laboratories

2.1.4 DNA constructs and vectors

GFP and eEF2Kca lentiviral constructs were previously described (Verpelli et al., 2010) and are expressed by the previously described 2nd generation lentiviral transfer vector FUW (Lois et al.,

2002). K170M was subcloned into the FUW vector using the restriction sites BamH1 and Asc1. The sieEF2K/siRNA 362 lentiviral construct was also previously described (Verpelli et al., 2010) and is expressed in the previously described 2nd generation lentiviral transfer vector pLVTHM (Wiznerowicz and Trono, 2003). It exhibits the following siRNA nucleotide sequence: gggagtggctgaaagacga. A scrambled form of sieEF2K was cloned into pLVTHM and exhibits the following nucleotide sequence: gctgagcgaaggagagat. sreEF2K was designed on the basis of rat eEF2K in the pEGFP-C1 vector by Polymerase chain reaction (PCR)-mutagenesis. It was then subcloned into the 3rd generation lentiviral transfer vector pUltra-hot ("Plasmid 24130: pUltra-hot". Addgene, *n.p.*, *n.d*, Web. 17 Dec. 2013*;* Addgene plasmid 24130; principal investigator: Malcolm Moore) using the restriction sites Xba1 and Sal1. Its resistance to sieEF2K is due to 6 mutations (made evident by bold type) in the siRNA nucleotide sequence which conserves the peptide sequence in the corresponding region of the gene: g**a**ga**a**tgg**tt**a**a**a**gg**a**t**ga. Syn2b was subcloned into the FUW vector using the restriction sites BamH1 and Asc1. All restriction enzymes were purchased by New England Biolabs.

2.1.5 Acknowledgment of materials, corresponding researchers and associated institutions

The NLGN1 antibody was a gift from Dr. N. Brose (Max Planck Institute of Experimental Medicine, Göttingen, Germany). The Syn antibody was a gift from Dr. Valtorta (Division of Neuroscience, San Raffaele Scientific Institute and Vita-Salute University, Milan, Italy). The Syn2 antibody was a gift from O. Franco (University of Genova, Genova, Italy). K170M cDNA was kindly provided by Dr. Chris G. Proud, (University of Southhampton, Southhampton, U.K.). Syn2b cDNA was kindly provided by George J. Augustine (Nanyang Technological University, Singapore, Singapore). The pUltra-hot vector was provided by Dr. M. A. S. Moore (Memorial Sloan-Kettering Cancer Center, New York, USA) via the webservice Addgene. Homozyguous eEF2K-KO mice were provided by Dr. Ryazanov (University of Medicine and Dentistry of New Jersey/Robert Wood Johnson Medical School, New Brunswick, NJ). TKO mice cultures were kindly provided by Dr. Flavia Valtorta (Division of Neuroscience, San Raffaele Scientific Institute and Vita-Salute University, Milan, Italy). TKO mice were provided by Dr. H.T. Kao (Brown University, Providence, RI, USA), and Dr. Paul Greengard (The Rockefeller University, NY, USA).

2.2 Methods

Methods were carried out according to cited publications, common protocols, and protocols provided by manufacturer. Important changes in protocoles are noted and described.

2.2.1 Cell culture

Principally, rat primary hippocampal and cortical cultures of days *in vitro* (DIV) 20 were used. Alternatively, mouse hippocampal cultures of DIV 20 were used (always noted).

2.2.1.1 Preparation of primary rat neuronal cultures

Primary rat neuronal cultures were prepared similarly to a previously described study (Verpelli et al., 2010) with slight modifications. Hippocampal or cortical neuron cultures were prepared from embryonic day (E) 18 rat embryos (Charles River). Neurons were plated at medium density (200 cells/mm²) on 12-well plates (Euroclone) with or without coverslips (VWR), coated with 0.01 mg/ml poly-L-Lys (Sigma-Aldrich), and cultured using home made B27 which represents a slight variation of a previously described formula (Chen et al., 2008). Every week (at DIV 4, 11, and 18), 40% of the volume was aspired and replaced by fresh medium (volume: 50% of the original volume). 12-well plates without coverslips were used for protein biochemical analysis, whereas 12-well plates with coverslips were used for immunocytochemical or electrophysiological analysis.

2.2.1.2 Preparation of primary mouse neuronal cultures

Primary mouse neuronal cultures were prepared from the hippocampi of E 17.5 embryos from wild type (WT) and TKO mice as previously described (Banker and Cowan, 1977). Neurons were plated at medium density (200 cells/mm²) on 12-well plates (Corning, NY, USA) with or without coverslips (VWR), and coated with 0.1 mg/mL poly-L-Lys (Sigma-Aldrich). Cells were plated in complete Neurobasal medium [Neurobasal (Invitrogen, Carlsbad, CA, USA) supplemented with 10% fetal bovine serum, 2% B27, 1% Pen/Strep, 1% L-Glutamax (Gibco ® Invitrogen)]. After 4 h, the medium was completely substituted with serum-free Neurobasal. Every week (at DIV 4, 11, and 18), 30% of the volume was aspired and replaced by fresh medium (volume: 40% of the original volume). 12-well plates without coverslips were used for protein biochemical analysis, whereas 12-well plates with coverslips were used for electrophysiological analysis.

2.2.1.3 Lentiviral production and infection of primary rat and mouse neuronal cultures

Genetically modified lentiviruses were produced as previously described (Naldini et al., 1996; Lois et al., 2002) and the production was carried out with 2nd and 3rd generation lentiviral transfer vectors. Mainly, lentiviral infection took place at DIV 1. If infection took place at another time point, it is noted.

2.2.1.4 Analysis of primary rat and mouse neuronal cultures

Protein biochemical, immunocytochemical, or electrophysiological analysis was carried out at DIV 20 unless otherwise stated.

2.2.2 Protein biochemistry

2.2.2.1 Preparation of samples

Cultured neurons or brain lysates were collected with precooled "buffered sucrose" [0.32 M sucrose (Sigma-Aldrich)/4mM HEPES-NaOH buffer (Sigma-Aldrich), pH 7.3, protease inhibitors (Roche)] and analyzed via Bradford protein assay (Bio-Rad) to asses protein concentration. For total lysate (TL), proteins were solubilized in 2-4x loading buffer/dye [(250 mM Tris, 8 % (w/v), 40 % (v/v) glycerol, 0.008 % (w/v) bromophenol blue (all Sigma-Aldrich)] in order to have a final protein concentration of 1 µg/µl in the sample. In other cases, fractionation took place prior to Bradford protein assay analysis resulting in a P1 fraction (enriched in cell bodies and dendritic fragments) and a P2 fraction (enriched in presynaptic and postsynaptic components) (Huttner et al., 1983; Grabrucker et al., 2011). Also in the case of P1 and P2 fractions, 2-4x loading buffer was added in order to have a final protein concentration of 1 µg/µl in the sample. When not stated otherwise, samples are from TL. Samples were then heated for 5 min at 95°C (thermoblock from FALC Instruments) and centrifuged for 1 min at 15,000 g (centrifuge purchased from VWR, model 521-3600). Then, 20 µg of samples were loaded in the pockets of 6-15% polyacrylamide gels (home made with reagents from Bio-Rad) and proteins were electrophoretically seperated by sodium dodecyl sulfate-Polyacrylamide gel electrophoresis (SDS-PAGE).

2.2.2.2 Sodium dodecyl sulfate-polyacrylamide gel electrophoresis and electroblotting

Proteins were electrophoretically seperated by SDS-PAGE under denaturing conditions (Laemmli, 1970) followed by electroblotting of the proteins onto a nitrocellulose membrane using the Trans-Blot Turbo System (Bio-Rad). Then the membranes were stained by Ponceau S Stain (Sigma-Aldrich) to control for efficient protein transfer of proteins and were subsequently washed twice in

Tris-buffered saline-Tween (TBS-T) [20 mM Tris pH 7.4, 150 mM NaCl (both Sigma-Aldrich), and 0.1% Tween 20 (Bio-Rad)].

2.2.2.3 Western Blot analysis

Blocking of membranes took place for at least 1.5 h at 4°C in blocking buffer (TBS-T and 5% dried nonfat milk). Primary antibodies were applied for 1-3 h in blocking buffer (here: with 3 instead of 5% dried nonfat milk). For rat neuronal culture lysates (except for those lysates analyzed in the context of paragraph 3.1.5), HRP-conjugated secondary antibodies (Jackson ImmunoResearch Laboratories) were used in blocking buffer (here: with 3 instead of 5% dried nonfat milk) and chemiluminescence was induced using an ECL kit (GE Healthcare). For brain lysates and rat/mouse neuronal culture lysates analyzed in the context of paragraph 3.1.5, fluorophore coupled secondary antibodies (LI-COR) were used and signal detection took place using an Odyssey scanner (LI-COR) after completely drying the membrane. After each antibody incubation, 3 washes (10 min each) took place with TBS-T. For fluorophore coupled secondary antibodies, 2 additional washes (10 min each) were added with Tris-buffered saline (TBS) [20 mM Tris pH 7.4, 150 mM NaCl (both Sigma-Aldrich)] to displace Tween 20 from the membrane in order to avoid fluorescence background signal. Immunoblot band intensity was quantified manually with ImageJ (US National Institutes of Health), an open source program. Normalization took place via actin for P1 and P2 samples. For TL, mainly tubulin was used for normalization; actin was only used fot TL normalization when P2 fractions were run in parallel in the gel.

2.2.3 Immunocytochemistry

For immunocytochemical analysis, neurons were fixed in methanol at -20°C or with 4% paraformaldehyde and 4% sucrose for 5-10 min at room temperature [for FM-dye, 0.05% glutaraldehyde (VWR) were added additionally] and then washed 3 times (10 min for each wash) with PBS [136.8 mM NaCl, 2.68 mM KCl, 10.1 mM Na_2HPO_4 and 1.76 mM KH_2PO_4 , pH 7.4 (all Sigma-Aldrich)]. Then, primary antibodies [diluted in GDB buffer: 30 mM phosphate buffer, pH 7.4, 0.2% gelatin, 0.5% Triton X-100, 0.8 M NaCl (all Sigma-Aldrich)] were applied for 1-3 h at room temperature. Secondary antibodies were also diluted in GDB buffer and applied for 1 h. After each antibody incubation, 3 washes (10 min each) took place with “high-salt buffer” [20mM Na_2HPO_4/NaH_2PO_4 and 0.5M NaCl, pH 7.4 (all Sigma-Aldrich)] and before mounting a final wash (for 10 min) was carried out with PBS. Before mounting, coverslips were briefly passed through ddH_2O to dilute salts. 4',6-diamidino-2-phenylindole (DAPI) staining (Life Technologies) was

carried out for 2 min (DAPI diluted in PBS to a final concentration of 0.5 µg/ml) and took place during the washing steps before mounting.

2.2.3.1 FM-Dye experiment

FM-dye staining was carried out with slight variation of a previously described protocole (Hering et al., 2003). More specifically, neurons were incubated for 1 min at room temperature in 3 µM FM 4-64FX (Molecular Probes) in high potassium buffer [90 mM KCl, 55 mM NaCl, 10 mM HEPES pH 7.4, 10 mM glucose, 2.6 mM $CaCl_2$, 1.3 mM $MgCl_2$ (all Sigma-Aldrich)] or in Tyrode solution [3mM KCl, 145 mM NaCl, 10 mM HEPES pH 7.4, 10 mM glucose, 2.6mM $CaCl_2$, 1.3 mM $MgCl_2$, 5 µM glycine (all Sigma-Aldrich)]. Then, 4-5 washes (3-5 min each) with Tyrode solution were carried out in the presence of 1 µM tetrodotoxin (TTX) before fixation. After fixation, immunocytochemical analysis followed as described in paragraph 2.2.3.

2.2.3.2 Image acquisition and Processing

Mounted coverslips were imaged with a confocal microscope (Zeiss 510 with Zeiss 63 x objective) at a resolution of 1024 x 1024 pixels. Images represent maximum intensity projections of five individual images taken at depth intervals of around 0.5 µm. Acquired images were then analyzed for puncta quantity and size sing ImageJ (analyze particles option, cutoff: 1 µm²). To analyze the GAD65 stain at the soma, a circle (30 µm diameter) was laid around the center of the DAPI stain and the average GAD65 stain was calculated. For the FM-dye stain, a MAP2 mask was generated on which the the average FM-dye signal was calculated.

2.2.4 Analysis of proteins by Liquid chromatography–mass spectrometry/mass spectrometry

After SDS-PAGE, gels were stained with home made colloidal Coomassie Brilliant Blue [20% methanol, 8% ammonium sulfate, 1.6% phosphoric acid, and 0.12% Coomassie G-250 (all Sigma-Aldrich)]. Gel slices were excised from the gels sampling the entire length of the lanes (15 slices each). After reduction with 10 mM dithiothreitol (DTT) (Sigma-Aldrich) , alkylation with 55 mM Iodoacetamide and overnight tryptic digestion (Shevchenko et al., 2006), peptide mixtures were desalted and concentrated on home made C18 Stage Tips µC18 (Rappsilber et al., 2007) and injected in a capillary chromatographic system (EasyLC, Proxeon Biosystems, Odense, Denmark). Peptide separation occurred on a RP homemade 15-cm reverse phase (RP) spraying fused silica capillary column (75 µm i.d.), packed in house with 3-µm ReproSil-Pur 120 C18-AQ (Dr. Maisch GmbH, Germany). A gradient of eluents A (H_2O with 2% v/v ACN, 0.5% v/v acetic acid) and B

(80% ACN with 0.5% v/v acetic acid) was used to achieve separation, from 7% B (at 0 min 0.2 μL/min flow rate) to 40% B (in 70 min, 0.2 μL/min flow rate). The LC system was connected to an LTQ-Orbitrap mass spectrometer (Thermo Fisher Scientific, Bremen, Germany) equipped with a nanoelectrospray ion source (Proxeon Biosystems, Odense, Denmark). Mass spectrometry (MS) and MS/MS spectra were acquired selecting the ten most intense ions per survey spectrum acquired in the orbitrap from m/z 300-1750 with 30.000 resolution. Target ions selected for the MS/MS were fragmented in the ion trap and dynamically excluded for 60s. Target values were 1,000,000 for survey scan and 100,000 for MS/MS scan. For accurate mass measurements, the lock-mass option was employed (Olsen et al., 2005). Technical replicates were conducted on the Liquid chromatography–mass spectrometry (LC-MS)/MS part of the analysis.

2.2.5 Real-time polymerase chain reaction

Total messenger RNA (mRNA) was analyzed by Real-time polymerase chain reaction (RT-PCR). For this, total RNA was extracted from primary rat cortical cultures infected with GFP or eEF2Kca at DIV 20, using the RNeasy Mini Kit and accompanying QIAshredder (Qiagen) according to the manufacturer's instructions. Contaminating DNA in the sample was degraded by on-column incubation with DNaseI (Qiagen) for 15 min. 1 μg per sample was reverse-transcribed using the SuperScript III (Life Technologies, Inc.) in accordance with the manufacturer's instructions. Gene expression was quantitatively analysed by amplification carried out with the ABI Prism 7000 Sequence Detection System and SDS software version 1.2.3 (Applied Biosystems, Inc., CA, USA). The target sequences were amplified from 50 ng of cDNA in the presence of TaqMan Gene Expression Master Mix. The TaqMan™ primer and probe assays (Life Technologies, Inc.) were eEF2 (ID # Rn00820849_g1), MAP1b (ID # Rn01399486_m1), TRIM3 (ID # Rn01509048_m1), Slc32a1 (namely VGAT, ID # Rn00824654_m1), Syn2 (ID # Rn00569739_m1), Gad2 (namely GAD65, ID # Rn00561244_m1), Dlg4 (namely PSD95, ID # Rn00571479_m1); the glyceraldehyde-3-phosphate dehydrogenase (GADPH; ID # Rn99999916_s1) was used as endogenous control. All of the assays were tested and confirmed as compatible for use with GAPDH as an endogenous control. The $2^{-\Delta\Delta CT}$ method was used to calculate the results, thus allowing the normalization of each sample to the endogenous control, and comparison with the calibrator for each experiment (set to a value of 1), as described in the figure legends.

2.2.6 Electrophysiology

2.2.6.1 *In vitro* experiments (primary rat/mouse neuronal cultures)

Whole-cell patch clamp recordings were performed at room temperature from DIV 20 primary cortical or hippocampal neurons perfused with external solution containing (in mM): 130 NaCl, 2.5 KCl, 2.2 $CaCl_2$, 1.5 $MgCl_2$, 10 D-glucose, 10 HEPES-NaOH (pH 7.4; osmolarity adjusted to 290 mOsm) for mIPSCs or Krebs'–Ringer's–HEPES solution containing (in mM): 125 NaCl, 5 KCl, 1.2 $MgSO_4$, 1.2 KH_2PO_4, 2 $CaCl_2$, 6 glucose, and 25 HEPES, pH 7.4 for mEPSCs. For mPSC recordings, blockers of voltage-dependent sodium channels (500 μM lidocaine) were included in the extracellular solution. This was done in combination with blockers for $GABA_A$Rs (20 μM bicuculline) or blockers for NMDARs, AMPARs/Kainate receptors [3mM Kynurenic acid (KYN)] for mEPSC or mIPSC recordings, respectively. The composition of the intracellular solution was (mM): 126 K-gluconate, 4 NaCl, 1 EGTA, 1 $MgSO_4$, 0.5 $CaCl_2$, 3 ATP (magnesium salt), 0.1 GTP (sodium salt), 10 glucose, 10 HEPES-KOH (pH 7.3; osmolarity adjusted to 280 mOsm) for mEPSCs recordings or 140 mM CsCl, 2 mM $MgCl_2$, 1 mM $CaCl_2$, 10 mM EGTA, 10 mM HEPES-CsOH, 2 mM ATP (disodium salt) (pH 7.3) for mIPSCs. Recordings were performed with an Multiclamp 700B amplifier (Axon CNS molecular devices, USA). Pipette resistance was 2-3 MΩ and series resistance was always below 20 MΩ. mEPSCs and mIPSCs were recorded at a holding potential of -70 mV over a period of 2-5 min, filtered at 2 kHz and digitized at 20 kHz using Clampex 10.1 software. Analysis was performed offline with Clampfit 10.1 software using a threshold crossing principle; detection level was set at 5 pA, and raw data were visually inspected to eliminate false events; cells with noisy or unstable baselines were discarded. mEPSC and mIPSCs population averages were obtained by aligning the events at the mid-point of the rising phase. The weighted decay time constant (Dt) of mEPSCs were calculated as described (Cingolani et al., 2008).

2.2.6.2 *Ex vivo* experiments (slices of eEF2K-KO mice and slices thereof)

WT and eEF2K-KO mice were anesthetized in a chamber saturated with chloroform and then decapitated. The brain was rapidly removed and placed in an ice-cold solution containing 220 mM sucrose, 2 mM KCl, 1.3 mM NaH_2PO_4, 12 mM $MgSO_4$, 0.2 mM $CaCl_2$, 10 mM glucose, 2.6 mM $NaHCO_3$ (pH 7.3, equilibrated with 95% O_2 and 5% CO_2), and 3 mM KYN. Coronal hippocampal slices (thickness, 250–300 μm) were prepared with a vibratome VT1000 S (Leica) and then incubated first for 40 min at 36°C and then for 30 min at room temperature in artificial CSF (aCSF), consisting of (in mM) 125 NaCl, 2.5 KCl, 1.25 NaH_2PO_4, 1 mM $MgCl_2$, 2 mM $CaCl_2$, 25 mM glucose, and 26 mM $NaHCO_3$ (pH 7.3, equilibrated with 95% O_2 and 5% CO_2).

Slices were transferred to a recording chamber perfused with aCSF at room temperature at a rate of about 2 ml/min. Whole-cell patch-clamp electrophysiological recordings were performed with an

Multiclamp 700B amplifier (Axon CNS molecular devices, USA) using an infrared-differential interference contrast microscope. Patch microelectrodes (borosilicate capillaries with a filament and an outer diameter of 1.5 μm; Sutter Instruments) were prepared with a four-step horizontal puller (Sutter Instruments) and had a resistance of 3–5 MΩ.

Spontaneously occuring IPSCs as well as tonic GABAergic currents were recorded at a holding potential of −65 mV with an internal solution containing 140 mM CsCl, 2 mM $MgCl_2$, 1 mM $CaCl_2$, 10 mM EGTA, 10 mM HEPES-CsOH, 2 mM ATP (disodium salt) (pH 7.3), and 5 mM QX-314 (lidocaine N-ethyl bromide). Access resistance was between 10 and 20 MΩ; if it changed by >20% during the recording, the recording was discarded.

All GABAergic currents were recorded in the presence of KYN (3 mM) in the external solution. For the recording of mIPSCs, lidocaine (500 μM) was added in the external solution. Currents were filtered at 2 kHz and digitized at 20 kHz using Clampex 10.1 software. Analysis was performed offline with Clampfit 10.1 software.

2.2.7 Electroencephalography analysis

2.2.7.1 Preparation of mice for electroencephalography analysis

WT and eEF2K-KO mice were anesthetized with an i.p. injection of 5% chloral hydrate dissolved in saline and given at a volume of 10 ml/kg. Four screw electrodes (Bilaney Consultants GMBH, Dusseldorf, Germany) were inserted bilaterally through the skull over cortex (anteroposterior, +2.0–3.0 mm; left–right 2.0 mm from bregma) as previously described (Manfredi et al., 2009) according to brain atlas coordinates (Franklin and Paxinos, 2008); a further electrode was placed into the nasal bone as ground. The five electrodes were connected to a pedestal (Bilaney, Dusseldorf, Germany) and fixed with acrylic cement (Palavit, New Galetti and Rossi, Milan, Italy). The animals were allowed to recover for a week from surgery before the experiment. After surgery, EEG activity was recorded in a Faraday chamber using a Power-Lab digital acquisition system (AD Instruments, Bella Vista, Australia; sampling rate 100 Hz, resolution 0.2 Hz) in freely moving awake mice.

2.2.7.2 Electroencephalography analysis under baseline conditions

Basal cerebral activity was recorded continuously for 22 hours (form 5:00 pm to 16:00 pm). A quantitative analysis of spectral power was processed using fast Fourier transform. Each 2-hour spectral power was calculated between 0 and 25 Hz, with a 0.2 Hz resolution, using the standard spectral power distribution: δ (0-4 Hz), θ (4.2-8 Hz), α (8.2-13 Hz) and β (13.2-25 Hz). Segments

with movement artifacts or electrical noise were excluded from statistical analysis. EEG traces were also analyzed for spike activity (number) as previously described (Manfredi et al., 2009).

2.2.7.3 Electroencephalography analysis after administration of chemoconvulsant substances

After 30 minutes of baseline, animals were given pilocarpine (300 mg/kg i.p.) or pentylenetatrazol (PTZ) (30 mg/kg i.p.) and immediately recorded for EEG activity. Atropine methylnitrate (5 mg/kg i.p.) was given 30 min before pilocarpine to reduce peripheral cholinergic side effects. Behaviour and EEG traces were analyzed as previously described (Nosten-Bertrand et al., 2008) for 2 hours after drug treatment. Seizures were scored as Racine's scale (1, mouth and facial movement; 2, head nodding; 3, forelimb clonus; 4, rearing with forelimb clonus; and 5, rearing and falling with forelimb clonus). The number of animals showing seizures (Racine scale 3-5), total number of seizures, the latency to the first seizure and lethality were also evaluated.

In accordance with a previous study (Erbayat-Altay et al., 2008), EEG seizures were characterized as absence (Racine scale 1-2) when associated with rhythmic 4-6Hz sharp waves of spindle-like events; myoclonic seizures (Racine scale 3) consisting of whole body jerk and bilateral forelimb movements associated with solitary spike or polyspike and slow wave; generalized clonic or tonic seizures (Racine scale 4-5) [whole body jerks consisting of a train of spikes (clonic) or a voltage attenuation (tonic phase) which lasted 30-60 sec]. Rhythmic sharp waves, spikes or polyspike were characterized by an amplitude at least two times higher than baseline. Seizures were video-monitored and reviewed off-line by a blinded independent investigator to exactly score the seizures. Lethality was monitored within 7 days after drug injection.

2.2.8 Genotyping of mice

For genotyping of mice, DNA was extracted from tails and analyzed by PCR as previously described (Gitler et al., 2004; Autry et al., 2011).

2.2.9 Data analysis and figure display

2.2.9.1 Data analysis and display

Data is expressed as means ± SEM or percentage, was analyzed for statistical significance, and was displayed by Prism 5 software (GraphPad, San Diego, CA). If there were only two groups whose means were compared, a student's t-test was carried out to assess statistical significance. The

accepted level of significance was $p \leq 0.05$. In all cases with three or more groups, a one factorial analysis of variance (ANOVA) was calculated for the data and if group means differed in a significant manner ($p \leq 0.05$), a post hoc Tukey test was calculated to assess statistical significance. The accepted level of significance for the post hoc test was $p \leq 0.05$.

2.2.9.2 Mass spectrometry data analysis by MaxQuant

Raw data was processed with MaxQuant version 1.1.1.36. Peptides were identified from the MS/MS spectra searched against the uniprot_cp_rat_2011_07 database using the Andromeda search engine (Cox et al., 2011). Cysteine carbamidomethylation was used as fixed modification, methionine oxidation and protein N-terminal acetylation as variable modifications. Mass deviation for MS/MS peaks was set at 0.5 m/z units and a maximum of two missed cleavages was allowed. The peptides and protein false discovery rates (FDR) were set to 0.01; the minimal length required for a peptide was six amino acids; a minimum of two peptides and at least one unique peptide were required for high-confidence protein identification; for quantitative analysis the options Re-quantify and second peptide were selected. The lists of identified proteins were filtered to eliminate reverse hits and known contaminants. The statistical program Perseus – in the MaxQuant environment – was used for determining the Significance B with a Benjamini-Hochberg FDR < 5%. For SILAC analysis, quantification of the up- and downregulated proteins followed the criteria: 1. weighted mean ratio (eEF2Kca/GFP) of the protein exhibited the same sign (< > 1) in all experiments; 2. the weighted mean ratio was significant in at least two experiments (significance evaluated by Benjamini-Hochberg FDR < 5%); 3. the ratio count of the peptide was greater than 1 (minimum Ratio Count = 2); 4. SD of weighted mean ratio did not exceed 0.25.

2.2.9.3 Figure display

Figures were generated with Microsoft Office PowerPoint 2003 for Windows (Microsoft) in combination with Adobe Photoshop 6.0 for Windows (Adobe).

2.2.10 Acknowledgement of experimenters and corresponding institutions

Electrophysiological analysis was carried out by Dr. Luca Murru (CNR Institute of Neuroscience and Department of Pharmacology, University of Milan, Milan, Italy). EEG recordings and analysis was carried out by Dr. Luisa Ponzoni and Dr. Daniela Braida (Department of Medical Biotechology and Translational Medicine, University of Milan, Milan, Italy). Breeding of TKO mice and generation of TKO culture was carried out by Dr. Fabrizia Guarnieri (Division of Neuroscience,

San Raffaele Scientific Institute and Vita-Salute University, Milan, Italy). Execution and analysis of mass spectrometry was carried out by Dr. Angela Cattaneo (Biomolecular Mass Spectrometry Unit, Division of Genetics and Cell Biology, San Raffaele Scientific Institute, Milan, Italy). The first SILAC experiment was carried out by Dr. Chiara Verpelli (CNR Institute of Neuroscience and Department of Pharmacology, University of Milan, Milan, Italy). Technical Support for RT-PCR analysis was given by Dr. Roberta Benfante (CNR Institute of Neuroscience and Department of Pharmacology, University of Milan, Milan, Italy). The PCR for cloning Syn2b into the FUW vector was carried out by Emmanuela Toffolo (Department of Medical Biotechnology and Translational Medicine, University of Milan, Milan, Italy). Dr. Elisa Faggiani (Neuromuscular Diseases and Neuroimmunology, Neurological Institute Foundation Carlo Besta, Milan, Italy) helped in the genotyping of eEF2K-KO mice.

Dr. Carlo Sala (CNR Institute of Neuroscience and Department of Pharmacology, University of Milan, Milan, Italy) provided expertise for the part regarding molecular biology, biochemistry, the *in vivo* work and corrected the text. Dr. Chiara Verpelli provided expertise for the part regarding biochemistry. Dr. Mariaelvina Sala (Department of Medical Biotechology and Translational Medicine, University of Milan, Milan, Italy) and Dr. Daniela Braida provided expertise for the part regarding the EEG analysis and behavioural studies. Dr. Roberta Benfante provided expertise for the part regarding RT-PCR. Dr. Angela Bachi (Biomolecular Mass Spectrometry Unit, Division of Genetics and Cell Biology, San Raffaele Scientific Institute, Milan, Italy) provided expertise for the part regarding the mass spectrometry experiments. Dr. Luca Murru provided expertise for the electrophysiological part of the study. Dr. Patrizia Rosa (CNR Institute of Neuroscience and Department of Pharmacology, University of Milan, Milan, Italy) and Dr. Silvia Bassani (CNR Institute of Neuroscience and Department of Pharmacology, University of Milan, Milan, Italy) provided expertise for the FM-dye experiment.

3 Results

3.1 eEF2K gain-of-function experiments *in vitro* (primary rat/mouse neuronal cultures)

3.1.1 eEF2K upregulates a small number of synaptic proteins while downregulating a subset of presynaptic vesicle-associated proteins

Previous studies on eEF2K have shown that this Ca^{2+}/Calmodulin dependent kinase diversely regulates the translation rate of a set of proteins at the excitatory postsynapse which is most probably due to its ability to phosphorylate and thereby inactivate its only known substrate eEF2. Importantly, eEF2K activity can be altered by acute and prolonged changes in neuronal activity suggesting that the eEF2K/eEF2 pathway may represent a way for neurons to decode neuronal activity and implement the type of proteomic changes required (Scheetz et al., 2000; Chotiner et al., 2003; Davidkova and Carroll, 2007; Sutton et al., 2007; Park et al., 2008; Verpelli et al., 2010; Autry et al., 2011).

To deepen our understanding of which synaptic proteins are regulated by chronic eEF2K activity we lentivirally overexpressed either a constitutively active form of eEF2K (eEF2Kca) described previously (Verpelli et al., 2010) or GFP as an infection control at DIV 1 in primary cultures of rat hippocampal neurons. At DIV 20, P2 crude synaptosomal fractions (fractions enriched in synaptic components) were prepared according to a previously described protocol (Li et al., 1996; Ohno et al., 2004) and were analyzed by mass spectrometry to identify changes in protein levels (Fig. 5 A). For this, we took advantage of a metabolic labeling method called stable isotope labeling in cell culture (SILAC) which yields more quantitative mass spectrometry results as opposed to label-free methods (Ibarrola et al., 2003; Ibarrola et al., 2004; Mann, 2006; Ong and Mann, 2006; Bachi and Bonaldi, 2008; Liao et al., 2008; Spellman et al., 2008; Zhang et al., 2012). In this context we also carried out a pilot experiment in which we verified that isotope integration was successful at about 95% (Fig. 4). Additionally, we verified by WB that eEF2K and peEF2 levels were successfully modified by eEF2Kca overexpression (Fig. 5 C, E). We also analyzed Caspase-3 cleavage as an indication of cell viability/apoptosis (Porter and Janicke, 1999; Zhang and Bhavnani, 2006) and could not detect differences between the groups (Fig. 5 B, D).

The SILAC-based mass spectrometry analysis was carried out on three independent experiments, each yielding about 1100 identified proteins in the P2 fractions. To identify proteins strongly regulated by eEF2K, stringent parameters were applied, revealing 4 up- and 32 downregulated

proteins (Tab. 1). To better understand which synaptic proteins are regulated by eEF2K, the list was reduced to members which have been shown to localize to the synapse namely eEF2, MAP1b, Tripartite motif-containing protein 3 (TRIM3), Cask, and Glypican 4 (Gpc4) (Hsueh et al., 1998; Tabuchi et al., 2002; Zalfa et al., 2003; Davidkova and Carroll, 2007; Hung et al., 2010; Verpelli et al., 2010; Dajas-Bailador et al., 2012; de Wit et al., 2013; Taha et al., 2013). The list of downregulated proteins was augmented by a revision of the raw data which revealed several downregulated presynaptic vesicle-associated proteins with stable trends, such as Syn2 (Valtorta et al., 1992; Medrihan et al., 2013), while major postsynaptic proteins were not affected (Tab. 2).

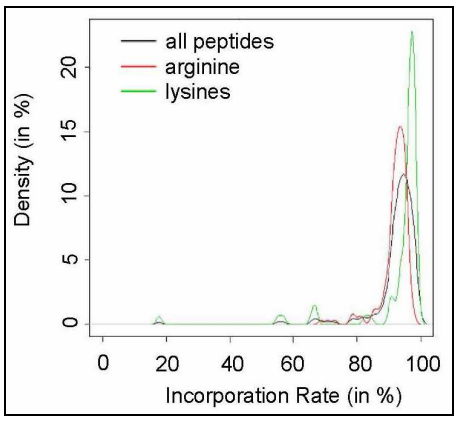

Figure 4: Successful incorporation of isotopes in SILAC procedure. To investigate the labeling efficiency in our experimental design, hippocampal neurons were grown from DIV 0 to DIV 20 with labeled/"heavy" amino acids: isotopes "Lys4" and "Arg6" (Cambridge Isotope Laboratories, Inc). At DIV 20, neurons were lysed and loaded on an SDS-Page. Then, a section of the gel was digested with trypsin, and analyzed by LC-MS/MS. Raw files were processed by MaxQuant and statistical data analysis was done using the R software package (ver. 2.10.1). The average labeling efficiency was 95% (N = 246; Bandwidth: 0.009905; incorporation rate of Arg: 93.6%; incorporation rate of Lys: 97.2%)

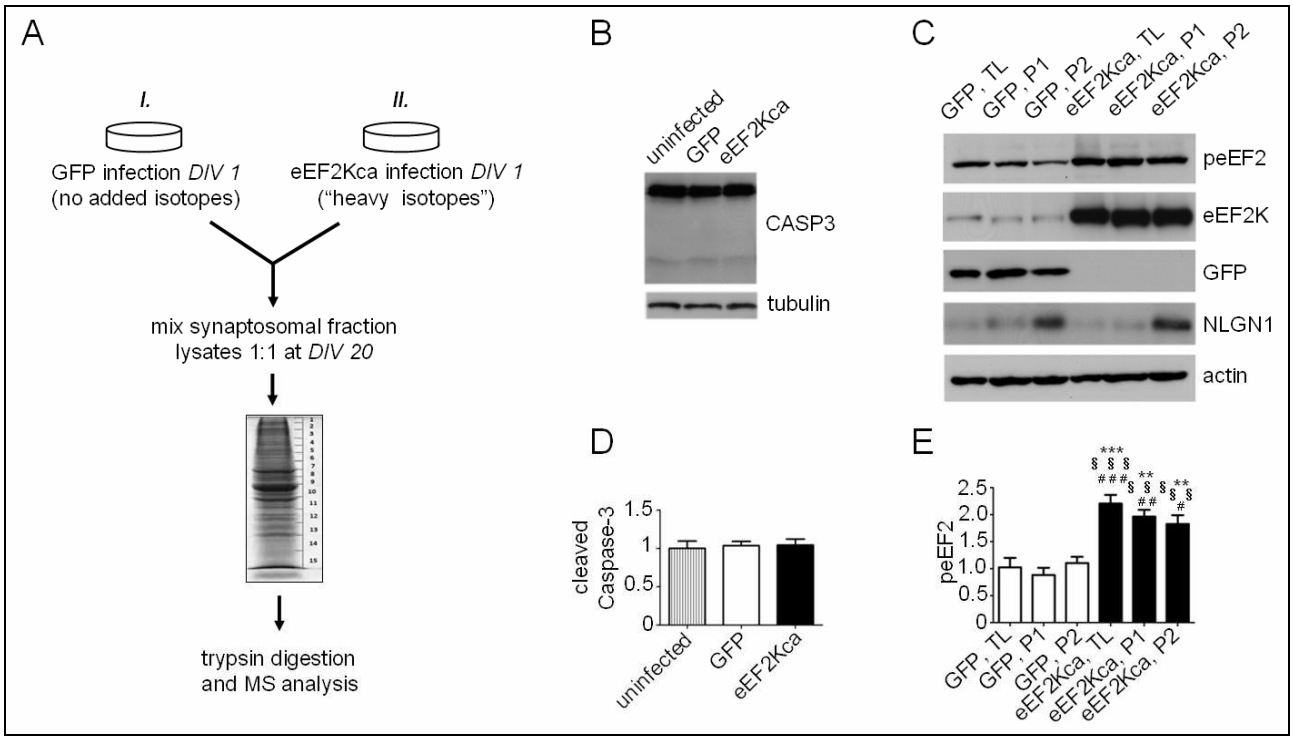

Figure 5: SILAC procedure and associated WB analysis to compare crude synaptosomal fractions of GFP and eEF2Kca. **A,** SILAC procedure. Primary cultures of rat hippocampal neurons were grown in media (*I.*) without or (*II.*) with labeled isotopes of Arg and Lys (from plating, i.e. DIV 0, onwards). Cultures were infected with lentiviruses at DIV 1 with either (*I.*) GFP as an infection control or (*II.*) eEF2Kca. At DIV 20, equal protein amounts of P2 lysates from GFP and eEF2Kca were mixed, subjected to an SDS-PAGE, and analyzed via mass spectrometry. Three independent experiments were performed. **B,** Cell viability appears comparable between analyzed groups of SILAC experiments. To assess cell viability/apoptosis, total lysates of DIV 20 neurons were analyzed by WB for Caspase-3 cleavage. **C,** WB analysis of fractions of GFP and eEF2Kca infected cells reveals successful induction of eEF2K gain-of-function and enrichment of synaptic proteins in P2 fraction. At DIV 20, total lysates (TL), nuclear fractions (P1), and crude synapotosomal fractions (P2) were analyzed by WB for peEF2, eEF2K, GFP, and NLGN1 **D + E,** Quantifications of band intensities of B and C, respectively (NLGN1, GFP, and eEF2K quantification not shown). Band intensity is normalized by actin. For B a Caspase-3 cleavage quotient was calculated (17 kDa band intensity of Caspase-3 corresponding to cleaved protein was devided by 35kDa band intensity corresponding to full length protein). Vertical axis shows the mean fold change vs. uninfected cells or GFP, TL, respectively (uninfected cells or GFP, TL set to a value of 1). Error bars are SEMs. At least four independent experiments were performed per condition. **, and *** $p < 0.01$, and 0.001 versus GFP, TL. §§, and §§§ $p < 0.01$, and 0.001 versus GFP, P1. #, ##, and ### $p < 0.05$, 0.01, and 0.001 versus GFP, P2 (ANOVA and post hoc Tukey test).

Regulation by eEF2K	Weighted Mean Ratio (eEF2Kca/ GFP)	SD of Weighted Mean Ratios	Protein Name	Common Name/ Abbreviation	Uniprot Accession Code
↑	1.38	0.04	Tripartite motif-containing protein 3; Brain-expressed RING finger protein; RING finger protein 22	Trim3;Berp;Rnf22	D4A8U3;O70277
↑	1.40	0.07	CDK108;Mu-crystallin homolog	Crym	Q9QYU4
↑	1.41	0.10	MAP1 light chain LC1;Microtubule-associated protein 1B;Neuraxin	MAP1b	F1LRL9;P15205
↑	2.23	0.25	Elongation factor 2	eEF2	P05197
↓	0.39	0.01	H1d;Histone H1.2	H1f2;Hist1h1c	P15865
↓	0.61	0.03	Serine hydroxymethyltrans-ferase	Shmt2	Q5U3Z7
↓	0.28	0.03	Putative uncharacterized protein ENSRNOP00000042464;Putative uncharacterized protein Hist1h2bm;Putative uncharacterized protein Hist1h2bn;RCG23099;Putative uncharacterized protein Hist1h2bp;Putative uncharacterized protein Hist1h2bb;Histone H2B type 1;Putative uncharacterized protein Hist3h2ba;RCG34360;Putative uncharacterized protein Hist2h2be	Hist1h2bm;Hist1h2bn;rCG_23099;Hist1h2bp;Hist1h2bb;Hist3h2ba;rCG_34360;Hist2h2be	D4A817;D4ABS3;D3ZNH4;D3ZLY9;F1LS18;D3Z8U0;D3ZWM5;Q00715;F1LP73;D3ZNZ9;D3ZZP9
↓	0.23	0.03	Histone H4;Osteogenic growth peptide	H4ft;Hist1h4b;Hist1h4m;Hist4;Hist4h4	P62804

↓	0.23	0.03	Histone H3;Putative uncharacterized protein Hist1h3f;Putative uncharacterized protein Hist2h3c2;Putative uncharacterized protein LOC684762;RCG45187;RCG45215;RCG51970;Putative uncharacterized protein ENSRNOP00000060626;Putative uncharacterized protein ENSRNOP00000008328;Histone H3.3;Histone H3.1;Putative uncharacterized protein LOC691496;RCG33140;Putative uncharacterized protein ENSRNOP00000051699	H3f3b;Hist1h3f;Hist2h3c2;LOC684762;rCG_45187;rCG_45215;rCG_51970;H3.3b;LOC691496;rCG_33140	B0BMY8;D3ZJ08;D3ZK97;D3ZQN4;P84245;Q6LED0;D4A0P4;D3ZVW5
↓	0.24	0.03	Putative uncharacterized protein Hist1h1b;RCG23067	Hist1h1b;rCG_23067	D3ZBN0
↓	0.35	0.04	Putative uncharacterized protein LOC685909;RCG35761, isoform CRA_b;Histone H2A.Z	LOC685909;rCG_35761;H2afz;H2az	D4AEC0;P0C0S7;D4A7X2
↓	0.59	0.04	ICD-M;IDP;Isocitrate dehydrogenase [NADP], mitochondrial;NADP(+)-specific ICDH;Oxalosuccinate decarboxylase	Idh2	P56574
↓	0.34	0.05	Histone H2A type 1;Histone H2A type 2-A;Histone H2A.2;Putative uncharacterized protein Hist2h2ac;RCG51861	Hist2h2aa3;Hist2h2ac;rCG_51861	P02262;P0CC09;D4ACV3
↓	0.65	0.06	Putative uncharacterized protein Maoa;Amine oxidase [flavin-containing] A;Monoamine oxidase type A	Maoa	D3ZFS8;P21396
↓	0.34	0.06	Putative uncharacterized protein 682318;RCG23057;Putative uncharacterized protein ENSRNOP00000051151;Histone H2A type 1-C;Histone H2A type 1-E;Histone H2A type 4;Histone H2A, testis;Histone H2A type 1-F;Histone H2A type 3;Histone H2A;Histone H2A.J;Putative uncharacterized protein H2afx;RCG57928	682318;rCG_23057;RGD1564767;H2afj;H2afx;rCG_57928	D3ZVK7;D3ZZ29;P0C169;P0C170;Q00728;Q64598;Q4FZT6;Q6I8Q6;A9UMV8;D3ZXP3
↓	0.66	0.08	Ornithine aminotransferase, mitochondrial;Ornithine--oxo-acid aminotransferase	Oat	P04182
↓	0.54	0.09	Putative uncharacterized protein;Putative uncharacterized protein Sfrs3;RCG61099, isoform CRA_b	Sfrs3;Sfrs3_predicted;rCG_61099	Q0ZFS8;D3ZL34
↓	0.51	0.10	Core histone macro-H2A.1;H2A.y;H2A/y;Putative uncharacterized protein H2afy	H2afy	F1LR17;Q02874;D3ZKI7;Q02874-2;D3ZZ57
↓	0.67	0.11	Chromosome segregation 1-like (S. cerevisiae) (Predicted);Putative uncharacterized protein Cse1l	Cse1l;Cse1l_predicted;rCG_32309	D3ZPR0
↓	0.62	0.12	AIR carboxylase;Multifunctional protein ADE2;Phosphoribosylaminoimidazole carboxylase;Phosphoribosylaminoimidazole-succinocarboxamide synthase;SAICAR synthetase;Putative uncharacterized protein Paics	Ade2;Airc;Paics	P51583;D4A763
↓	0.64	0.14	Putative uncharacterized protein Actbl2;Similar to cytoplasmic beta-actin (Predicted)	Actbl2;rCG_44795;RGD1309504_predicted	D3ZRN3
↓	0.52	0.14	Acyl-CoA synthetase family member 2, mitochondrial	Acsf2	Q499N5
↓	0.61	0.14	Aldehyde dehydrogenase, mitochondrial;ALDH class 2;ALDH1;ALDH-E2	Aldh2	P11884;F1LN88
↓	0.48	0.14	Glial fibrillary acidic protein	Gfap	F1LSI8;P47819;P47819-2
↓	0.25	0.16	Glycogen phosphorylase, muscle form;Myophosphorylase	Pygm	P09812
↓	0.67	0.16	3,2-trans-enoyl-CoA isomerase, mitochondrial;Delta(3),Delta(2)-enoyl-CoA isomerase;Dodecenoyl-CoA isomerase;Dodecenoyl-coenzyme A delta isomerase;Dodecenoyl-Coenzyme A delta isomerase (3,2 trans-enoyl-Coenzyme A isomerase)	Dci;rCG_33892	P23965;Q68G41
↓	0.45	0.17	Putative uncharacterized protein RGD1563668;Amphoterin;Heparin-binding protein p30;High mobility group protein 1;High mobility group protein B1;Putative uncharacterized protein Hmg1l1;RCG50935;Putative uncharacterized protein RGD1560584;Putative uncharacterized protein ENSRNOP00000045117;Putative uncharacterized protein ENSRNOP00000041486;Putative uncharacterized protein ENSRNOP00000043786;Putative uncharacterized protein	RGD1563668;Hmg1;Hmg-1;Hmgb1;Hmg1l1;rCG_50935;RGD1560584;Hmgb1-ps3	D3ZL49;F1MA29;P63159;D3ZCR3;D3ZXR5;D4A9T3;D3ZLG3;D3Z7Z9;F1LTL3;F1LNG6;D3ZLA7;D3ZYR6;D3ZJN6;D3Z8A3;D3ZWY0;

			ENSRNOP00000046511;Putative uncharacterized protein ENSRNOP00000044633;Putative uncharacterized protein ENSRNOP00000046375;Putative uncharacterized protein ENSRNOP00000062422;Putative uncharacterized protein ENSRNOP00000063848;Putative uncharacterized protein ENSRNOP00000050063;Putative uncharacterized protein ENSRNOP00000048413;Putative uncharacterized protein ENSRNOP00000055435;Putative uncharacterized protein ENSRNOP00000044484;Putative uncharacterized protein ENSRNOP00000063563;Putative uncharacterized protein ENSRNOP00000061953;Putative uncharacterized protein Hmgb1-ps3;Putative uncharacterized protein ENSRNOP00000038289;Putative uncharacterized protein ENSRNOP00000042728;Putative uncharacterized protein ENSRNOP00000039114;Putative uncharacterized protein ENSRNOP00000051063		D3ZA18;D3ZFH8;D3ZC69;D3ZXP6;D3ZZD8;D4A2L7;D3ZGW6;D4AEI9;D4A4X8;D3ZMK0;F1LXZ8;F1LTK2;D3ZRY5
↓	0.60	0.18	Vimentin	Vim	P31000
↓	0.37	0.18	Putatuive uncharacterized protein Cask	Cask	D4A5M4
↓	0.63	0.18	2,4-dienoyl-CoA reductase [NADPH];2,4-dienoyl-CoA reductase, mitochondrial	Decr;Decr1	Q64591
↓	0.69	0.18	Sideroflexin-5;Tricarboxylate carrier BBG-TCC;Putative uncharacterized protein ENSRNOP00000054347	Sfxn5	Q8CFD0;D4A441
↓	0.25	0.18	Eukaryotic translation initiation factor 5;Putative uncharacterized protein ENSRNOP00000045192;Putative uncharacterized protein RGD1564400	Eif5;RGD1564400	Q07205;D4AEA4;D3ZRG2
↓	0.76	0.19			E9PTV2
↓	0.65	0.21	Rhodanese;Thiosulfate sulfurtransferase;Putative uncharacterized protein Tst	Tst	P24329;D3ZF47
↓	0.58	0.22	Glypican 4	Gpc4	Q642B0

Table 1: List of eEF2K-regulated proteins in crude synaptosomal fractions. The mass spectrometry analysis was applied to three independent experiments and successfully identified about 1100 proteins in the P2 fractions in each round. Then, MaxQuant ver.1.1.1.36 and Perseus were used to highlight proteins whose relative quantity strongly changed in eEF2Kca. For this analysis, four different parameters were utilized: 1. weighted mean ratio (eEF2Kca/GFP) of the protein exhibited the same sign (<> 1) in all experiments; 2. the weighted mean ratio was significant in at least two experiments (significance evaluated by Benjamini-Hochberg FDR < 5%); 3. the ratio count of the peptide was greater than 1 (minimum Ratio Count = 2); 4. SD of weighted mean ratio did not exceed 0.25. The analysis revealed 4 up- and 32 downregulated proteins (ratio of eEF2Kca to GFP greater and smaller than one, respectively). The list is ordered by up- and downregulated proteins and SD of the weighted mean ratio.

Regulation by eEF2K	Ratio (eEF2Kca/GFP), experiment 1	Ratio (eEF2Kca/GFP), experiment 2	Ratio (eEF2Kca/GFP), experiment 3	Protein Name	Abbreviation	Uniprot Accession Code
↑	1.41	1.40	1.33	Tripartite motif-containing protein 3	TRIM3	D4A8U3
↑	1.39	1.32	1.53	Microtubule-associated protein 1B	MAP1b	F1LRL9, P15205
↑	2.31	2.44	1.95	Elongation factor 2	eEF2	P05197
↓	0.76	0.74	0.77	Synapsin-2a; Synapsin-2b	Syn2a; Syn2b	Q63537; Q63537-2
↓	0.71	0.78	0.85	Synaptotagmin-1	Syt1	P21707
↓	0.64	0.41	X	Vesicular GABA transporter	Vgat	O35458
↓	0.24	0.50	X	Putative uncharactrized protein Cask	Cask	D4A5M4
↓	0.32	0.73	0.70	Glypican 4	Gpc4	Q642B0
=	X	1.05	1.02	Homer protein homolog 1; Homer protein homolog 1b	Homer 1; Homer 1b	Q9Z214; Q9Z214-2
=	0.96	0.99	0.91	Synaptophysin	Syp	P07825
=	X	0.92	1.00	PSD-95/SAP90-related protein 1, Synapse-associated protein 102, Disks large homolog 3	PSRP1, SAP-102, Dlg3	Q62936, Q62936-2, D4A3M2, D3ZKM1
=	1.11	1.05	1.22	Synaptobrevin-2;Vesicle-associated membrane protein 2;Cellubrevin;Synaptobrevin-3;Vesicle-associated membrane protein 3	Syb2;Vamp2;Syb3 ;Vamp3	F1LNI9;F1LRP6;P63045;P63025

Table 2: List of synaptic and presynaptic vesicle-associated proteins regulated by eEF2K. To better understand which synaptic proteins are regulated by eEF2K, we searched for proteins with well-established synaptic localization in the list of eEF2K-regulated proteins in crude synaptosomal fractions (Tab. 1). For the upregulated proteins the list therefore was reduced to eEF2, MAP1b, and TRIM-3, all of which have been described to be present at the synapse (though they are not exclusively localized to the synapses). For the downregulated proteins the list was reduced to Cask and Gpc4, both of which have a well-described presynaptic localization (though Cask is also found postsynaptically). Since this proteomic data suggested that eEF2K appears to downregulate proteins with presynaptic localization, we reviewed the raw data and found several downregulated presynaptic vesicle-associated proteins such as Syn2 (but not its family member Syn3 and only a very small downregulation of Syn1 of about 9%), SYT1 (no info on other family members since they were not identified), and VGAT. Interestingly, the revision of the raw data also showed that major postsynaptic proteins such as Homer1 were not downregulated by eEF2K. The list shows the aforementioned regulated proteins, as well as some selected non-regulated proteins (bottom part of table). The list is ordered by SD of the weighted mean ratio.

3.1.2 Protein regulation depends on eEF2K activity, does not take place at transcriptional level, and is complex

Using the same experimental framework (infection DIV 1, analysis DIV 20) without SILAC labeling we verified the quantitative changes of selected eEF2K-regulated proteins by western blotting using primary cultures of rat cortical neurons (Fig. 6 A, B). This analysis allowed us to distinguish between the P1 and P2 fraction (P1 is the complementary fraction to P2 and is therefore relatively enriched in nuclear components) and also allowed us to discern between the two Syn2 isoforms. We realized that the proteomic regulations can be whitnessed in both fractions and that actually Syn2b (and not Syn2a) levels were signficantly decreased in eEF2Kca (Fig. 6 A, B). We

also analyzed the mRNA levels of the proteins by quantitative real-time PCR and found no difference between GFP and eEF2Kca, suggesting that the proteins are not regulated at the transcriptional level (Fig. 7).

We then generated a lentivirus expressing a catalytically inactive form of eEF2K (K170M) previously described (Pigott et al., 2012; Pyr Dit Ruys et al., 2012) which preserves endogenous peEF2 levels (Fig. 8 A, C). K170M lentiviral overexpression took place in the same experimental framework in combination with either an small interference ribonucleic acid (siRNA) of eEF2K called siRNA 362 (henceforth referred to as sieEF2K), which was previously described (Verpelli et al., 2010) or with a scrambled form of this siRNA (scrambled). In parallel, an overexpression of GFP or an sieEF2K-resistant form of eEF2K (sreEF2K) was carried out, as well (Fig. 8 A). Consecutive WB analysis was mainly focused on eEF2 and MAP1B as representatives of regulated proteins. We found that both MAP1b and eEF2 upregulation does not take place in K170M (Fig. 8 A, C). Taken together, these results suggests that in hippocampal and cortical neurons the eEF2K-regulated proteins become regulated due to the catalytic activity of eEF2K and not due to changes at the transcriptional level, indicating that the observed quantitative changes are probably due to changes at the translational level.

Interestingly, we also noticed that MAP1B levels directly depend on the amount of eEF2K which is not the case for eEF2 since sieEF2K led to a downregulation of MAP1B (and was rescueable by sreEF2K) but not eEF2 (Fig. 8 A, B). This suggests that there may be different classes of proteins whose quantity changes differentially in response to a gain-of-function of eEF2K. To investigate this concept further, neurons were infected with GFP or eEF2Kca at DIV 1 or DIV 10 and analysis was carried out one week after infection (as opposed to 19 days after infection like in the principal experimental framework). We found that eEF2 upregulation only took place if the infection was at DIV 1 whereas MAP1B and peEF2 up- and Syn2b downregulation took place independently of infection time point (Fig. 9 A, B, C). This suggests that the proteomic changes induced by eEF2K overexpression probably take place within 1 week after infection. Furthermore, these results suggest that there may be proteins regulated by eEF2K which have a strict correlation with eEF2K and peEF2 levels (like MAP1b) while others (like eEF2) may be regulated in a more complex fashion.

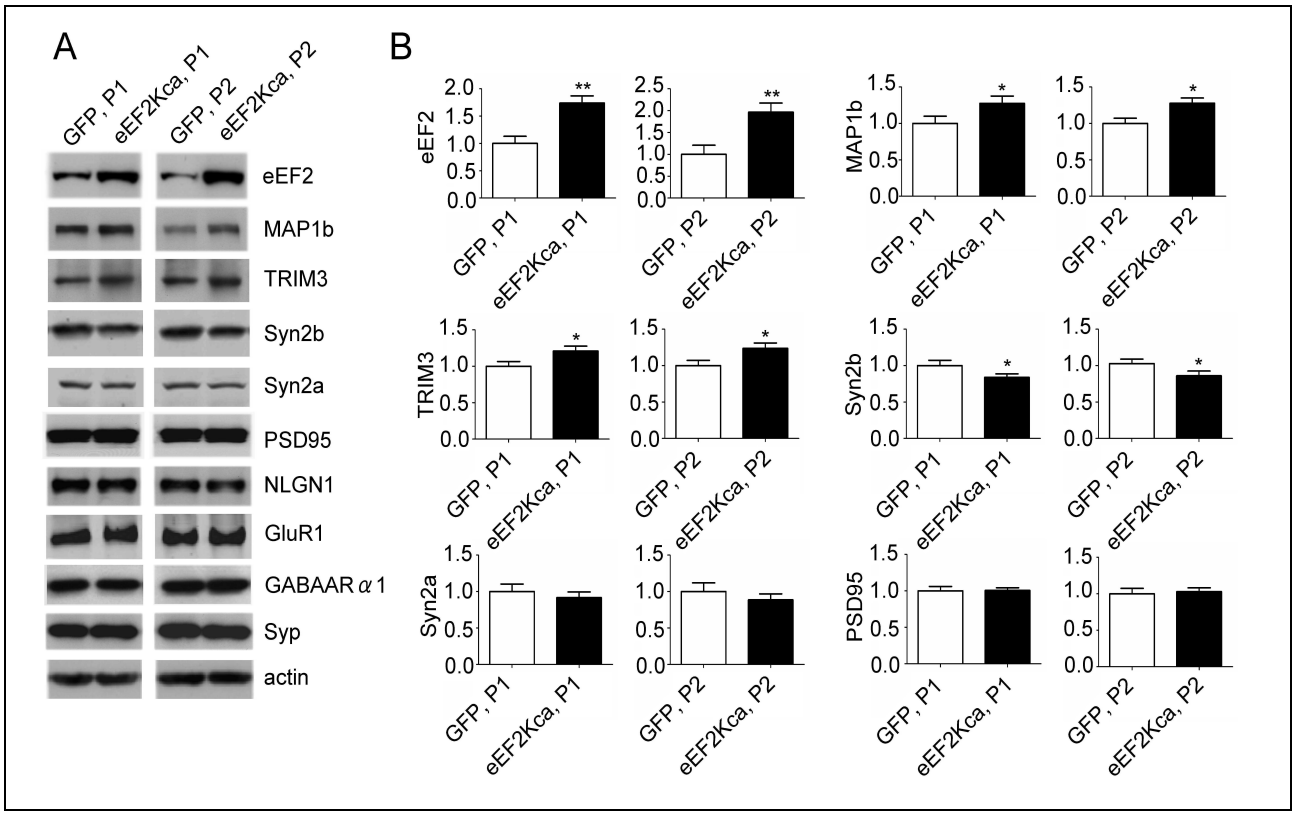

Figure 6: WB confirmation of selected eEF2K-regulated synaptic proteins. **A,** eEF2K-regulated proteins (see Tab. 2) can be verified by WB. Primary cortical rat cultures were infected with lentiviruses at DIV 1. At DIV 20, nuclear fractions (P1) and crude synaptosomal fractions (P2) were analyzed by WB for eEF2, MAP1b, TRIM3, and Syn2. Selected proteins not regulated by eEF2K (PSD95, NLGN1, GluR1, $GABA_AR\alpha1$, and Syp) are shown, as well. **B,** Quantifications of band intensities of A (only of regulated proteins and PSD95). Band intensities are normalized by actin. Vertical axis shows the mean fold change vs. GFP (GFP set to a value of 1). Error bars are SEMs. At least five independent experiments were performed per analyzed protein. * $p < 0.05$, ** $p < 0.01$ versus GFP (student's t-Test).

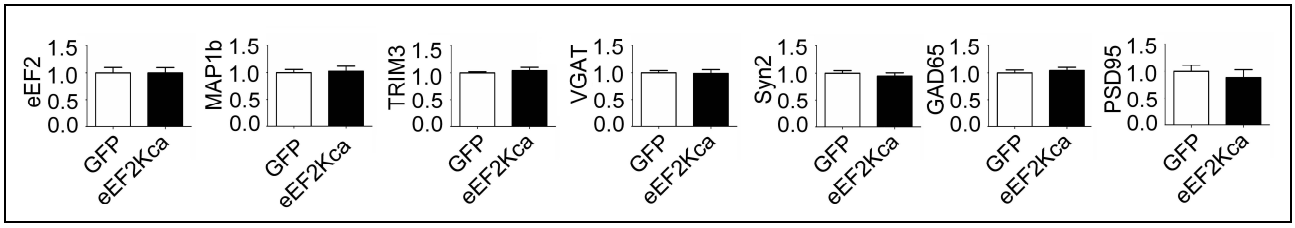

Figure 7: Quantitative RT-PCR analysis reveals that eEF2K does not regulate identified proteins at the level of transcription. Primary cortical rat cultures were infected with lentiviruses at DIV 1 with GFP or eEF2Kca. At DIV 20, lysates were analyzed by quantitative RT-PCR for selected eEF2K-regulated proteins (eEF2, MAP1, TRIM3, VGAT, Syn2, GAD65; see Fig. 11 for the regulation of GAD65) and a non-regulated protein (PSD-95). mRNA levels were standardized by GAPDH. Vertical axis shows the mean fold change vs. GFP (GFP set to a value of 1). Error bars are SEMs. Three independent experiments were performed per analyzed gene.

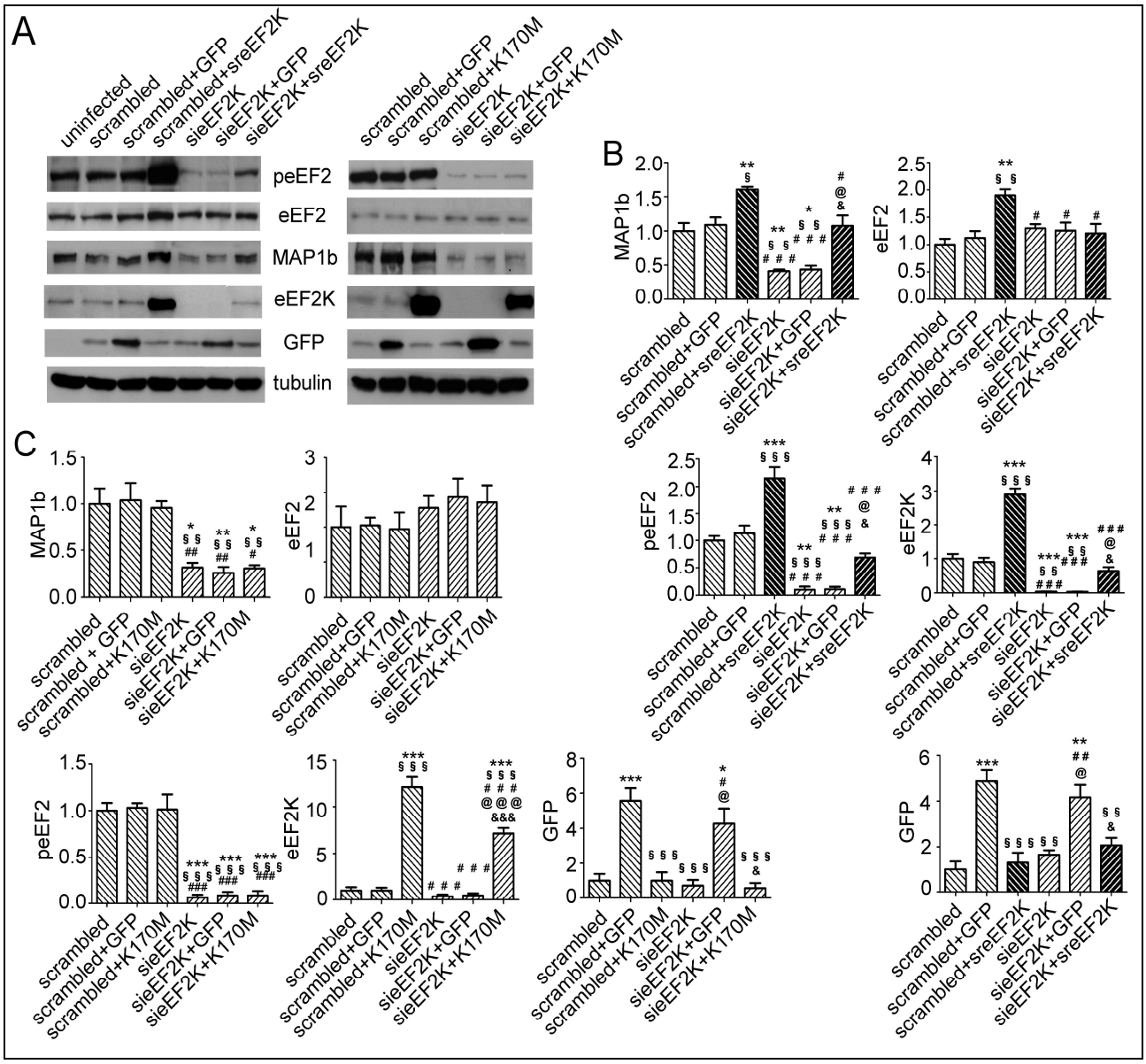

Figure 8: eEF2K activity is necessary for eEF2K-dependent protein regulation to occur but the regulation is not strictly correlated with eEF2K activity for all proteins. **A,** WB analysis reveals that eEF2K activity is essential for the regulation of eEF2 and MAP1b levels but only MAP1b levels correlate strictly with eEF2K activity. Primary cortical rat cultures were infected with lentiviruses at DIV 1 with either an siRNA for eEF2K (sieEF2K) or a scrambled siRNA (scrambled). These infections were also carried out in combination with GFP, an sieEF2K resistant form of eEF2K (sreEF2K), or a catalytically inactive form of eEF2K (K170M). At DIV 20, lysates were analyzed by WB for peEF2, eEF2, MAP1b, eEF2K, and GFP. **B + C,** Quantifications of band intensities of A. Band intensities are normalized by tubulin. Vertical axis shows the mean fold change vs. scrambled (scrambled set to a value of 1). Error bars are SEMs. At least three independent experiments were performed per condition. *, **, and *** $p < 0.05$, 0.01, and 0.001 versus scrambled. §, §§, and §§§ $p < 0.05$, 0.01, and 0.001 versus scrambled+GFP. #, ##, and ### $p < 0.05$, 0.01, and 0.001 versus scambled+sreEF2K or scrambled+K170M (B or C, respectively). @, @@, and @@@ $p < 0.05$, 0.01, and 0.001 versus sieEF2K. &, &&, and &&& $p < 0.05$, 0.01, and 0.001 versus sieEF2K+GFP (ANOVA and post hoc Tukey test).

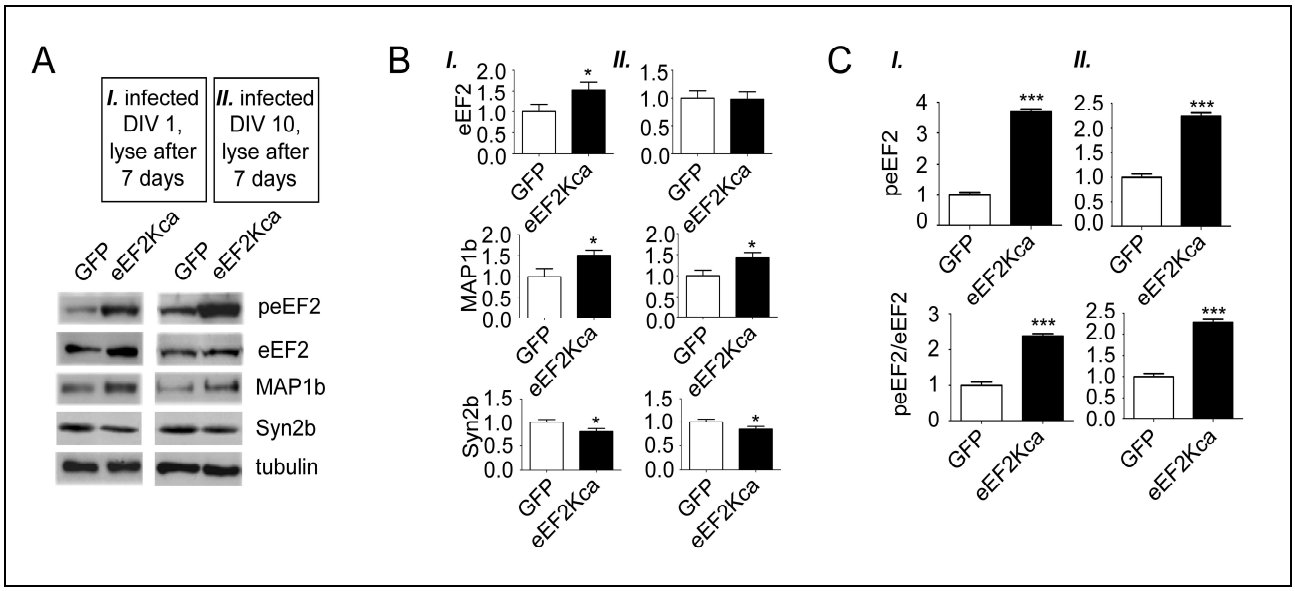

Figure 9: eEF2K-dependent protein regulation is complex. **A,** WB analysis reveals that the timepoint of eEF2Kca infection has an effect on the levels of the eEF2K-regulated proteins eEF2 and MAP1b. Primary cortical rat cultures were infected with lentiviruses at DIV 1 or DIV 10 with GFP or eEF2Kca. One week after infection, lysates were analyzed via WB for peEF2, eEF2, MAP1b, and Syn2b. **B + C,** Quantifications of band intensities of A. Band intensities are normalized by tubulin. Vertical axis shows the mean fold change vs. GFP (GFP set to a value of 1). Error bars are SEMs. * $p < 0.05$, *** $p < 0.001$ versus GFP (student's t-Test).

3.1.3 eEF2K activity downregulates puncta of presynaptic vesicle-associated proteins and is most evident at the inhibitory synapse

Since eEF2K activity downregulates the quantity of several presynaptic and presynaptic vesicle-associated proteins, we wondered whether these effects would also be reflected by a change of their distribution and/or accumulation at the presynapse. At the same time we were curious to find out if eEF2K activity has differential effects on inhibitory and excitatory synapses. To this end, we carried out an immunocytochemical analysis in the aforementioned principal experimental framework (lentiviral infection of primary cortical rat cultures at DIV 1 fixation DIV 20) where we analyzed the puncta amount and puncta size of several pre- and postsynaptic markers of the GABAergic (i.e. inhibitory) and glutamatergic (i.e. excitatory) synapse: Syn1/2 (GABAergic/glutamatergic presynapse), VGAT (GABAergic presynapse), GAD65 (GABAergic presynapse), VGLUT (glutamatergic presynapse), as well as $GABA_AR\alpha1$ (GABAergic postsynapse), GluR1 (glutamatergic postsynapse), and PSD95 (glutamatergic postsynapse) (Lee et al., 2003; Castejon et al., 2004; Tafoya et al., 2006; Bragina et al., 2007; Bethmann et al., 2008; Gitler et al., 2008). Infection was carried out with GFP, eEF2Kca, or K170M in order to have an infection control and also a control of the catalytic activity of eEF2K. Qualitatively speaking, infection efficiency was at nearly 100% (Simmons et al., 2006) and Microtubule-associated protein 2 (MAP2) stainings seemed comparable between the groups, indicating that the basic morphology and microtubular organization in the neurons (and their dendritic compartments) is unaltered by eEF2K

overexpression (Fig. 10 A) (Hendry and Bhandari, 1992; Li et al., 2000; Teng et al., 2001; Chen et al., 2012).

As expected from the proteomic results (see Fig. 6 A, B), a small but significant downregulation of both Syn1/2 puncta amount and puncta size was evident in eEF2Kca (relative to GFP and K170M). Judging by the proteomic results, our assumption is that the effect is mainly due to a downregulation Syn2b (see Tab. 2). Instead, the downregulation did not apply to costained PSD95. This suggests that eEF2K activity causes Syn1/2 molecules to be less abundant and/or less accumulated at the glutamatergic and GABAergic presynapse which, in turn, implicates functional changes in SV dynamics (Valtorta et al., 2011). This result also indicates that eEF2K activity does not have a big effect on the scaffold of the glutamatergic postsynaptic compartment (Sheng and Hoogenraad, 2007). Of notice, the (spatial) correlation of Syn1/2 and PSD95 puncta was not changed in the groups, which indicates that the basic organization of the glutamatergic synapse (namely the degree of juxtaposition of pre- and postsynapse) is unaltered by overexpressing eEF2K (Garner and Kindler, 1996; Castejon et al., 2004) (Fig. 10 B, C). Another result in line with the proteomic data is that we observed a downregulation of puncta of the vesicular GABA transporter VGAT in eEF2Kca (relative to GFP and K170M). Instead, this is not the case for the vesicular glutamate transporter VGLUT nor the postsynaptic GABAR and GluR subunits $GABA_AR\alpha1$ and GluR1, respectively (Fig. 11 E, F). This means that eEF2K activity may have a strong effect on the uptake of GABA into synaptic vesicles while not affecting GABARs/GluRs or GABAR/GluR-dependent events at the postsynaptic level which is in agreement with the results of the WB analysis (see Fig. 6 A).

Since eEF2K activity downregulates VGAT puncta, we wondered whether this would also be observed with presynaptic markers which are functionally and biochemically associated with VGAT and are therefore colocalized with it. One such marker is GAD65 (Jin et al., 2003; Tafoya et al., 2006; Zander et al., 2010), a protein which was not identified in the mass spectrometry analysis, probably due to technical limitations (Wysocki et al., 2005). GAD65 is also of particular interest for understanding whether eEF2K activity has a significant effect on the presynaptic compartment of the inhibitory synapse (and the GABA system in general for that matter), since it is an enzyme critically involved in the presynaptic synthesis of GABA (Pinal and Tobin, 1998; Tian et al., 1999; Walls et al., 2010). Additionally, GAD65 allows one to discern between inhibitory and excitatory neurons because it is accumulated in the soma of GABAergic neurons, where it is actively synthesized (Kanaani et al., 2002; Mi et al., 2002). We noticed a clear downregulation GAD65 puncta both in inhibitory and excitatory neurons. Inhibitory neurons also displayed a reduction in GAD65 puncta size and in the somatic signal of GAD65 (Fig. 11 A, B, C, D). This indicates that

eEF2Kca activity may have a strong effect on the inhibitory presynaptic compartment by downregulating GAD65 quantity and/or accumulation, thereby presumably reducing the availability of the inhibitory neurotransmitter GABA at the synapse and in SVs.

Taken together, this data indicates that eEF2K gain-of-function in primary neuronal cultures leads to a downregulation of certain presynaptic vesicle-associated markers (like Syn1/2, VGAT, and GAD65) while leaving major postsynaptic markers (like PSD95, $GABA_AR\alpha1$, and GluR1) associated with scaffolding and GABA/glutamate signalling unchanged. Therefore, eEF2K presumably does not change the general architecture or function of the postsynapse but instead probably has a strong impact on SV dynamics (and possibly SV content in the case of inhibitory presynaptic compartments). Of note, the fact that eEF2Kca only leads to a downregulation of a subset of synaptic proteins while leaving the amount of other synaptic proteins unchanged (see also Tab. 2) also indicates that the total amount of (functional) synapses is probably not altered by eEF2K activity but instead the function of each individual presynaptic compartment may very well be affected.

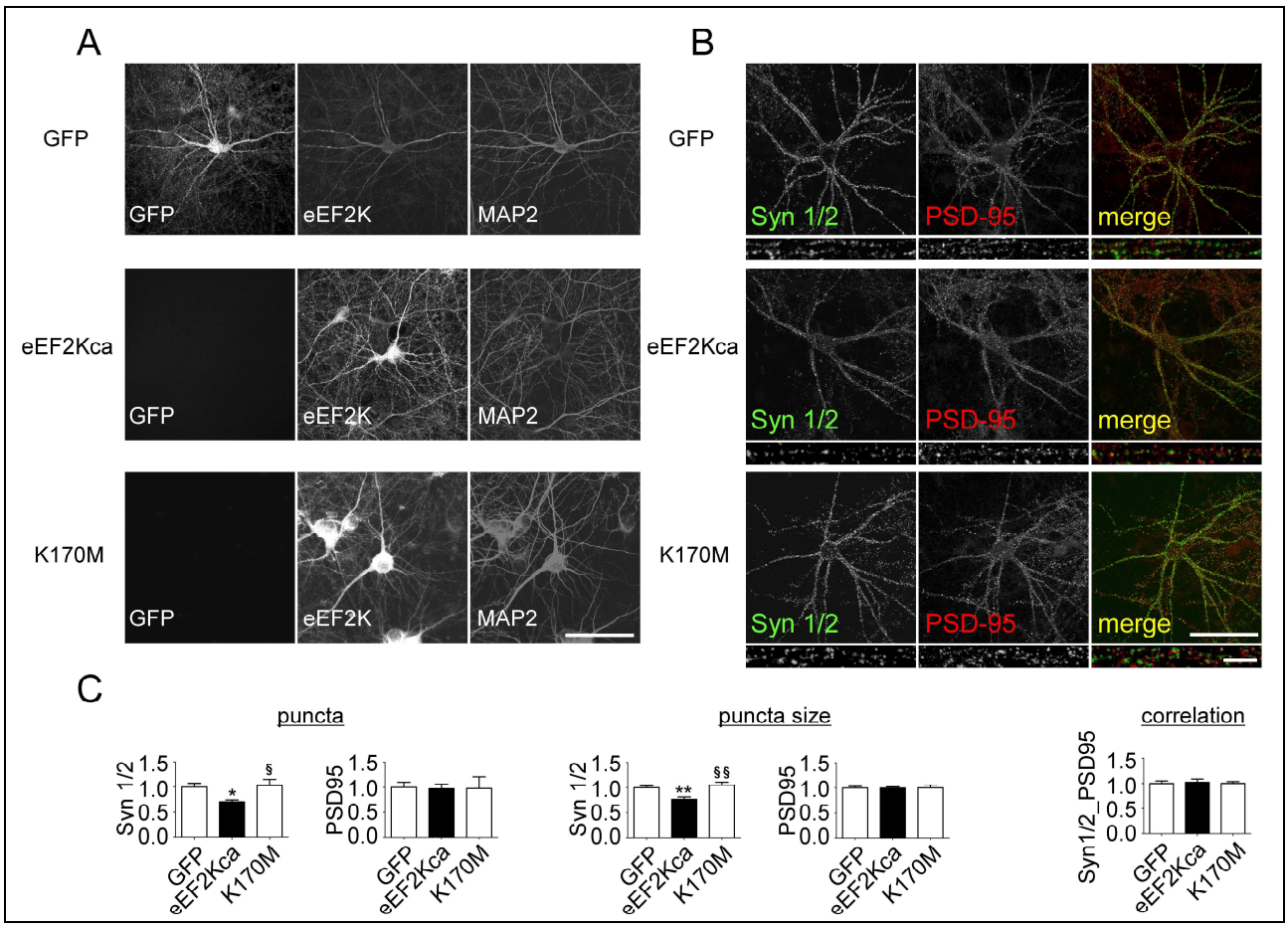

Figure 10: eEF2K activity downregulates puncta of vesicle-associated proteins of the inhibitory and excitatory presynapse but does not affect neuronal morphology, nor the basic organization of the excitatory postsynapse. **A,** High infection efficiency and comparable MAP2 stains of GFP, eEF2Kca, and K170M. Primary cortical rat cultures were infected with GFP, eEF2Kca, or K170M at DIV 1. At DIV 20 neurons were fixated and subjected to immunocytochemical analysis for eEF2K and MAP2 (costained). GFP reflects fluorescence of GFP reporter gene. Imaged neurons were selected at random. Scale bar, 100 µm. **B,** eEF2K activity leads to a reduction of Syn1/2 puncta and puncta size but does not affect PSD95 puncta, nor the correlation of Synapsin and PSD95 puncta. Primary cortical rat cultures were infected with GFP, eEF2Kca, or K170M at DIV 1. At DIV 20 neurons were fixated and subjected to immunocytochemical analysis of Syn1/2 and PSD95 (costained). Images of entire neurons and one of their (straightened, magnified) dendrites are shown. Imaged neurons were selected on the basis of prominent Syn1/2 stains. Scale bar, 100 µm. Scale bar magnified image, 10 µm. **C,** Quantifications of puncta (amount), puncta size, and correlation of markers from B (quantifications carried out on image of entire neuron). Vertical axis shows the mean fold change vs. GFP (GFP set to a value of 1). Error bars are SEMs. At least six independent experiments (on average three imaged neurons per experiment) were performed per condition. *, ** $p < 0.05$ and 0.01 versus GFP. § and §§ $p < 0.05$ and 0.01 versus eEF2Kca (ANOVA and post hoc Tukey test).

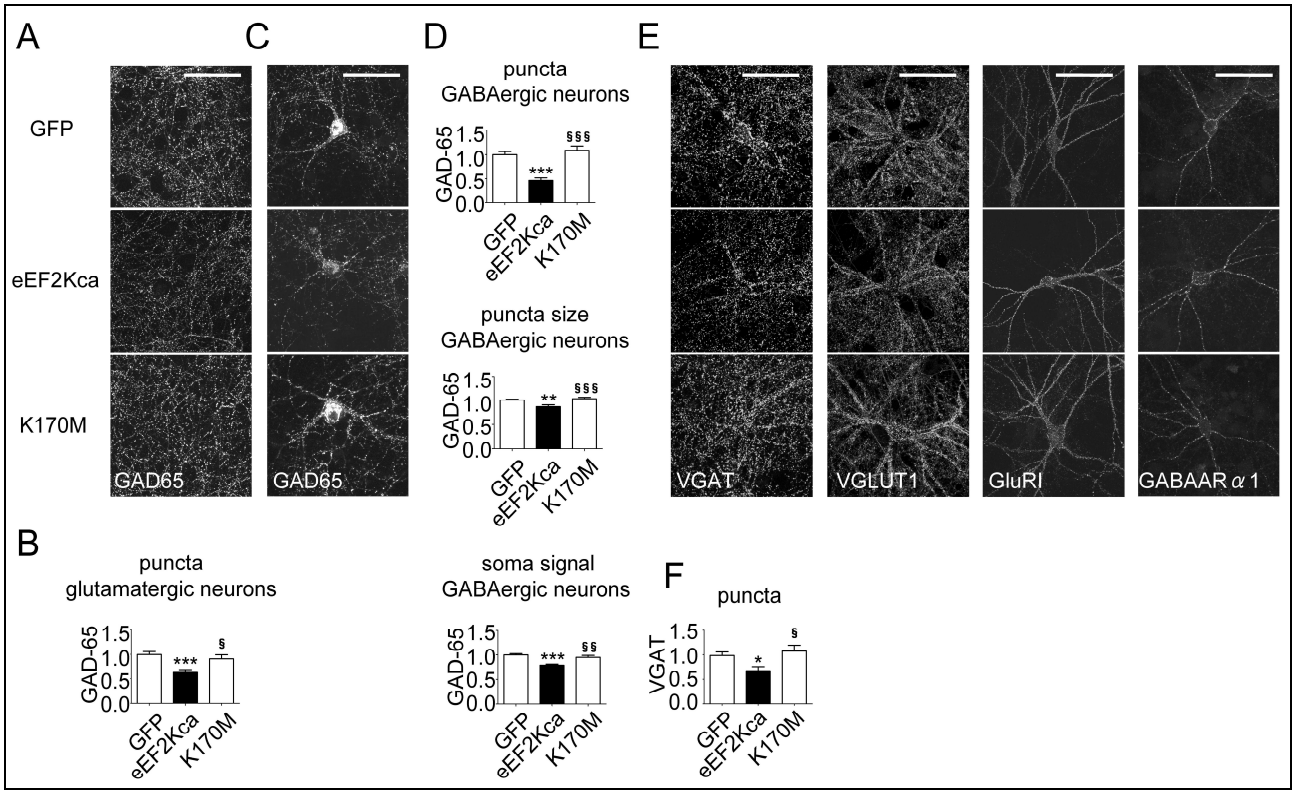

Figure 11: eEF2K activity downregulates puncta of GABA-signalling- and vesicle-associated proteins of the inhibitory presynapse but does not affect postsynaptic GABA and glutamate receptors. **A,** eEF2K activity downregulates GAD65 puncta of excitatory neurons. Primary cortical rat cultures were infected with GFP, eEF2Kca, or K170M at DIV 1. At DIV 20 neurons were fixated and subjected to immunocytochemical analysis for GAD65. Imaging was restricted to cells without prominent GAD65 signal near DAPI stain (DAPI stain not shown). Scale bar, 100 µm. **C,** eEF2K activity downregulates GAD65 puncta and puncta size of inhibitory neurons, as well as the GAD65 signal at the soma of these cells. Primary cortical rat cultures were infected with GFP, eEF2Kca, or K170M at DIV 1. At DIV 20 neurons were fixated and subjected to immunocytochemical analysis for GAD65. Imaging was restricted to cells with prominent GAD65 signal near DAPI stain (DAPI stain not shown). Scale bar, 100 µm. **E,** eEF2K activity downregulates VGAT, but not VGLUT, GluR1, nor $GABA_AR\alpha1$ puncta. Primary cortical rat cultures were infected with GFP, eEF2Kca, or K170M at DIV 1. At DIV 20 neurons were fixated and subjected to immunocytochemical analysis for VGLUT, VGAT, GluR1, and $GABA_AR\alpha1$. Imaged neurons were selected on the basis of a prominent stain. Scale bar, 100 µm. **B, D, F,** Quantifications of puncta (amount) and puncta size from A, C, and E, respectively (also quantification of soma signal for C). Vertical axis shows the mean fold change vs. GFP (GFP set to a value of 1). Error bars are SEMs. At least five independent experiments (on average three imaged neurons per experiment) were performed per condition. * and *** $p < 0.05$ and 0.001 versus GFP. § and §§ $p < 0.05$ and 0.01 versus eEF2Kca (ANOVA and post hoc Tukey test).

3.1.4 eEF2K activity downregulates vesicle release

Since our results strongly indicate that eEF2K activity downregulates presynaptic vesicle-associated proteins like Syn2b, we wanted to analyze whether this would also be reflected in functional changes of the presynaptic compartment. One of the described functions of Syns is the control of SV release (Sihra et al., 1989; Valtorta et al., 2011; Medrihan et al., 2013) so we were curious to see

if eEF2K activity downregulates vesicle release. We addressed this question with an FM-dye experiment, which gives an indication of vesicle release. It does so by the use of a fluorescent dye that binds to membranes and therefore becomes internalized into the neuron after vesicle release (which is made evident by activating the neurons) and associated endocytosis (Hering et al., 2003; He and Wu, 2007; Kim and Thayer, 2009; Saheki and De Camilli, 2012). Using a slightly modified experimental design previously described (Hering et al., 2003), we found that activated neurons release fewer vesicles in eEF2Kca than in GFP, whereas the release does not differ between GFP and K170M, indicating that eEF2K activity is responsible for a reduction of vesicle release. Of note, a separate analysis revealed that even under baseline conditions neurons release fewer vesicles in eEF2Kca than in GFP (Fig. 12 A, B).

This result means that eEF2K activity, indeed, downregulates a central function of the presynaptic compartment, namely: eEF2K appears to downregulate vesicle release, presumably via its downregulation of vesicle-associated proteins like Syn2b. This reduction of vesicle release could be either due to eEF2K activity causing a reduction in the number of functional synapses or it could be due to eEF2K activity causing a reduction in the efficacy (i.e. release probability) of each individual presynaptic compartment. Judging by our immunocytochemical and proteomic results (see Tab. 2, Fig. 6, and paragraph 3.1.3), the latter possibility is more probable.

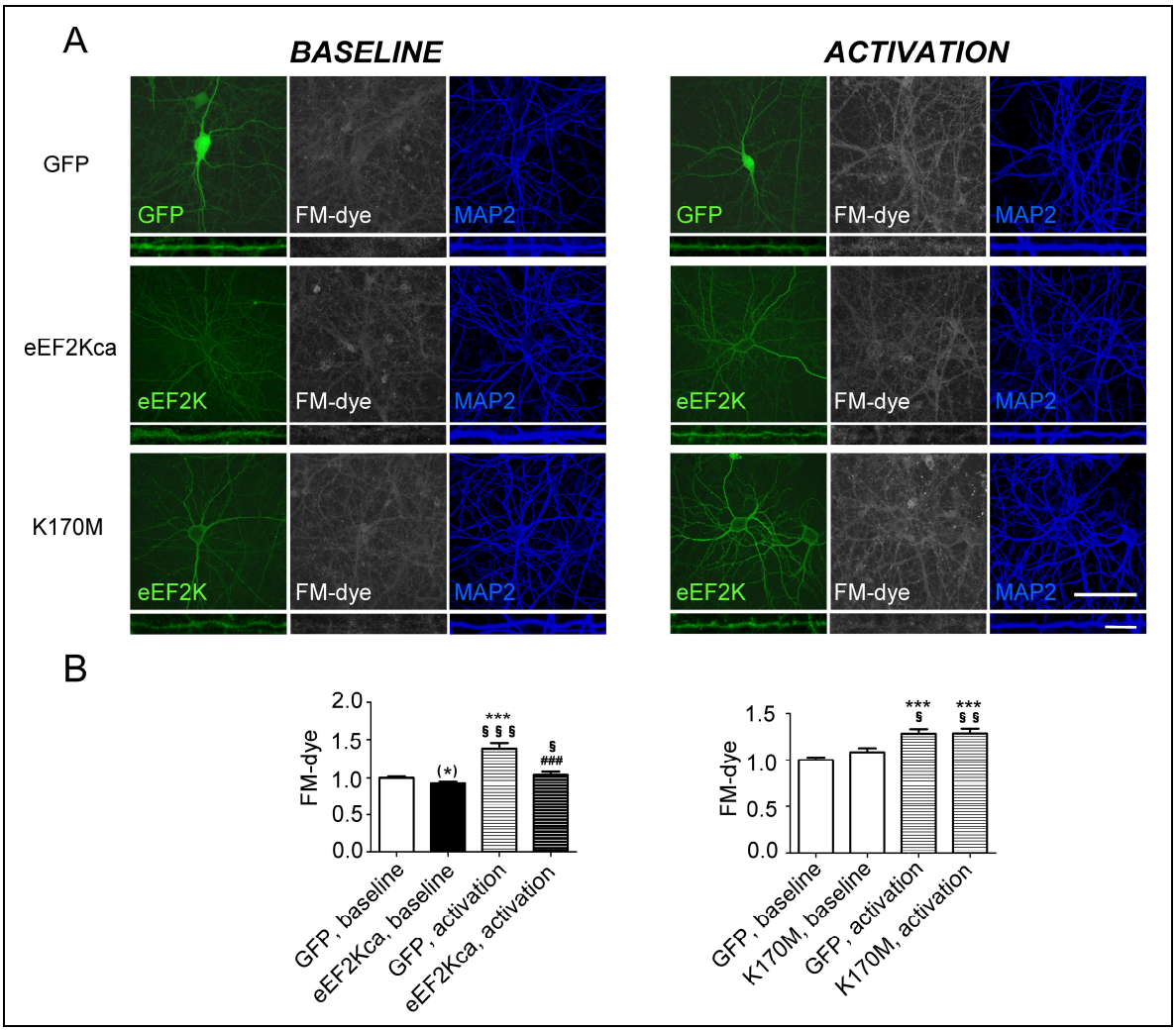

Figure 12: eEF2K activity downregulates vesicle release. **A,** eEF2K activity downregulates FM 4-64 FX dye incorporation following neuronal activation. Primary cortical rat cultures were infected with GFP, eEF2Kca, or K170M at DIV 1. At DIV 20 neurons were activated with high potassium buffer (right side of figure; "ACTIVATION") or were treated with Tyrode solution as a (non-activated) control (left side of figure; "BASELINE") (c.f. materials and methods). Neurons were then fixated and subjected to immunocytochemical analysis for MAP2. eEF2K was costained for eEF2Kca and K170M. GFP reflects fluorescence of GFP reporter gene. FM-dye reflects signal from FM 4-64 FX dye. Images of entire neurons and one of their (straightened, magnified) dendrites are shown. Imaging was restricted to cells with prominent GFP signal/ eEF2K stain. Scale bar, 100 µm. Scale bar magnified image, 10 µm**. B,** Quantification of A, mean pixel intensity of FM-dye on MAP2 mask (quantifications carried out on image of entire neuron). Vertical axis shows the mean fold change vs. GFP, baseline (GFP, baseline set to a value of 1). Error bars are SEMs. Three independent experiments (on average five imaged neurons per experiment) were performed per condition. *** $p < 0.001$ versus GFP, baseline. §, §§, and §§§ $p < 0.05$, 0.01, and 0.001 versus eEF2Kca, baseline or K170M, baseline (left or right quantification, respectively) (ANOVA and post hoc Tukey test). (*) $p < 0.05$ versus GFP, baseline (analysis only carried out for eEF2Kca, baseline and K170M, baseline) (student's t-Test).

3.1.5 eEF2K activity downregulates mPSC frequency by downregulating Syns/Syn2b and depotentiates mIPSCs

To further examine the effect of eEF2K activity on vesicle release and the functionality of the synapse, we employed electrophysiology to analyse mPSCs in the aforementioned experimental framework (infection of rat cortical neurons with GFP, eEF2Kca, or K170M at DIV 1, recording DIV 20). A change in mPSC frequency can be due to a change in vesicle release probability (or the amount of functional synapses) and is therefore usually interpreted as a change in presynaptic function. Instead, a change in mPSC decay time, amplitude, and area/charge transfer is usually

interpreted as a functional change at the postsynapse, reflecting changes in kinetics, efficacy, or quantity of receptors, though a change in mPSC amplitude/area may also reflect a reduction in the amount of released neurotransmitters (Fatt and Katz, 1952; Van der Kloot, 1991; Queenan et al., 2001; Tyler and Pozzo-Miller, 2001; Han and Stevens, 2009). Importantly, we also tested whether Syns -and the eEF2K-regulated isoform Syn2b in particular- are related to (and possibly the root cause of) eEF2K-induced changes of mPSC since there is literature indicating that changes in levels of Syn2b are related to changes in mPSCs (Gitler et al., 2008; Medrihan et al., 2013).

We found that eEF2K activity markedly reduced the frequency of mEPSCs while leaving other mEPSC parameters unaffected (Fig. 13 A, B). Interestingly, the same phenomenon was observed in mouse primary hippocampal neurons infected with GFP or eEF2Kca (Fig. 14. A, B) while no difference in mEPSC frequency was detected between GFP and eEF2Kca in neurons derived from Syn 1-3 KO (TKO) mice (Fig. 14 A, B). Worthy of note, both in wildtype and TKO primary mouse hippocampal neurons eEF2Kca induced similar proteomic changes as observed initially in rat hippocampal and cortical neurons (Fig. 15. A, B; see also Fig. 6), indicating two things: firstly, eEF2K activity has a very general effect on the synaptic proteome and presynaptic function (here: reduction of mEPSC frequency), since similar eEF2K-induced changes can be observed in rat or mouse neuronal (i.e. cortical or hippocampal) cultures; secondly, the fact that eEF2Kca does not reduce mEPSC frequency in TKO cultures cannot be explained by a TKO-specific eEF2K-dependent regulation of the proteome. These results indicate that eEF2K activity reduces mEPSC frequency by downregulating Syn levels. Importantly, we found that eEF2Kca does not reduce the frequency of mEPSCs when co-overexpressed with Syn2b (Fig. 16 A, B), indicating that eEF2K reduces mEPSC frequency by downregulating Syn2b levels.

We also found that eEF2K activity reduced the frequency of mIPSCs, however, also the decay time, area, and amplitude were markedly reduced (Fig. 13 A, B). In mouse hippocampal neurons mIPSC frequency and decay time were reduced (Fig. 14 A, B). Instead, no differences in mIPSC frequency were detected between GFP and eEF2Kca in neurons derived from TKO mice but the reduction in mIPSC decay time took place, nonetheless (Fig. 14 A, B). These results indicate that eEF2K activity reduces mIPSC frequency by downregulating synapsin levels, whereas mIPSC decay time (and possibly the other mIPSC parameters) are reduced in a synapsin-independent fashion.

Taken together, these results indicate that eEF2K activity reduces mPSC frequency and therefore probably reduces release at the excitatory and inhibitory presynapse (we exlude the possibility of a change in the amount of functional synapses, see Tab. 2, Fig. 6, and paragraph 3.1.3). This effect appears to be mediated by the downregulation of the Syn family and Syn2b in particular. Instead, eEF2K does not appear to affect the efficacy of ionotropic GluRs at the excitatory postsynapse

since mEPSC decay time, area, and amplitude are unchanged. On the contrary, eEF2K activity does appear to downregulate $GABA_AR$ kinetics/efficacy at the inhibitory postsynapse since the mIPSC decay time is downregulated and this effect presumably occurs in a Syn-independent manner. In rat cortical cultures, eEF2K activity additionally leads to a downregulation of mIPSC area and amplitude. This may reflect a downregulation of $GABA_AR$ efficacy and/or quantity but it may also reflect a downregulation of GABA in the GABAergic vesicles (see Fig. 11).

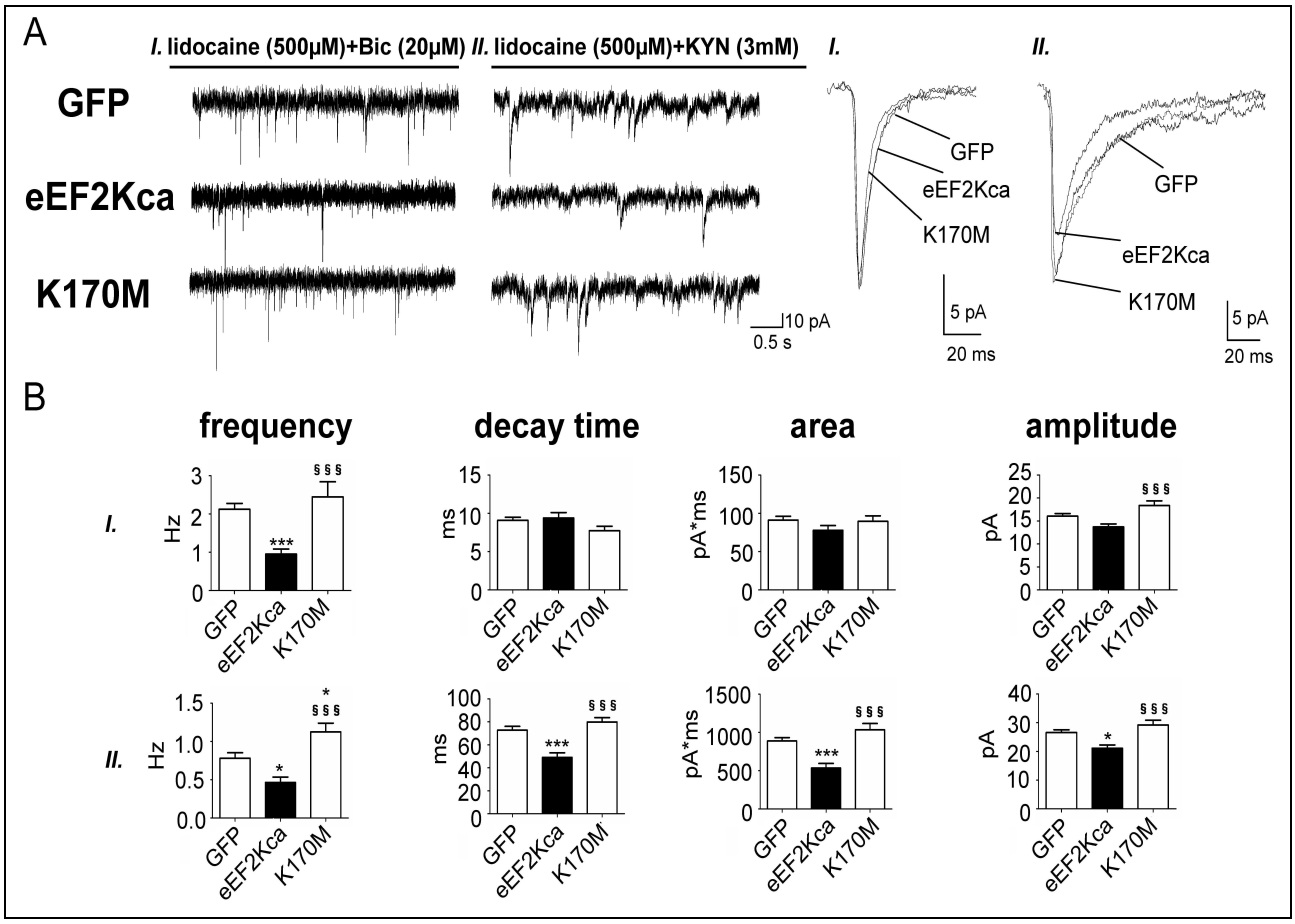

Figure 13: eEF2K activity downregulates mPSC frequency and depotentiates mIPSCs. **A,** eEF2K activity downregulates mEPSC and mIPSC frequency but also downregulates mIPSC decay time, area, and amplitude. Primary cortical rat cultures were infected with GFP, eEF2Kca, or K170M at DIV 1. At DIV 20 neurons were subjected to electrophysiological analysis of mPSCs. Neurons were chosen at random for recordings. Representative traces of mEPSCs (*I.*) and mIPSCs (*II.*) are shown for GFP, eEF2Kca, and K170M **B,** Quantification of A. Vertical axis shows Hz (for frequency), ms (for decay time), pA*ms (for area), and pA (for amplitude). Error bars are SEMs. Three independent experiments (on average seven recorded neurons per experiment) were performed per condition. * and *** $p < 0.05$ and 0.001 versus GFP. §§§ $p < 0.001$ versus eEF2Kca (ANOVA and post hoc Tukey test).

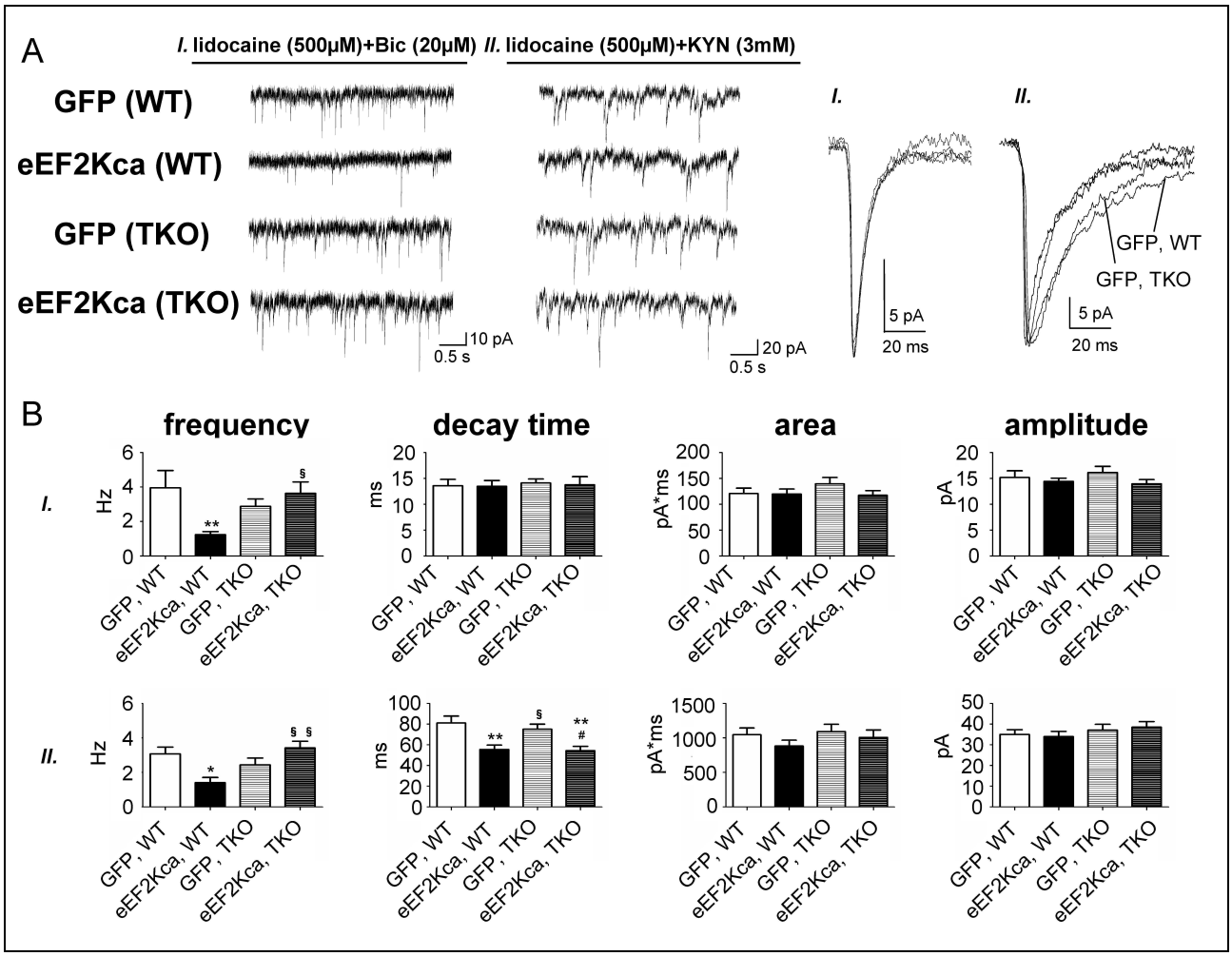

Figure 14: eEF2K-dependent mPSC frequency downregulation is Syn-dependent but the mIPSC depotentiation is not. **A,** eEF2K downregulates mEPSC and mIPSC frequency but also downregulates mIPSC decay time. Primary hippocampal mouse cultures (WT and TKO) were infected with GFP or eEF2Kca at DIV 1. At DIV 20 neurons were subjected to electrophysiological analysis of mPSCs. Neurons were chosen at random for recordings. Representative traces of mEPSCs (*I.*) and mIPSCs (*II.*) are shown for GFP, WT/TKO and eEF2Kca, WT/TKO **B,** Quantification of A. Vertical axis shows Hz (for frequency), ms (for decay time), pA*ms (for area), and pA (for amplitude). Error bars are SEMs. Three independent experiments (on average six recorded neurons per experiment) were performed per condition. * and ** $p < 0.05$ and 0.01 versus GFP, WT. § and §§ $p < 0.05$ and 0.01 versus eEF2Kca, WT. # $p < 0.05$ versus GFP, TKO (ANOVA and post hoc Tukey test).

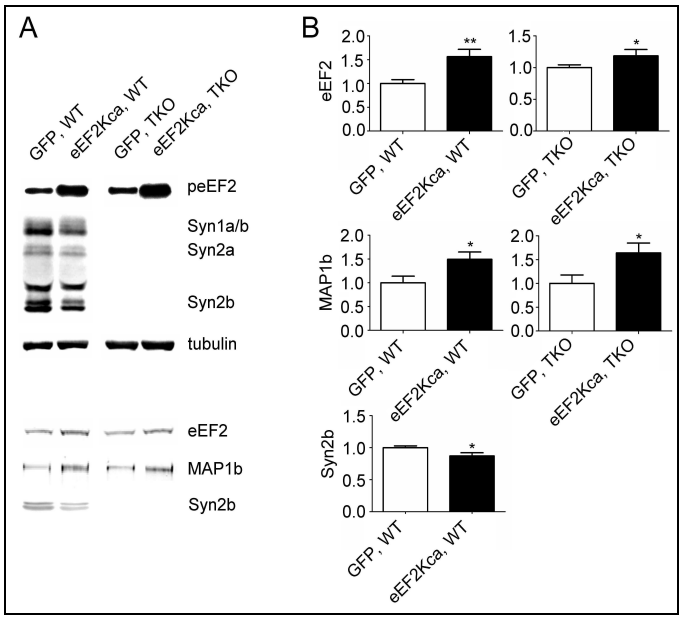

Figure 15: eEF2K overexpression induces similar proteomic changes in WT and TKO hippocampal mouse cultures as in rat cortical/hippocampal cultures. **A,** WB analysis reveals that eEF2Kca induces an upregulation of eEF2 and MAP1b while downregulating Syn2b. Primary hippocampal mouse cultures (WT and TKO) were infected with lentiviruses at DIV 1 with GFP or eEF2Kca. At DIV 20, lysates were analyzed via WB for peEF2, Syn, eEF2, MAP1b, and Syn2b. **B,** Quantifications of band intensities of A. Band intensities are normalized by tubulin. Vertical axis shows the mean fold change vs. GFP WT/TKO (GFP WT/TKO set to a value of 1). Error bars are SEMs. Three independent experiments were performed per condition. * and ** $p < 0.05$, and 0.01 versus GFP WT/TKO (student's t-Test).

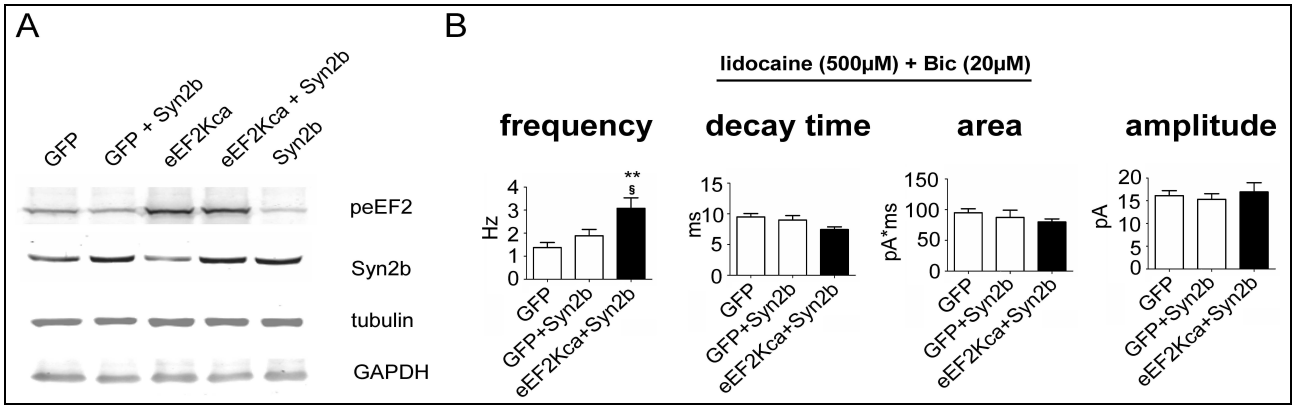

Figure 16: eEF2K reduces mEPSC frequency via Syn2b. **A,** Syn2b co-overexpression with GFP or eEF2Kca is comparable in terms of observed Syn2b levels. Primary cortical rat cultures were infected with GFP alone, GFP and Syn2b, eEF2Kca alone, eEF2Kca and Syn2b, or Syn2b alone at DIV 1. At DIV 20 neurons were analyzed by WB for peEF2 or Syn2b (quantification not shown). **B,** Syn2b co-overexpression can rescue eEF2K-mediated mEPSC frequency downregulation. Primary cortical rat cultures were infected with GFP alone, GFP and Syn2b, or eEF2Kca and Syn2b at DIV 1. At DIV 20 neurons were subjected to electrophysiological analysis of mEPSCs. Neurons were chosen at random for recording. Quantifications (but not representative traces) are shown. Vertical axis shows Hz (for frequency), ms (for decay time), pA*ms (for area), and pA (for amplitude). Error bars are SEMs. Three independent experiments (on average four recorded neurons per experiment) were performed per condition. ** $p < 0.01$ versus GFP. § < 0.05 versus GFP and Syn2b (ANOVA and post hoc Tukey test).

3.2 eEF2K loss-of-function *in vivo* and *ex vivo* (eEF2K-KO mice and slices thereof)

3.2.1 eEF2K-KO mice exhibit increased Syn2b expression levels

To examine correlates of our *in vitro* results *in vivo/ex vivo* we chose to examine previously described eEF2K-KO mice (Ryazanov, 2002), i.e. we chose a chronic loss-of-function design in which we expected opposite effects of the (chronic) gain-of-function experiments *in vitro*. Genetic deletion of eEF2K activity *in vivo* causes no obvious phenotypes in mice (normal weight and behaviour, normal baseline brain activity levels and excitatory transmission, intact incidental learning) despite a profound reduction in peEF2 levels, though there is literature demonstrating impairments in synaptic plasticity and associative learning (Ryazanov, 2002; Park et al., 2008; Gildish et al., 2012; Nosyreva et al., 2013). Of note, there are also publications which show that the eEF2K/eEF2 pathway is involved in stress-responses both *in vitro* and *in vivo* (Dorovkov et al., 2002; Dagestad et al., 2006; Autry et al., 2011; Gronli et al., 2012; Nosyreva et al., 2013), suggesting that eEF2K-KO mice may exhibit altered responses to stressful events, which could be due to changes in the GABAergic transmission (Griebel and Holmes, 2013).

We started our *in vivo* analysis by looking at proteomic changes in eEF2K-KO mice and focused our attention on three proteins that were regulated by eEF2K *in vitro*: eEF2, MAP1b, and Syn2b. We analyzed cortical P2 fractions and P2 fractions of brain slices containing the hippocampus that were used for electrophysiological analysis (see paragraph 3.2.2). In line with published data, quantitative WB analysis revealed a profound downregulation of peEF2 levels in eEF2K-KO mice relative to WT littermates, indicating that eEF2K activity is, indeed, abolished in the KO mice (Fig. 17 A). Importantly, a small but significant upregulation of Syn2b levels was observed (Fig. 17 A, B). The analysis of eEF2 or MAP1b levels revealed no difference between eEF2K-KO mice and their WT littermates (data not shown). These results indicate that eEF2K activity negatively regulates Syn2b expression levels not only *in vitro* (see paragraph 3.1.2) but also *in vivo*. Instead, eEF2K activity does not appear to regulate expression levels of eEF2 or MAP1b *in vivo*, the former of which has also been observed by other groups working on eEF2K-KO mice (Park et al., 2008). This indicates that eEF2K activity may regulate some- but not all- proteins similarly *in vitro* and *in vivo*.

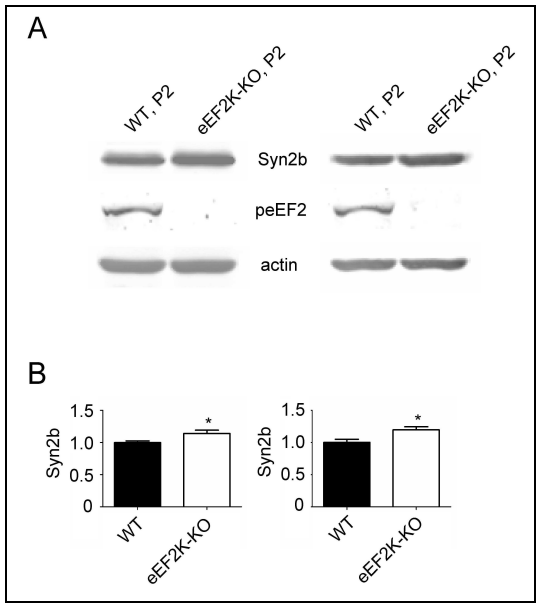

Figure 17: eEF2K-KO mice have increased Syn2b levels. **A,** WB analysis reveals abolished peEF2 and increased Syn2b levels in eEF2K-KO mice. P2 fractions of eEF2K-KO and WT littermates were prepared from cortex (left side of figure) and brain slices containing the hippocampus (right side of figure). P2 fractions were analyzed by WB for Syn2b and peEF2. **B,** Quantifications of band intensities of A. Band intensities are normalized by actin. Vertical axis shows the mean fold change vs. WT (WT set to a value of 1). Error bars are SEMs. At least five independent experiments were performed per condition. * $p < 0.05$ versus WT (student's t-Test).

3.2.2 eEF2K-KO mice have increased mIPSC frequency and potentiated mIPSCs

Since we saw a strong effect of eEF2K activity *in vitro* on the functionality of both the pre- and postsynaptic compartment of the hippocampal/cortical GABAergic synapse (as opposed to an effect only on the presynaptic compartment of the glutamatergic synapse; see paragraph 3.1.5), we decided to focus our attention of the electrophysiological *ex vivo* experiments on the inhibitory synapse. More specifically, we decided to analyze mIPSCs of eEF2K-KO and WT mice littermates in granule cells of the (hippocampal) dentate gyrus which have well described electrophysiological properties related to GABAergic transmission (Mody et al., 1992; Staley et al., 1992; Glykys and Mody, 2007; Liang et al., 2008; Hortnagl et al., 2013). Worthy of note, mIPSC frequency is decreased in granule cells of Syn2-KO mice which was another reason for us to look at mIPSCs because we expected an increase of mIPSC frequency in eEF2K-KO mice as they exhibit increased Syn2b levels (see Fig. 17) (Medrihan et al., 2013).

As expected, the analysis revealed a strong increase in mIPSC frequency in eEF2K-KO mice relative to WT littermates (Fig. 18 A, B). This result indicates that not only *in vitro* but also *ex vivo* eEF2K activity negatively controls vesicle release at the GABAergic synapse, even though- as mentioned before- changes in mIPSC frequency may also be related to changes in the amount of functional GABAergic synapses. As is the case *in vitro*, the change in mIPSC frequency may be mediated (at least in part) by changes in Syn2b expression levels *ex vivo*, as well (see paragraph

3.1.5 and 3.2.1), but we do not have a formal proof of this. The *ex vivo* results are also in line with the *in vitro* results because eEF2K-KO mice exhibit not only an increase in mIPSC frequency but also in amplitude (Fig. 18 A, B), suggesting that eEF2K activity either negatively regulates the efficacy and/or quantity of $GABA_A$Rs but this result could also reflect a negative control of GABA in the GABAergic vesicles. Of note, the comparison of our electrophysiological results regarding mIPSC decay time in primary hippocampal neurons and in hippocampal granule cells in eEF2K-KO mice (Fig. 18, see also paragraph 3.1.5) also indicates that eEF2K activity may have differential effects on the kinetics of $GABA_A$Rs *in vitro* and *ex vivo*.

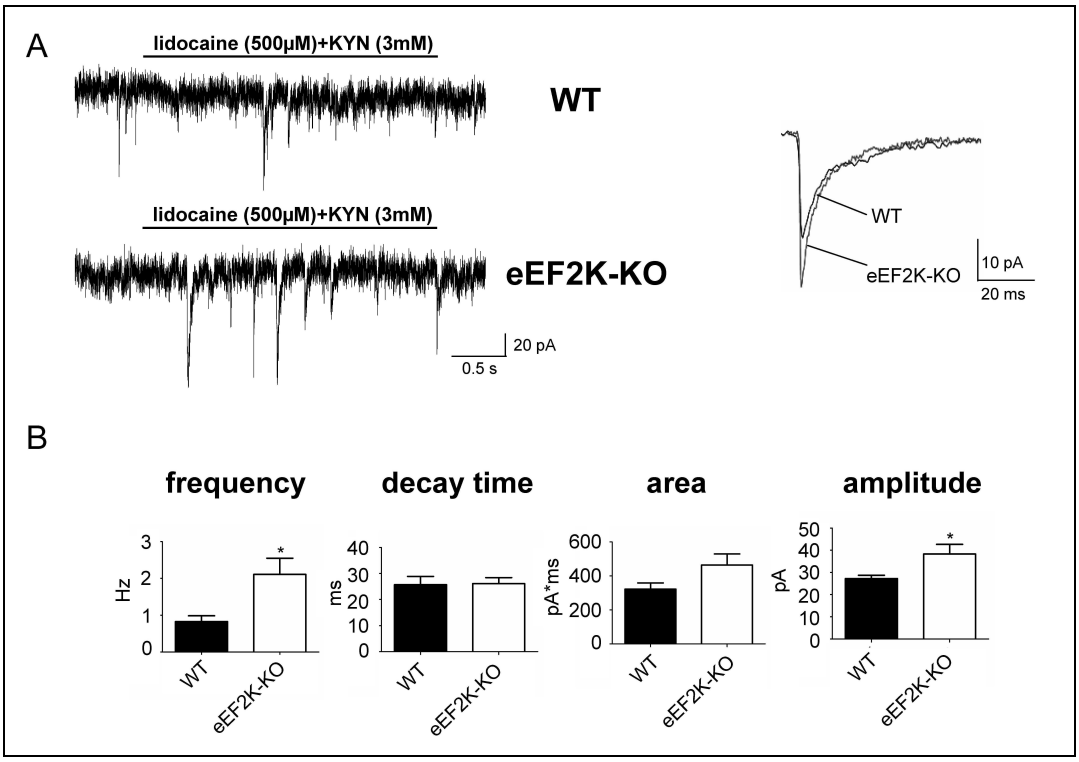

Figure 18: eEF2K-KO mice exhibit an increased mIPSC frequency and potentiated mIPSCs. **A,** Electrophysiological analysis of granule cells from (hippocampal) dentate gyrus reveals that slices from eEF2K-KO mice show an increase in mIPSC frequency and amplitude. Hippocampal slices of eEF2K-KO mice and WT littermates were prepared for electrophysiological analysis of mIPSCs in granule cells of the dentate gyrus. Representative traces of mIPSCs are shown for WT and eEF2K-KO animals. **B,** Quantification of A. Vertical axis shows Hz (for frequency), ms (for decay time), pA*ms (for area), and pA (for amplitude). Error bars are SEMs. Eleven neurons were analyzed per group. * $p < 0.05$ versus WT (student's t-Test).

3.2.3 eEF2K-KO mice present increased tonic inhibiton

In order to have a more complete understanding of how eEF2K activity may affect the GABAergic system *in vivo/ex vivo*, we decided to analyze tonic inhibition. This is a form of neuronal inibition mediated by extrasynaptic $GABA_A$R with high affinity for GABA, which are tonically activated by low concentrations of ambient/extrasynaptic GABA that presumably stems mainly from spillover of synaptically released GABA (Wei et al., 2003; Belelli et al., 2009; Egawa and Fukuda, 2013). Tonic

inhibition is clearly differentiable from the brief and intense phasic inhibition which is mediated by synaptically located $GABA_A$Rs but, importantly, has a "strong integral inhibitory force" (Egawa and Fukuda, 2013) and therefore sets the "tone" of the GABAergic system (between 75-90% of total inhibition is due to tonic inhibition, depending on the cell type and brain region) (Nusser and Mody, 2002; Scimemi et al., 2005; Belelli et al., 2009; Errington et al., 2011; Richardson et al., 2011). Again, we chose to do electrophysiological recordings of eEF2K-KO mice and WT littermates in granule cells of the (hippocampal) dentate gyrus where tonic inhibition is well-described and accounts for around 75% of total inhibition (Nusser and Mody, 2002; Wei et al., 2003; Scimemi et al., 2005; Glykys and Mody, 2007).

The experimental framework we implemented to analyze tonic inhibition represents a slight modification of an existing design (Farisello et al., 2012) which registers both phasic and tonic currents and consists of three consecutive phases (Fig. 19 A): first, GABAergic currents under relatively physiological conditions are measured (KYN), then after stimulation with saturating amounts of exogenous GABA (GABA + KYN), and lastly after blocking $GABA_A$R currents with a potent $GABA_A$R antagonist (Bic + KYN). This gives an indication of tonic inhibition due to (endogenously) released GABA and associated spillover under "baseline"/physiological conditions (measured by the current shift Bic + KYN vs. KYN) and tonic inhibition which may present itself under conditions of elevated network activity (measured by the current shift GABA + KYN vs. KYN), such as during explorative behaviour or during seizures, where GABA concentrations can vary up to fivefold (Minamoto et al., 1992; During and Spencer, 1993; Bianchi et al., 2003; Smolders et al., 2004; Scimemi et al., 2005; Bragina et al., 2008; Farisello et al., 2012). Of note, the current shift GABA + KYN vs. KYN is commonly interpreted as a change in the efficacy and/or amount of extracellular $GABA_A$Rs since GABA is given in excess (Farisello et al., 2012). Lastly, one must keep in mind that tonic currents can be influenced by the activity of GABA transporters, which reduce amount of freely diffuseable GABA, and of course also depend on the amount of GABAergic synapses (Nusser and Mody, 2002; Scimemi et al., 2005; Qi et al., 2006; Bragina et al., 2008).

Interestingly, the analysis revealed that eEF2K-KO mice show a marked increase in tonic inhibition relative to WT littermates. More specifically, the current shift GABA + KYN vs. KYN was increased, however, the current shift Bic + KYN vs. KYN was not (Fig. 19 A, B). This indicates that *ex vivo* eEF2K activity negatively regulates tonic inhibition but only when network activity is strongly increased, such as during seizures (Scimemi et al., 2005). This may be due to less efficative and/or abundant extracellular $GABA_A$Rs whose impact only becomes apparent if network activity (and associated GABA spillover) is elevated or it may be due to an increase in the activity

of GABA transporters under these conditions. Alternatively, eEF2K activity may also negatively control the number of GABAergic synapses which may cause detectable effects only under conditions of high network activity. And lastly, eEF2K activity may negatively regulate GABA release (see also paragraph 3.2.2) but this may only have a significant impact on tonic inhibiton when neurons become highly active. However, given that the current shift Bic + KYN vs. KYN is unaltered, the latter two explanations seem rather hypothetical (Farisello et al., 2012) and are (to the best of our knowledge) not backed up by a substantial amount of published data. Of note, the phasic currents (measurement of spontaneously occuring IPSCs) did not differ between eEF2K-KO and WT mice (data not shown), suggesting that eEF2K activity may actually have a stronger effect on tonic rather than on phasic inhibition *ex vivo*. This, in turn, could suggest that *ex vivo* eEF2K activity may negatively control the efficacy and/or quantity of extrasynaptic rather than synaptic $GABA_A$Rs, though our previous data also suggests an effect on synaptically located $GABA_A$Rs (see Fig. 18). Taken together with the results from paragraph 3.2.2., the data suggests that eEF2K activity regulates the functionality of the postsynaptic compartment of the GABAergic synapse not only *in vitro* but also *ex vivo*. More specifically, it appears to negatively regulate the efficacy and/or quantity of postsynaptic $GABA_A$Rs.

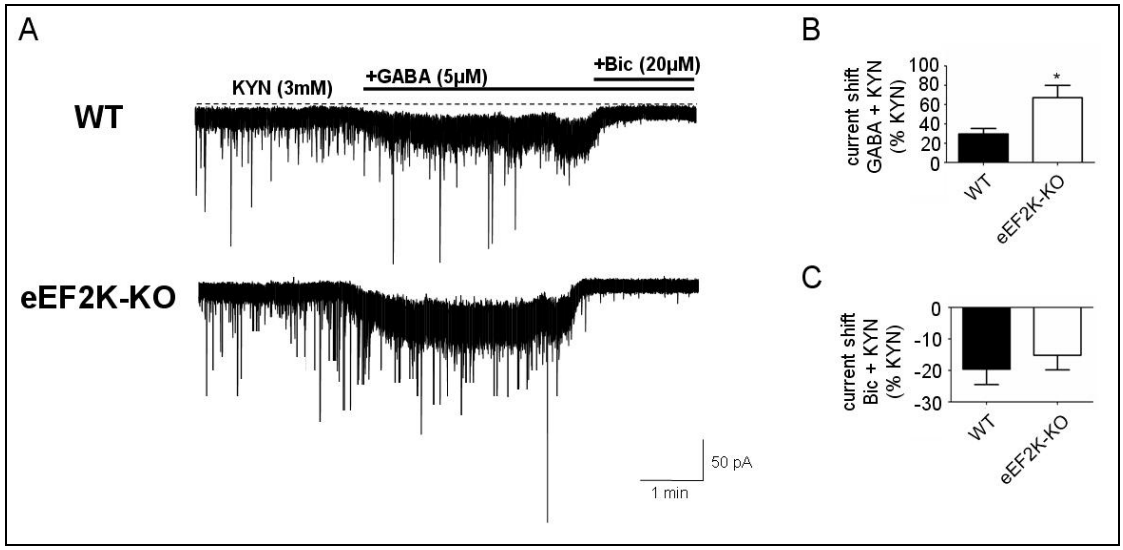

Figure 19: eEF2K-KO mice exhibit increased tonic inhibition. **A,** Electrophysiological analysis of granule cells from (hippocampal) dentate gyrus reveals that slices of eEF2K-KO mice exhibit an increased current shift from baseline when exogenous GABA is given in saturating concentrations but not under physiological conditions. Hippocampal slices of eEF2K-KO mice and WT littermates were prepared for electrophysiological analysis of GABAergic currents in granule cells of the dentate gyrus. GABAergic currents are measured during consecutive stages; first during KYN (3 mM), then during GABA (5 µM) + KYN (3 mM), and finally during Bic (20 µM) + KYN (3 mM). The dotted line represents the zero-current level. Representative traces are shown for WT and eEF2K-KO animals. **B,** Quantification of A. Vertical axis shows (tonic) GABAergic currents during GABA + KYN (as % of KYN). Error bars are SEMs. 16 neurons were analyzed per group. * $p < 0.05$ versus WT (student's t-Test). **C,** Quantification of A. Vertical axis shows (tonic) GABAergic currents during Bic + KYN (as % of KYN). Error bars are SEMs. 10-13 neurons were analyzed per group.

3.2.4 eEF2K-KO mice exhibit a reduced susceptibility to chemoconvulsant agents

Since we found that eEF2K-KO mice exhibit increased tonic inhibition and potentiated mIPSCs (see paragraph 3.2.2 and 3.2.3), we wanted to test if these mice show a decreased susceptibility to seizures relative to WT controls when they are challenged with convulsive substances. Indeed, there is an abundance of literature showing that the GABAergic system and associated phenomenon like tonic inhibition are causally related to seizures; e.g. many antiepileptic drugs activate the GABAergic response and a lower tonic inhibition appears to be one of the root causes of status epilepticus and seizures (Meldrum and Horton, 1980; Czuczwar, 1999; Mohler et al., 2002; Kobayashi and Buckmaster, 2003; Richerson, 2004; Klitgaard, 2005; Glykys and Mody, 2006; Farisello et al., 2012; Houser et al., 2012; Joshi and Kapur, 2012). Thus, we formulated the hypothesis that the absence of eEF2K activity should decrease the propensity for the development of seizures.

We, therefore, chose to induce seizures by PTZ and pilocarpine in eEF2K-KO and WT mice while carrying out EEG recordings and analysis as previously described (Erbayat-Altay et al., 2008; Sala et al., 2010; Corradini et al., 2012). A sub-convulsive dose of PTZ (Jelenkovic et al., 2002) and a convulsive dose of pilocarpine (Vezzani, 2009) was used, which induced myoclonic or clonic & clonic-tonic seizure responses in WT mice, respectively (Fig. 21 A, B). As expected, eEF2K-KO mice exhibited a reduced response in both conditions, showing absence seizures for the PTZ treatment and a shift towards myoclonic seizures for the pilocarpine treatment. Additionally, classically analyzed EEG parameters clearly pointed towards a protection of eEF2K-KO mice from seizures (Fig. 21 A, B). These results strongly indicate that absence of eEF2K activity is associated with a decreased propensity for seizures. Notably, neither the relative weight of the EEG frequency bands nor the spontaneously occurring EEG spikes differed between eEF2K-KO and WT mice under baseline conditions (Fig. 20), indicating that while the absence of eEF2K activity decreases the susceptibility to seizures it does not have an effect on the activity level of the brain under baseline conditions (Whittingstall and Logothetis, 2009). In line with this, preliminary behavioural experiments testing for anxiety and other stress-related parameters (data not shown) did not reveal a difference between eEF2K-KO and WT mice which is in line with previous results published by another group (Ryazanov, 2002; Nosyreva et al., 2013).

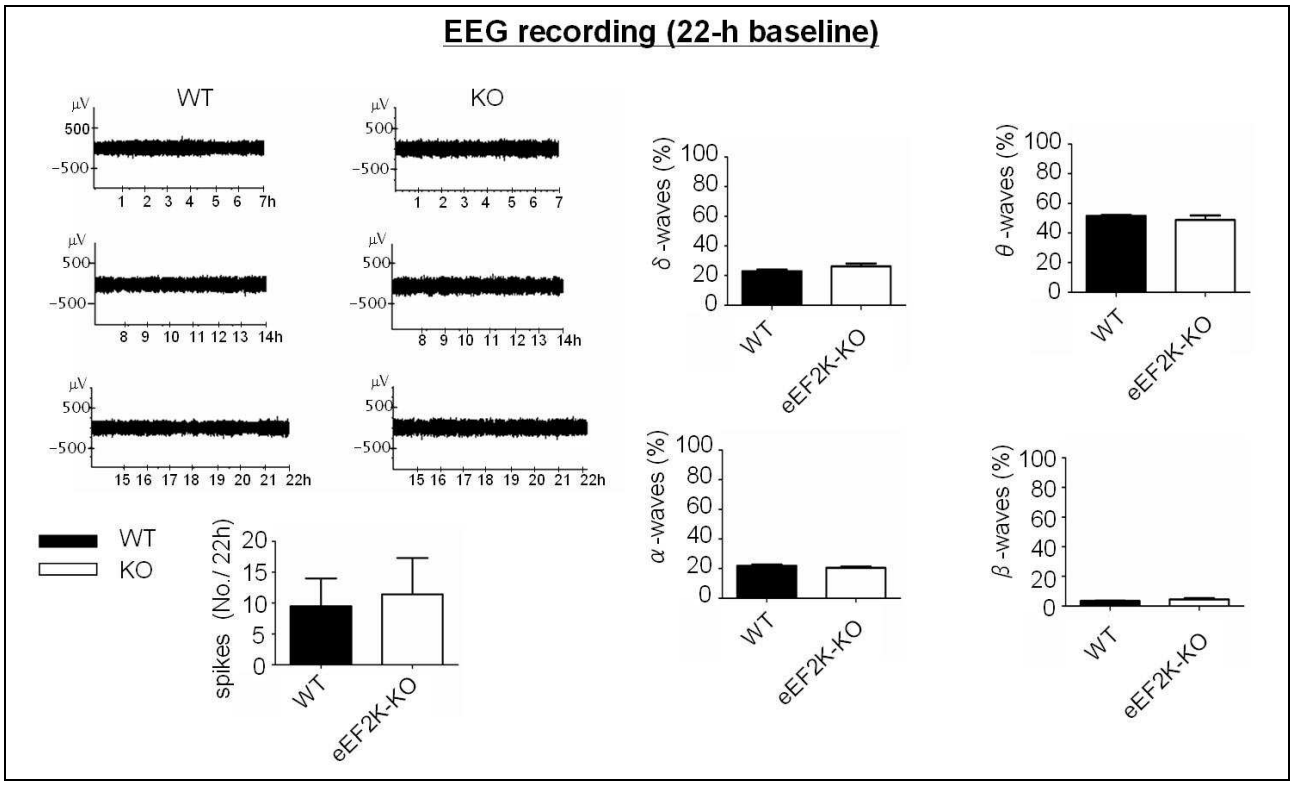

Figure 20: eEF2K-KO mice exhibit normal baseline brain activity. EEG traces of two representative mice (WT and KO) and relative analysis reveals normal brain activity under baseline conditions in both genotypes. Quantifications of EEG parameters are also shown. Vertical axis shows relative δ, θ, α, and β EEG frequency bands (% of total spectral power) and No. of EEG spikes per 22 hours. Error bars are SEMs. N= 11 WT and N = 7 KO.

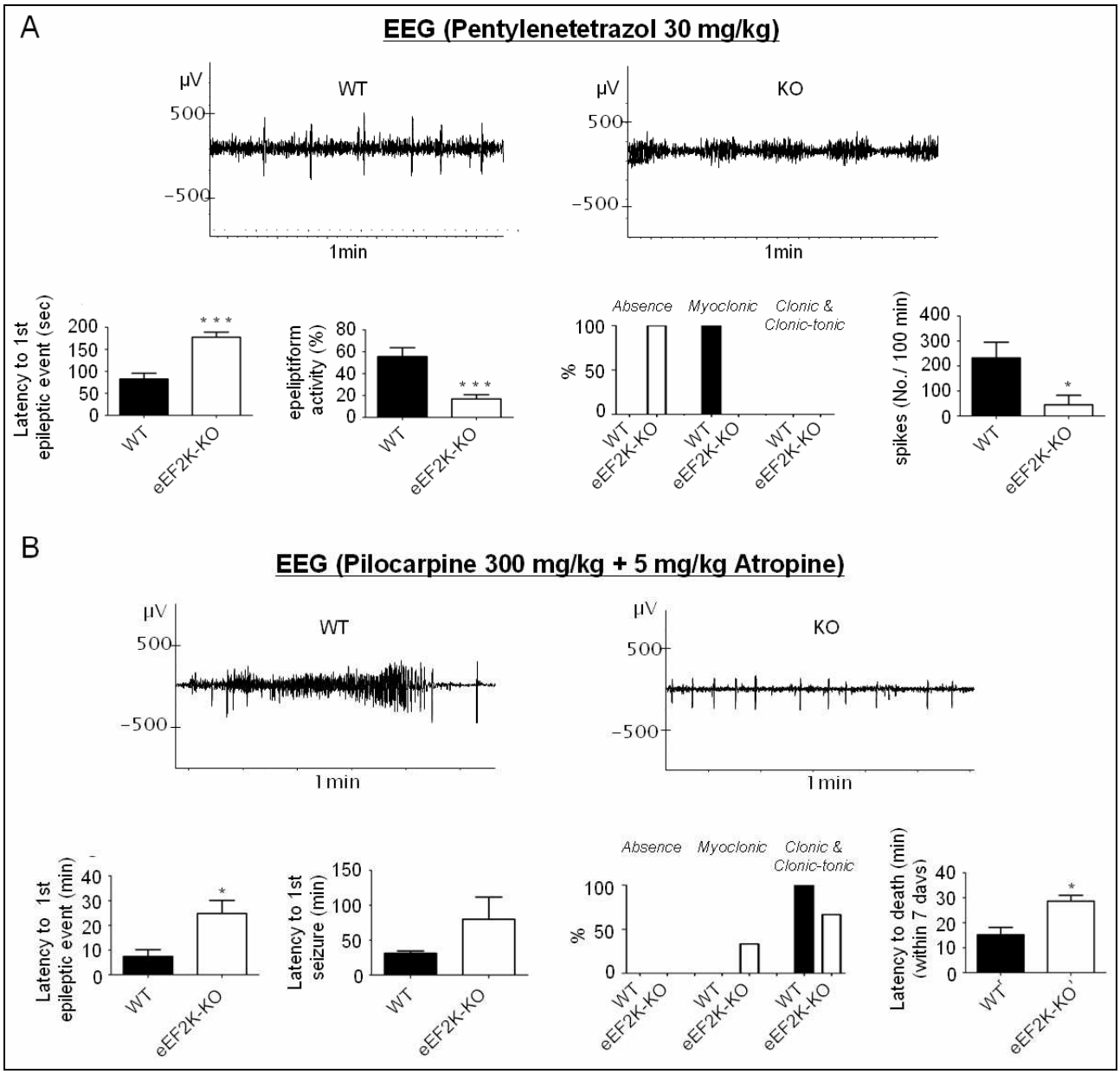

Figure 21: eEF2K-KO mice are clearly less prone to seizures. **A, B,** EEG traces and analysis of eEF2K-KO mice reveals reduced responses to the convulsive substances PTZ (A) and pilocarpine (B). Quantifications of several behavioural and EEG parameters are also shown.Vertical axis shows latency to first epileptic seizure (racine stage 3-5), time spent in epileptiform activity, No. of EEG spikes per 100 min, and latency to death in animals showing tonic-clonic seizures. Error bars are SEMs. N= 7 for each group. * $p < 0.05$ and *** $P< 0.001$ versus WT (Student's t-Test).

4 Discussion

4.1 Summary of main findings

The findings of our study mainly indicate two things (see Fig. 22): 1. chronic eEF2K activity downregulates the efficacy of the presynaptic compartment of both the excitatory and inhibitory synapse; 2. chronic eEF2K activity downregulates the efficacy of the inhibitory but not excitatory postsynaptic compartment.

More specifically, eEF2K activity downregulates vesicle release by reducing Syn2b expression levels and it presumably does so by downregulating its translation rate since eEF2K activity leads to the phosphorylation and inactivation of eEF2, its only known substrate (Browne and Proud, 2002; Ryazanov, 2002). Additionally, at the GABAergic presynapse the amount of neurotransmitters in each vesicle may be reduced, as well, since eEF2K appears to downregulate GAD65 expression levels. To the best of our knowledge, we are the first group to show presynaptic effects induced by eEF2K, possibly since most research on this kinase in neuroscience has focused on acute, short-, and medium-term effects of eEF2K activity at the (excitatory) postsynaptic compartment, mainly in the context of NMDAR/mGluR activation and synaptic plasticity (Scheetz et al., 2000; Chotiner et al., 2003; Davidkova and Carroll, 2007; Piccoli et al., 2007; Sutton et al., 2007; Park et al., 2008; Verpelli et al., 2010; Autry et al., 2011). Additionally, eEF2K downregulates the efficacy/and or quantity of $GABA_A$Rs, presumably by reducing the expression levels of yet unknown proteins. Perhaps, eEF2K activity changes expression levels of certain $GABA_A$R subunits and could thereby affect the total amount or composition of $GABA_A$Rs which may cause the aforementioned changes in $GABA_A$R efficacy (Kilman et al., 2002; Liang et al., 2004; Eyre et al., 2012).

Taken together, the findings of this study suggest that chronic eEF2K activity has a larger effect on the function of the GABAergic synapse/inhibitory system as opposed to the glutamatergic synapse/excitatory system. This, in turn, means that eEF2K may affect the excitation/inhibition balance which is relevant for applied research on and treatment of disorders of the nervous system and neurological disorders such as seizures/status epilepticus and epilepsy (Kilman et al., 2002; Fritschy, 2008; Yizhar et al., 2011). Indeed, our *in vivo* results point towards practical applications of manipulating eEF2K activity levels in the context of epilepsy since eEF2K-KO mice have a stronger GABAergic system and- expectedly- also exhibit a decreased susceptibility to seizures. Apparently, even though eEF2K-KO (and eEF2K-KI) mice have a normal degree of brain activity and exhibit normal behaviour under baseline conditions (Park et al., 2008; Gildish et al., 2012;

Nosyreva et al., 2013) (see also paragraph 3.2.4), they clearly exhibit increased GABAergic inhibition under conditions which mimic a state of elevated network activity (see paragraph 3.2.3). This, in turn, suggests that chronic absence of eEF2K activity may positively regulate a stress-induced response of the organism aimed at regulating network activity. Therefore, one might be able to reduce seizure magnitude or susceptibility in patients by chronic administration of eEF2K inhibitors. Unfortunately, there are only few papers showing that commercially available eEF2K inhibitors like NH125 or rottlerin (Arora et al., 2003; Sutton et al., 2007; Autry et al., 2011) pass the blood–brain barrier (Autry et al., 2011) and several groups (including our own, data not shown) have found the inhibitors to be ineffective in reducing peEF2 levels both *in vivo* and *in vitro* (Chen et al., 2011; Devkota et al., 2012). It is important to point out that even though there are publications which show that the eEF2K/eEF2 pathway is involved in stress-responses (Ryazanov, 2002; Dagestad et al., 2006; Autry et al., 2011; Gronli et al., 2012; Nosyreva et al., 2013), our study is the first which associates eEF2K activity with the GABAergic system and seizure susceptibility.

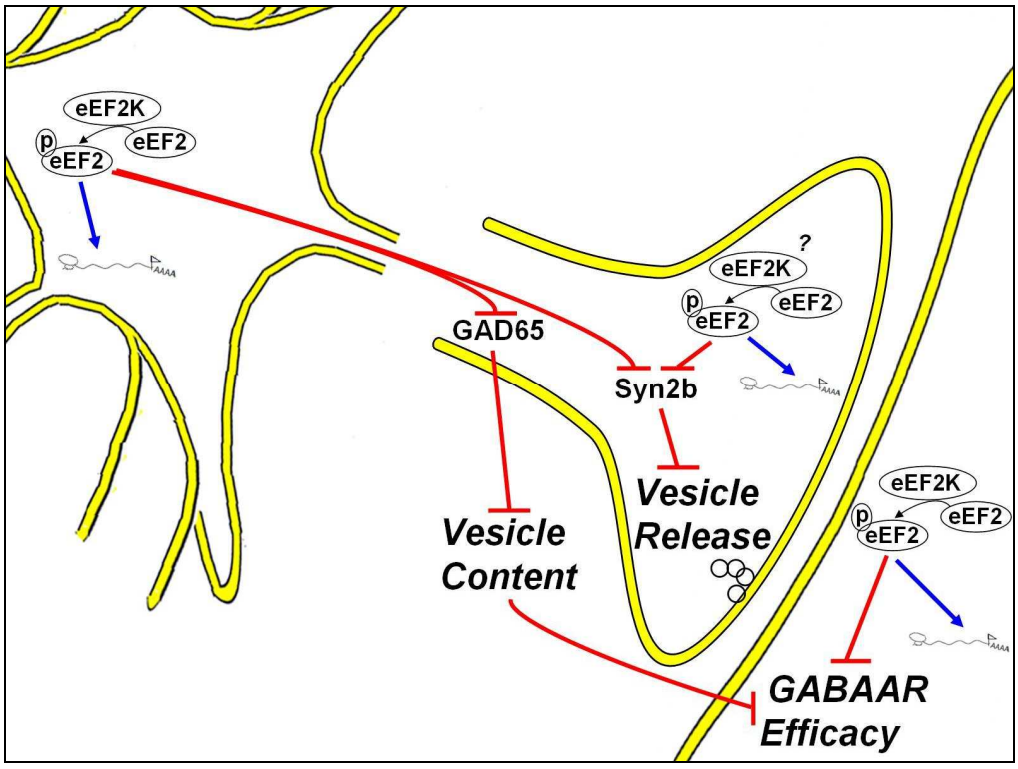

Figure 22: eEF2K activity reduces the efficacy of the GABAergic synapse by regulating the expression levels of a subset of synaptic proteins. eEF2K phosphorylates and thereby inactivates eEF2, resulting in strongly reduced somatic and synaptic protein translation (Nairn et al., 1985; Mitsui et al., 1993; Ryazanov et al., 1997; Scheetz et al., 2000; Sutton et al., 2007) while the translation rate of a subset of synaptic proteins is increased (Scheetz et al., 2000; Chotiner et al., 2003; Davidkova and Carroll, 2007; Park et al., 2008; Autry et al., 2011). The process of eEF2 phosphorylation is indicated by the curved black arrow, whereas the up- and downregulation of mRNA translation is shown by the blue arrow and red T-bar, respectively ("AAAA" indicates polyadenylated mRNA which is accessible for protein translation). Our study shows that somatically or presynaptically localized eEF2K activity of the presynaptic neuron (left side of figure) leads to an upregulation of a subset of synaptic proteins such as MAP1b (not shown). It also leads to a downregulation of a subset of presynaptic and presynaptic vesicle-associated proteins, such as Syn2b and GAD 65. The downregulation of Syn2b leads to a reduction in vesicle release (reduction shown by red T-bar). Additionally, the downregulation of GAD65 levels probably leads to a reduction in the amount of GABA present in each vesicle (reduction shown by red T-bar) at the GABAergic

presynapse, which in turn could affect $GABA_AR$ efficacy (reduction shown by red T-bar). Somatically or postsynaptically localized eEF2K activity of the postsynaptic neuron (right side of figure) leads to an upregulation of a subset of synaptic proteins such as MAP1b or TRIM-3 (both not shown). It also leads to a downregulation of $GABA_AR$ efficacy at the inhibitory postsynapse (reduction shown by red T-bar), presumably by controlling expression levels of yet unknown proteins (e.g. a subset of $GABA_AR$ subunits).

4.2 Data revision and outlook

4.2.1 eEF2K gain-of-function experiments *in vitro* (primary rat/mouse neuronal cultures)

In order to look at proteomic and functional changes induced by chronic eEF2K gain-of-function, we chose primary neuronal cultures as our experimental model since they are easily accessible to experimental manipulations- e.g. lentiviral infection to increase the amount of eEF2K expressed in neurons (Boulton et al., 1992; Ding and Kilpatrick, 2013). It is important to note that eEF2K gain-of-function (via lentiviral infection of eEF2Kca) was introduced in immature neurons (DIV 1) and the analysis was carried out on mature neurons (DIV 20). This means that the data of this *in vitro* approach may not only reflect what kind of effect eEF2K has on mature networks but may also reflect changes in mature networks that actually stem from eEF2K-dependent developmental processes. Indeed, carrying out the infection with eEF2Kca at DIV 10 (where neurons are already much more mature than at DIV 1 but are not considered fully matured yet) (Murata and Constantine-Paton, 2013) had an effect on the expression rate of one of the proteins that were identified to be regulated by eEF2K when infection took place at DIV 1 (see Fig. 9), indicating that developmental processes may, in part, be reflected by the analysis.

To analyze eEF2K-dependent proteomic changes that occur after chronic overexpression/gain-of-function of eEF2K, we implemented a highly quantitative SILAC-based mass spectrometry approach (Ibarrola et al., 2003; Ong and Mann, 2006; Liao et al., 2008). With this approach we identified "eEF2K-regulated" proteins by comparing the relative quantity of identified peptides/proteins in the P2 fraction of eEF2Kca with the relative quantity in the P2 fraction of the GFP control (see paragraph 3.1.1). "Upregulated" proteins are proteins which exhibit an eEF2Kca to GFP ratio which is greater than one, whereas "downregulated" proteins exhibit an eEF2Kca to GFP ratio which is smaller than one. Since the P2 fraction is enriched in synaptic components (Li et al., 1996; Ohno et al., 2004) (see also Fig. 5), proteomic changes in this fraction are indicative of changes in protein levels at the synapse (both of the pre- and postsynaptic compartment) and are probably due to eEF2K-dependent regulation at the translational level involving the phosphorylation/inactivation of eEF2, the only known substrate of eEF2K (Mitsui et al., 1993; Browne and Proud, 2002). As a consequence of eEF2 inactivation, global translation is reduced but

the local translation at the synapse of a small subset of synaptic proteins is actually increased by yet not well-understood mechanisms (Marin et al., 1997; Scheetz et al., 2000; Park et al., 2008). This eEF2K-dependent local translation has been described at the postsynapse (of the excitatory synapse) but it is conceivable that this form of local translation may also take place in the presynaptic compartment (Yoon et al., ; Lin and Holt, 2007; Akins et al., 2009). Therefore, the proteomic changes we see in the P2 fraction could be the result of eEF2K-dependent translation control at the soma or at the synapse (i.e. local) but based on our experimental setup we cannot distinguish between the two. It is also important to keep in mind the technical limitations of the SILAC-based mass spectrometry readout: any mass spectrometry analysis is biased towards proteins which are relatively abundant and/or easily detectable (e.g. proteins which are easily ionizeable) (Wysocki et al., 2005). Additionally, metabolic labeling methods like SILAC are intrinsically biased towards proteins with high turnover rates and depend on cell growth which poses a technical challenge for implementing SILAC in neurons as opposed to mitotically deviding cells (Ong and Mann, 2006; Wu et al., 2012). Nonetheless, since synaptic proteins have a half-lifetime between two to five days (Cohen et al., 2013) and our isotope integration took place for 20 days we can be quite sure that the SILAC procedure was successfully implemented to assess proteomic changes, especially since we were able to demonstrate an average isotope incorporation rate of 95% in our experimental design (Fig. 4).

In our SILAC-based screen we identified three synaptic proteins whose expression levels are upregulated by chronic eEF2K gain-of-function: MAP1b, eEF2, and TRIM3 (Fig. 6). All of these proteins have been described to be localized to the synapse and have well-described synaptic functions (Davidkova and Carroll, 2007; Park et al., 2008; Hung et al., 2010), though it is noteworthy that they are not exclusively localized to the synapse (Verpelli et al., 2010; Bhanot et al., 2011; Labonte et al., 2013). Interestingly, Davidkova and Carroll demonstrated that acute mGluR-induced upregulation of MAP1b depends on eEF2K activity (Davidkova and Carroll, 2007) which indicates that eEF2K may upregulate MAP1b levels both chronically and in response to acute stimuli. In contrast, upregulation of eEF2 and TRIM3 has (to the best of our knowledge) not been related to eEF2K activity. Due to the fact that eEF2K vastly downregulates global translation (Ryazanov et al., 1988; Scheetz et al., 2000; Browne and Proud, 2002; Dorovkov et al., 2002), “upregulated” proteins as identified in our screen may also represent proteins whose translation rate is downregulated less strongly than that of the majority of proteins. One way to analyze whether eEF2K indeed increases the translation rate of the proteins at hand is to carry out protocols aimed at activating eEF2K- e.g. via NMDAR activation (Scheetz et al., 2000) or by the use of eEF2K activators (Chen et al., 2011; Devkota et al., 2012)- and then register whether the expression levels

of the identified proteins increase accordingly. Instead, the synaptic proteins whose expression levels are downregulated by chronic eEF2K gain-of-function comprise several presynaptic proteins, many of which are vesicle-associated like Syn2b (Tab. 2, Fig. 6) (Medrihan et al., 2013). This suggests that eEF2K activity downregulates the expression level of presynaptic vs. postsynaptic proteins, a concept that we then validated in the course of the study with an immunocytochemical approach (see paragraph 3.1.3). To the best of our knowledge there is no publication showing eEF2K-dependent proteomic changes at the presynapse but rather at the postsynapse, which may be due to the fact that most eEF2K-related research at the synapse has focused on GluR-mediated changes in eEF2K activity (Scheetz et al., 1997, 2000; Verpelli et al., 2010; Autry et al., 2011).

We then focused on MAP1B and eEF2 as representatives of eEF2K-regulated proteins and showed that their regulation does not depend on changes at the transcriptional level and does not depend on an increase in eEF2K molecules per se but, as expected, depends on an increase in eEF2K activity (for this we used K170M, a catalytically inactive form of eEF2; see paragraph 3.1.2). This indicates that proteomic changes induced by eEF2K are probably due to its control of translation via eEF2-phosphorylation (Browne and Proud, 2002). However, we cannot exclude the possibility that eEF2K activity leads to proteomic changes by affecting the stabilization/degradation of the regulated proteins (Vogel and Marcotte, 2012). To clarify whether changes in protein levels are really due to changes at the translational level one could compare the polysome profiles of eEF2K-regulated mRNAs (like that of MAP1b) between GFP and eEF2Kca (Schratt et al., 2004; Roffe et al., 2010; Moreno et al., 2012). E.g. in the case of upregulated proteins one would expect a shift of the profile towards the polyribosomal fraction in eEF2Kca relative to GFP which would indicate that the active translation of the mRNAs is higher in eEF2Kca than in the GFP control. Another important question is whether eEF2K activity directly or indirectly affects the expression level of eEF2K-regulated proteins. E.g. eEF2K activity may affect the expression level of a certain protein which is involved in protein synthesis (like e.g. eEF2, see Tab. 1 or 2) which, in turn, might lead to subsequent changes in the proteome. One (laborious) way of addressing this point would be to chronically manipulate the expression level of each regulated protein (e.g. eEF2) independently of eEF2K in a way which mimics the change induced by chronic eEF2K overexpression (here: one would have to increase eEF2 expression levels). If subsequent proteomic changes resemble those of overexpressing eEF2K (e.g. upregulation of MAP1b), eEF2K activity probably does not directly affect the expression level of the eEF2K-regulated proteins but rather does so indirectly via the regulation of a mediating protein (here: eEF2).

To analyze eEF2K-dependent functional changes at the synapse that occur after chronic overexpression/gain-of-function of eEF2K, we compared GFP, eEF2Kca, and K170M at DIV 20

with immunocytochemical and electrophysiological approaches (see paragraph 3.1.3, 3.1.4., and 3.1.5). In line with our previous finding that eEF2K downregulates the expression rate of presynaptic vesicle-associated proteins which are known to change SV dynamics like Syn2b, we found that eEF2K activity downregulates vesicle release. Importantly, using Syn TKO cultures and a Syn2b rescue design (3.1.5) we were able to show that the eEF2K-induced downregulation of Syn2b leads to a reduction of vesicle release, pointing towards the central role of Syn2b in mediating the eEF2K-induced effects at the presynapse. Taken together, these results suggest that eEF2K downregulates the efficacy of the presynaptic compartment/ vesicle release by reducing the expression levels of a subset of presynaptic vesicle-associated proteins such as Syn2b. However, one must be cautious about explaining the strong effect that eEF2K activity has on vesicle release solely by the regulation of Syn2b since the downregulation is only around 25 % (Tab. 2) but in the context of the rescue experiment the Syn2b levels were increased well above GFP baseline levels in eEF2Kca by co-overexpression of Syn2b (Fig. 16). This consideration is especially relevant since there are indications that Syn2b overexpression can result in increased vesicle release (Gitler et al., 2008) which could mean that the Syn2b overexpression might outdo any effect that eEF2K overexpression may have on vesicle release. Also, since eEF2K downregulates global translation one has to ask the question how eEF2K achieves protein specific downregulation of protein expression rates, like for Syn2b- our study does not give an answer to this question but we believe it merits further research. Nonetheless, our results are in line with published data which shows that there are proteins whose expression rates are particularly repressed by eEF2K activity- one example is BDNF at the excitatory postsynapse (Autry et al., 2011).

Importantly, the electrophysiological analysis also revealed another interesting effect that chronic eEF2K gain-of-function has on the synapse: apparently eEF2K activity leads to a downregulation of the efficacy of the postsynaptic compartment of the inhibitory synapse but does not affect the efficacy of the excitatory postsynapse. More specifically, in rat primary cortical cultures eEF2K appears to downregulate the mIPSC area, decay time, and amplitude whereas the corresponding mEPSC parameters are not changed (3.1.5). This means that chronic eEF2K activity probably downregulates $GABA_AR$ quantity, kinetics, and/or efficacy (i.e. the ability of $GABA_ARs$ to exert an inhibitory effect on the postsynaptic neuron in response to activation via the endogenous ligand, GABA). Worthy of note, we can show that this postsynaptic effect that eEF2K has on the inhibitory synapse takes place independently of Syn regulation and therefore dissociates Syn2b downregulation from the downregulation of $GABA_AR$ efficacy. Instead, the effect could very well be due to other proteomic regulations that occur during eEF2K gain-of-function, such as MAP1b

upregulation, especially since MAP1b has been associated with GABAR anchoring at the inhibitory postsynapse (Allison et al., 2000).

4.2.2 eEF2K loss-of-function *in vivo* and *ex vivo* (eEF2K-KO mice and slices thereof)

We also wondered if our *in vitro* results could be replicated *in vivo* and what kind of effects a chronic change of eEF2K activity may have on a highly orchestrated neural network such as the brain of a mammal which obviously has a much higher level of complexity and cellular organization than a primary neuronal culture (Boulton et al., 1992). Our main motivation for this was to see whether changing eEF2K activity may have practical applications for patients suffering from neurological disorders such as epilepsy, since our *in vitro* results indicated an eEF2K-dependent effect on the excitation/inhibition balance (Kilman et al., 2002; Fritschy, 2008; Yizhar et al., 2011) (see also paragraph 3.1.5). For this, we analyzed eEF2K-KO mice which represent a genetic model to analyze the effects of chronic absence of physiological eEF2K activity. In this model we expected opposite effects of the (chronic) gain-of-function experiments *in vitro*. This assumption seems justified as gene-dosage effects have been previously described for eEF2K in neurons, both *in vivo/ex vivo* and *in vitro* (Park et al., 2008; Im et al., 2009; Verpelli et al., 2010; Gildish et al., 2012). However, it is important to keep in mind the limitations of such genetic models since genetic deletion *in vivo* has been shown to cause compensatory effects that mask obvious phenotypes which would otherwise be observed, thereby limitating the power of these approaches to reveal effects associated with gene deletion (Thyagarajan et al., 2003; van Amerongen and Berns, 2006; Barbaric et al., 2007). In line with this fact, eEF2K-KO mice have no obvious phenotypes (normal weight and behaviour, normal baseline brain activity levels and excitatory transmission) (Ryazanov, 2002; Park et al., 2008; Nosyreva et al., 2013) (see also paragraph 3.2.4). Nonetheless, there are published phenotypes of eEF2K-KO mice (Park et al., 2008; Autry et al., 2011; Nosyreva et al., 2013) and associations of the eEF2K/eEF2 pathway with stress (Ryazanov, 2002; Dagestad et al., 2006; Gronli et al., 2012) which may be related to changes in the excitation/inhibition balance caused by eEF2K activity (Griebel and Holmes, 2013).

Our WB analysis revealed that eEF2K-KO mice have a small increase in Syn2b expression levels but the levels of MAP1b and eEF2 do not appear to be altered (see paragraph 3.2.1). This means that not all but some proteomic changes are specular in our *in vitro* and *in vivo* design. Interestingly, a subsequent electrophysiological (see paragraph 3.2.2) analysis revealed that eEF2K-KO mice exhibit an increase in mIPSC frequency which may be due to the increase of Syn2b levels though

we have no formal proof of this. This suggests that eEF2K activity negatively regulates vesicle release at the GABAergic synapse not only *in vitro* but also *in vivo*. This concept is absolutely novel and has (to the best of our knowledge) not been described in literature. As expected from our *in vitro* results, there was also an increase of mIPSC amplitude and a strong trend for an increase in mIPSC area in the KO mice indicating that eEF2K activity negatively regulates the efficacy of the GABAergic postsynapse/$GABA_A$Rs both *in vitro* and *in vivo*. Interestingly, eEF2K-KO mice also presented a stronger tonic inhibition under conditions which may present themselves under elevated network (see paragraph 3.2.3). Taken together, these results indicate that *in vivo* physiological eEF2K activity negatively regulates the efficacy of the GABAergic system and this effect may become particularly pronounced when there is an increase of network activity, e.g. in the context of stressful events like kindling or seizures. Accordingly, eEF2K-KO mice responded much less to seizure induction by chemoconvulsant substances than WT mice (see paragraph 3.2.4) which may be due to their larger GABAergic response that presents itself in the context of stressful events. The results of this *in vivo* study therefore indicate that eEF2K may be a good target for chronically administered antiepileptic drugs aimed at inhibiting eEF2K since chronic loss of eEF2K activity does not change the baseline brain activity level of an organism nor does it change its behaviour. But importantly, chronic loss of eEF2K activity does appear to reduce the susceptibility of the organism to develop seizures.

These interesting *in vivo* results raise a lot of questions which could be addressed in future studies. For example, is eEF2K really a good target for antiepileptic drugs? This would have to be addressed by the use of an efficient and specific eEF2K inhibitor that passes the blood–brain barrier. As mentioned in 4.1 the available inhibitors do not appear to fulfill these criteria. If our hypothesis is correct, chronic use of an adequate eEF2K inhibitor should not affect the patient under normal conditions, i.e. it should not change the well-being of the patient when the activity level of his brain is within the physiological range. Instead, if the patient experiences a strong increase in network activity (such as during seizures), eEF2K should exhibit a moderating effect on neuronal activation. However, we cannot guarantee that downregulation of eEF2K activity (as in the case of chronically administered eEF2K inhibitors) would show similar effects as an absence of eEF2K activity (as in eEF2K-KO mice). E.g. it could be that eEF2K-KO mice compensate eEF2K deficits under physiological conditions by changing the expression of other proteins but do not compensate the deficits when the neuronal network is being "challenged", such as during elevated network activity (Barbaric et al., 2007; Bragina et al., 2008; Nosyreva et al., 2013). This could lead to the faulty hypothesis that chronic reduction of eEF2K activity should only show effects under elevated network activity. Additionally, one must keep in mind that eEF2K is a ubiquitous protein and

therefore changes in eEF2K activity may affect not only the brain but all organs of the body or may result in changes in the responses of the organism to pathophysiological conditions like cancer (Nairn et al., 1985; Ahmed et al., 2005; Leprivier et al., 2013).

Another interesting question to address in further studies is to better understand by which means eEF2K activity affects the excitation/inhibition imbalance and how this may relate to the fact that eEF2K-KO mice have a reduced susceptibility for seizures. For example, it would be interesting to decipher if changes in eEF2K activity *in vivo* really change the translation rate of specific proteins and whether these changes are the cause of the stronger GABAergic system that we witnessed in eEF2K-KO mice. Lastly, a fascinating question is whether eEF2K and the eEF2K/eEF2 pathway have an essential biological function at the synapse- what kind of an evolutionary advantage might the employment of this translation control machinery have in the context of synapse- and network-functionality? One idea proposed by researchers is that the eEF2K/eEF2 pathway acts as a decoding device for neuronal activity at the synapse, which dynamically changes the synaptic proteome in response to changes in network activity, possibly in order to enable specific changes in protein expression that are demanded by different states of network activity (Davidkova and Carroll, 2007; Sutton et al., 2007; Park et al., 2008; Autry et al., 2011; Nosyreva et al., 2013). Since our study indicates that eEF2K activity and the extent of seizures are related, it would be interesting to see if the eEF2K/eEF2 pathway is utilized by organisms to control network activity and associated events like seizures. This would mean that the eEF2K/eEF2 pathway does not only act as decoding device for network activity but may, itself, control the extent of network activity.

5 Abbreviations

Common abbreviations are not shown. Of note, the International System of Units was applied throughout this study.

a	= adeonsine
aa	= amino acids
AMPK	= AMP-activated protein kinase
AMPAR	= α-amino-3-hydroxy-5-methyl-4-isoxazolepropionic acid receptor
ANOVA	= analysis of variance
Arc	= activity-regulated cytoskeletal-associated protein
Arg	= Arginine
ATP	= adenosine triphosphate
BDNF	= Brain-derived neurotrophic factor
Bic	= Bicuculline
c	= cytosine
CaM	= calmodulin
CaMKII	= Ca^{2+}/Calmodulin-dependent kinase II
CaMKIII	= Ca^{2+}/Calmodulin-dependent kinase III
C-terminal	= carboxyl-terminus
Cy	= cyanine/ cyanine dye
DAPI	= 4',6-diamidino-2-phenylindole
dd	= double distilled
DIV	= days in vitro
DNA	= deoxyribonucleic acid
DTT	= dithiothreitol
E	= embryonic day
e.g.	= for example
eEF2	= eukaryotic elongation factor 2
eEF2K	= eukaryotic elongation factor 2 kinase
eEF2Kca	= constituitively active eukaryotic elongation factor 2 kinase
eEF2K-KO	= eukaryotic elongation factor 2 kinase-knockout
eEF2K-KI	= eukaryotic elongation factor 2 kinase-knockin
EEG	= electroencephalography
EPSC	= excitatory postsynaptic current
FDR	= false discovery rate
Fig.	= Figure
FITC	= Fluorescein isothiocyanate
g	= guanine
GABA	= gamma-Aminobutyric acid
$GABA_AR$	= $GABA_A$ receptor
$GABA_AR\alpha1$	= α1 subunit of the $GABA_A$ receptor
GABAR	= GABA receptor
GAPDH	= glyceraldehyde 3-phosphate dehydrogenase
GFP	= Green fluorescent protein
GluR	= glutamate receptor
GluR1/GRIA1	= subunit 1 of the AMPAR

GTP	= guanosine triphosphate
i.e.	= that means
i.p.	= intraperitoneal injection
IF	= immunofluorescence
IgG	= Immunoglobulin G
IPSC	= inhibitory postsynaptic current
K170M	= catalytically inactive eukaryotic elongation factor 2 kinase
kDa	= kilodalton
KYN	= Kynurenic acid
LC-MS/HPLC-MS	= Liquid chromatography–mass spectrometry
Lys	= Lysine
MAP1b	= Microtubule-associated protein 1B
MAP2	= Microtubule-associated protein 2
MEK/ERK	= mitogen-activated protein/extracellular signal-regulated kinase
mEPSC	= miniature excitatory postsynaptic current
Met	= Methionine
mGluR-LTD	= mGluR-dependent-Long Term Depression
mIPSC	= miniature inhibitory postsynaptic current
mPSC	= miniature postsynaptic current
mRNA	= messenger ribonucleic acid
MS	= mass spectrometry
mTOR	= mammalian target of rapamycin
N	= number of raw values per experimental group
n.d.	= no publishing date
n.p.	= no publisher name
NMDAR	= N-methyl-D-aspartate receptor
NLGN1	= neuroligin-1
No.	= number
N-terminal	= amino-terminus
P	= postnatal day
P1	= nuclear fraction
P2	= (crude) synaptosomal fraction
PCR	= polymerase chain reaction
p70S6K	= P70S6 kinase
p90RSK1	= p90 ribosomal S6 kinase
PSD95	= Postsynaptic Density protein 95
PSC	= postsynaptic current
PTZ	= pentylenetatrazol
RNA	= ribonucleic acid
RT-PCR	= Real-time polymerase chain reaction
Ser	= Serine
SAP	= Synapse-associated protein
SD	= standard deviation; σ
SDS	= sodium dodecyl sulfate
SDS-PAGE	= sodium dodecyl sulfate-Polyacrylamide gel electrophoresis
SEM	= standard error of mean
sieEF2K	= small interference ribonucleic acid 362
SILAC	= stable isotope labeling in cell culture
siRNA	= small interference ribonucleic acid
sreEF2K	= small interference ribonucleic acid 362-resistant form of

	eukaryotic elongation factor 2 kinase
SV	= synaptic vesicles
Syp	= Synaptophysin
Syn	= Synapsin
SYT	= Synaptotagmin
t	= thymine
Tab.	= table
Thr	= Threonin
TL	= total lysate
TKO	= Synapsin 1-3 knockout
TBS	= Tris-buffered saline
TBS-T	= Tris-buffered saline-Tween
tRNA	= Transfer ribonucleic acid
TTX	= tetrodotoxin
v	= volume
VGAT	= vesicular gamma-Aminobutyric acid transporter
VGLUT	= vesicular glutamate transporter
w	= weight
WB	= Western Blot
WT	= wild type

6 Acknowledgement

I want to thank my kind and sweet girlfriend for all the support she has given and all the sacrifices she has made in order for me to be able to carry out my PhD here in Italy. I know it was hard, but we have made it! I also want to thank my mother for encouraging me to always try my best and follow the dreams I have. I miss you. Your suffering may not have had any sense at all, but at least it got me interested in how the brain works. I want to thank my father who has taught me to organize myself well in order to succeed. And I also want to thank my kind grandparents who have always been a positive influence on me and are my role models- you are/were great people and I am so very thankful for all the time we spent together. Importantly, I also want to thank my sisters - you are really special and interesting people who I totally enjoy to communicate with- you have so many interesting things going on, I think we could hang out for years and still have a million things to talk about. I love you all! I also want to take this moment to thank the parents of my girlfriend, my good friends from the pizzeria next door, and all the people from my flat-sharing communities who have always been very supportive and are great people.

Of course, I also want to take this moment to thank the people involved in the study. Firstly, thanks to my boss and tutor Carlo for giving me the chance to carry out the PhD in his lab and for all the things I have learned during my time here. Your dedication to the project was great and I really appreciate that you always found time to discuss scientific problems at hand. Thanks also to my other boss and tutor Chiara for the support and talks we had about the project. I am happy that the both of you put a great deal of trust in my scientific skills and I hope my hard work and the outcome of this study have justified your positive attitude towards me. I also want to take this moment to acknowledge my colleagues, the people I had most contact with in the lab: Cinzia, Cate, Vale, and Adele. First of all, you are really nice people and I enjoyed working with each one of you for different reasons. Cinzia, I enjoyed that we could joke around without having to think twice about what we have just said! I hope you find (a new) Mr. Right sooner or later. Cate, you are a cool, chilled-out person and represent the typical Italian person that you want to hang out with. Vale, you were always very supportive and friendly, you were kind of the “mother” of the lab. Adele, we got to know each other a bit later but I really appreciate your sensibility and respect for other people. I also want to thank our technician Elisa, who has helped out so much during the project- how many gels did you run for the genotyping? I wish you the best for your new job. Thanks also to Luca for all the great experiments we carried out together- you are precise in your work and I really enjoyed working with you, also since you are a good guy. Thanks also to Daniela and Francesca from the

"Piccoli" lab- you are nice people and I wish you all the best for your projects. Thanks also to Giovanni for putting us into contact with other groups working on Synapsins. Thanks to Stefano and Luciano for all the great talks we had- I really enjoyed visiting you in the lab downstairs. Thanks to Luisa, Daniela, and Mariaelvina Sala for the great collaboration on EEG. I enjoyed coming over to your place- we always had something to chuckle about! I think we really worked well together. Thanks to Jonathan and Giulio for the time invested in the project and the good time we had on meetings and going out in Milan- you are cool guys and will be very successful in your fields, for sure. Thanks to Fabrizia, Angela and Angela, Elisa, and Maura for all the dedication during the project- it was a pleasure collaborating with you. And thanks to all the other collaborators and students in the lab who I cannot mention at this point because there are just so many of them! I really want to thank all of the people I have mentioned so far because you have been kind to me and you were one of the reasons my stay here in Italy was fun and exciting.

Lastly, I want to thank the Marie Curie programme SyMBaD ("SyMBaD – ITN Marie Curie, Grant Agreement n° 238608 –7th Framework Programme of the EU"), the University of Milan, and "CNR: Institute of Neuroscience Milan" for financing and making it possible that I could carry out my PhD here in Milan.

7 References

Ahmed M, Forsberg J, Bergsten P (2005) Protein profiling of human pancreatic islets by two-dimensional gel electrophoresis and mass spectrometry. J Proteome Res 4:931-940.

Akins MR, Berk-Rauch HE, Fallon JR (2009) Presynaptic translation: stepping out of the postsynaptic shadow. Front Neural Circuits 3:17.

Allison DW, Chervin AS, Gelfand VI, Craig AM (2000) Postsynaptic scaffolds of excitatory and inhibitory synapses in hippocampal neurons: maintenance of core components independent of actin filaments and microtubules. J Neurosci 20:4545-4554.

Arancibia-Carcamo IL, Moss SJ (2006) Molecular organization and assembly of the central inhibitory postsynapse. Results Probl Cell Differ 43:25-47.

Arora S, Yang JM, Kinzy TG, Utsumi R, Okamoto T, Kitayama T, Ortiz PA, Hait WN (2003) Identification and characterization of an inhibitor of eukaryotic elongation factor 2 kinase against human cancer cell lines. Cancer Res 63:6894-6899.

Autry AE, Adachi M, Nosyreva E, Na ES, Los MF, Cheng PF, Kavalali ET, Monteggia LM (2011) NMDA receptor blockade at rest triggers rapid behavioural antidepressant responses. Nature 475:91-95.

Bachi A, Bonaldi T (2008) Quantitative proteomics as a new piece of the systems biology puzzle. J Proteomics 71:357-367.

Banker GA, Cowan WM (1977) Rat hippocampal neurons in dispersed cell culture. Brain Res 126:397-342.

Barbaric I, Miller G, Dear TN (2007) Appearances can be deceiving: phenotypes of knockout mice. Brief Funct Genomic Proteomic 6:91-103.

Belelli D, Harrison NL, Maguire J, Macdonald RL, Walker MC, Cope DW (2009) Extrasynaptic GABAA receptors: form, pharmacology, and function. J Neurosci 29:12757-12763.

Bethmann K, Fritschy JM, Brandt C, Loscher W (2008) Antiepileptic drug resistant rats differ from drug responsive rats in GABA A receptor subunit expression in a model of temporal lobe epilepsy. Neurobiol Dis 31:169-187.

Bhanot K, Young KG, Kothary R (2011) MAP1B and clathrin are novel interacting partners of the giant cyto-linker dystonin. J Proteome Res 10:5118-5127.

Bianchi L, Ballini C, Colivicchi MA, Della Corte L, Giovannini MG, Pepeu G (2003) Investigation on acetylcholine, aspartate, glutamate and GABA extracellular levels from ventral hippocampus during repeated exploratory activity in the rat. Neurochem Res 28:565-573.

Boulton AA, Baker GB, Walz W (1992) Practical cell culture techniques. Totowa, N.J.: Humana Press.

Bragina L, Candiracci C, Barbaresi P, Giovedi S, Benfenati F, Conti F (2007) Heterogeneity of glutamatergic and GABAergic release machinery in cerebral cortex. Neuroscience 146:1829-1840.

Bragina L, Marchionni I, Omrani A, Cozzi A, Pellegrini-Giampietro DE, Cherubini E, Conti F (2008) GAT-1 regulates both tonic and phasic GABA(A) receptor-mediated inhibition in the cerebral cortex. J Neurochem 105:1781-1793.

Breedlove SM, Rosenzweig MR, Watson NV (2007) Biological psychology : an introduction to behavioral, cognitive, and clinical neuroscience, 5th Edition. Sunderland, Mass.: Sinauer Associates.

Browne GJ, Proud CG (2002) Regulation of peptide-chain elongation in mammalian cells. Eur J Biochem 269:5360-5368.

Browne GJ, Finn SG, Proud CG (2004) Stimulation of the AMP-activated protein kinase leads to activation of eukaryotic elongation factor 2 kinase and to its phosphorylation at a novel site, serine 398. J Biol Chem 279:12220-12231.

Castejon OJ, Fuller L, Dailey ME (2004) Localization of synapsin-I and PSD-95 in developing postnatal rat cerebellar cortex. Brain Res Dev Brain Res 151:25-32.

Chen X, Lepier A, Berninger B, Tolkovsky AM, Herbert J (2012) Cultured subventricular zone progenitor cells transduced with neurogenin-2 become mature glutamatergic neurons and integrate into the dentate gyrus. PLoS One 7:e31547.

Chen Y, Stevens B, Chang J, Milbrandt J, Barres BA, Hell JW (2008) NS21: re-defined and modified supplement B27 for neuronal cultures. J Neurosci Methods 171:239-247.

Chen Z, Gopalakrishnan SM, Bui MH, Soni NB, Warrior U, Johnson EF, Donnelly JB, Glaser KB (2011) 1-Benzyl-3-cetyl-2-methylimidazolium iodide (NH125) induces phosphorylation of eukaryotic elongation factor-2 (eEF2): a cautionary note on the anticancer mechanism of an eEF2 kinase inhibitor. J Biol Chem 286:43951-43958.

Chotiner JK, Khorasani H, Nairn AC, O'Dell TJ, Watson JB (2003) Adenylyl cyclase-dependent form of chemical long-term potentiation triggers translational regulation at the elongation step. Neuroscience 116:743-752.

Chuderland D, Seger R (2008) Calcium regulates ERK signaling by modulating its protein-protein interactions. Commun Integr Biol 1:4-5.

Cingolani LA, Thalhammer A, Yu LM, Catalano M, Ramos T, Colicos MA, Goda Y (2008) Activity-dependent regulation of synaptic AMPA receptor composition and abundance by beta3 integrins. Neuron 58:749-762.

Citri A, Malenka RC (2008) Synaptic plasticity: multiple forms, functions, and mechanisms. Neuropsychopharmacology 33:18-41.

Clapham DE (2007) Calcium signaling. Cell 131:1047-1058.

Cohen LD, Zuchman R, Sorokina O, Muller A, Dieterich DC, Armstrong JD, Ziv T, Ziv NE (2013) Metabolic turnover of synaptic proteins: kinetics, interdependencies and implications for synaptic maintenance. PLoS One 8:e63191.

Corradini I, Donzelli A, Antonucci F, Welzl H, Loos M, Martucci R, De Astis S, Pattini L, Inverardi F, Wolfer D, Caleo M, Bozzi Y, Verderio C, Frassoni C, Braida D, Clerici M, Lipp HP, Sala M, Matteoli M (2012) Epileptiform Activity and Cognitive Deficits in SNAP-25+/- Mice are Normalized by Antiepileptic Drugs. Cereb Cortex.

Cox J, Neuhauser N, Michalski A, Scheltema RA, Olsen JV, Mann M (2011) Andromeda: a peptide search engine integrated into the MaxQuant environment. J Proteome Res 10:1794-1805.

Czuczwar SJ (1999) [GABA-ergic system and antiepileptic drugs]. Neurol Neurochir Pol 33:1373-1380.

Dagestad G, Kuipers SD, Messaoudi E, Bramham CR (2006) Chronic fluoxetine induces region-specific changes in translation factor eIF4E and eEF2 activity in the rat brain. Eur J Neurosci 23:2814-2818.

Dajas-Bailador F, Bonev B, Garcez P, Stanley P, Guillemot F, Papalopulu N (2012) microRNA-9 regulates axon extension and branching by targeting Map1b in mouse cortical neurons. Nat Neurosci.

Davidkova G, Carroll RC (2007) Characterization of the role of microtubule-associated protein 1B in metabotropic glutamate receptor-mediated endocytosis of AMPA receptors in hippocampus. J Neurosci 27:13273-13278.

de Wit J, O'Sullivan ML, Savas JN, Condomitti G, Caccese MC, Vennekens KM, Yates JR, 3rd, Ghosh A (2013) Unbiased discovery of glypican as a receptor for LRRTM4 in regulating excitatory synapse development. Neuron 79:696-711.

Devkota AK, Tavares CD, Warthaka M, Abramczyk O, Marshall KD, Kaoud TS, Gorgulu K, Ozpolat B, Dalby KN (2012) Investigating the kinetic mechanism of inhibition of elongation

factor 2 kinase by NH125: evidence of a common in vitro artifact. Biochemistry 51:2100-2112.
Diggle TA, Seehra CK, Hase S, Redpath NT (1999) Analysis of the domain structure of elongation factor-2 kinase by mutagenesis. FEBS Lett 457:189-192.
Ding B, Kilpatrick DL (2013) Lentiviral vector production, titration, and transduction of primary neurons. Methods Mol Biol 1018:119-131.
Dingledine R, Borges K, Bowie D, Traynelis SF (1999) The glutamate receptor ion channels. Pharmacol Rev 51:7-61.
Dorovkov MV, Pavur KS, Petrov AN, Ryazanov AG (2002) Regulation of elongation factor-2 kinase by pH. Biochemistry 41:13444-13450.
Drennan D, Ryazanov AG (2004) Alpha-kinases: analysis of the family and comparison with conventional protein kinases. Prog Biophys Mol Biol 85:1-32.
During MJ, Spencer DD (1993) Extracellular hippocampal glutamate and spontaneous seizure in the conscious human brain. Lancet 341:1607-1610.
Egawa K, Fukuda A (2013) Pathophysiological power of improper tonic GABAA conductances in mature and immature models. Front Neural Circuits 7:170.
Erbayat-Altay E, Yamada KA, Wong M, Thio LL (2008) Increased severity of pentylenetetrazol induced seizures in leptin deficient ob/ob mice. Neurosci Lett 433:82-86.
Errington AC, Cope DW, Crunelli V (2011) Augmentation of Tonic GABA(A) Inhibition in Absence Epilepsy: Therapeutic Value of Inverse Agonists at Extrasynaptic GABA(A) Receptors. Adv Pharmacol Sci 2011:790590.
Eyre MD, Renzi M, Farrant M, Nusser Z (2012) Setting the time course of inhibitory synaptic currents by mixing multiple GABA(A) receptor alpha subunit isoforms. J Neurosci 32:5853-5867.
Fainzilber M, Budnik V, Segal RA, Kreutz MR (2011) From synapse to nucleus and back again--communication over distance within neurons. J Neurosci 31:16045-16048.
Farisello P, Boido D, Nieus T, Medrihan L, Cesca F, Valtorta F, Baldelli P, Benfenati F (2012) Synaptic and extrasynaptic origin of the excitation/inhibition imbalance in the hippocampus of synapsin I/II/III knockout mice. Cereb Cortex 23:581-593.
Fatt P, Katz B (1952) Spontaneous subthreshold activity at motor nerve endings. J Physiol 117:109-128.
Fortin DA, Srivastava T, Dwarakanath D, Pierre P, Nygaard S, Derkach VA, Soderling TR (2013) Brain-derived neurotrophic factor activation of CaM-kinase kinase via transient receptor potential canonical channels induces the translation and synaptic incorporation of GluA1-containing calcium-permeable AMPA receptors. J Neurosci 32:8127-8137.
Frank T, Rutherford MA, Strenzke N, Neef A, Pangrsic T, Khimich D, Fejtova A, Gundelfinger ED, Liberman MC, Harke B, Bryan KE, Lee A, Egner A, Riedel D, Moser T (2010) Bassoon and the synaptic ribbon organize Ca(2)+ channels and vesicles to add release sites and promote refilling. Neuron 68:724-738.
Franklin KBJ, Paxinos G (2008) The mouse brain in stereotaxic coordinates, 3rd Edition. Amsterdam ; Boston: Academic Press.
Fritschy JM (2008) Epilepsy, E/I Balance and GABA(A) Receptor Plasticity. Front Mol Neurosci 1:5.
Garner CC, Kindler S (1996) Synaptic proteins and the assembly of synaptic junctions. Trends Cell Biol 6:429-433.
Giesemann T, Schwarz G, Nawrotzki R, Berhorster K, Rothkegel M, Schluter K, Schrader N, Schindelin H, Mendel RR, Kirsch J, Jockusch BM (2003) Complex formation between the postsynaptic scaffolding protein gephyrin, profilin, and Mena: a possible link to the microfilament system. J Neurosci 23:8330-8339.

Gildish I, Manor D, David O, Sharma V, Williams D, Agarwala U, Wang X, Kenney JW, Proud CG, Rosenblum K (2012) Impaired associative taste learning and abnormal brain activation in kinase-defective eEF2K mice. Learn Mem 19:116-125.

Gitler D, Cheng Q, Greengard P, Augustine GJ (2008) Synapsin IIa controls the reserve pool of glutamatergic synaptic vesicles. J Neurosci 28:10835-10843.

Gitler D, Xu Y, Kao HT, Lin D, Lim S, Feng J, Greengard P, Augustine GJ (2004) Molecular determinants of synapsin targeting to presynaptic terminals. J Neurosci 24:3711-3720.

Glykys J, Mody I (2006) Hippocampal network hyperactivity after selective reduction of tonic inhibition in GABA A receptor alpha5 subunit-deficient mice. J Neurophysiol 95:2796-2807.

Glykys J, Mody I (2007) Activation of GABAA receptors: views from outside the synaptic cleft. Neuron 56:763-770.

Gonzalez-Teran B, Cortes JR, Manieri E, Matesanz N, Verdugo A, Rodriguez ME, Gonzalez-Rodriguez A, Valverde A, Martin P, Davis RJ, Sabio G (2012) Eukaryotic elongation factor 2 controls TNF-alpha translation in LPS-induced hepatitis. J Clin Invest 123:164-178.

Grabrucker AM, Knight MJ, Proepper C, Bockmann J, Joubert M, Rowan M, Nienhaus GU, Garner CC, Bowie JU, Kreutz MR, Gundelfinger ED, Boeckers TM (2011) Concerted action of zinc and ProSAP/Shank in synaptogenesis and synapse maturation. Embo J 30:569-581.

Griebel G, Holmes A (2013) 50 years of hurdles and hope in anxiolytic drug discovery. Nat Rev Drug Discov 12:667-687.

Gronli J, Dagestad G, Milde AM, Murison R, Bramham CR (2012) Post-transcriptional effects and interactions between chronic mild stress and acute sleep deprivation: regulation of translation factor and cytoplasmic polyadenylation element-binding protein phosphorylation. Behav Brain Res 235:251-262.

Han EB, Stevens CF (2009) Development regulates a switch between post- and presynaptic strengthening in response to activity deprivation. Proc Natl Acad Sci U S A 106:10817-10822.

Haydon PG (2000) Neuroglial networks: neurons and glia talk to each other. Curr Biol 10:R712-714.

He L, Wu LG (2007) The debate on the kiss-and-run fusion at synapses. Trends Neurosci 30:447-455.

Hendry SH, Bhandari MA (1992) Neuronal organization and plasticity in adult monkey visual cortex: immunoreactivity for microtubule-associated protein 2. Vis Neurosci 9:445-459.

Hering H, Lin CC, Sheng M (2003) Lipid rafts in the maintenance of synapses, dendritic spines, and surface AMPA receptor stability. J Neurosci 23:3262-3271.

Hong-Brown LQ, Brown CR, Huber DS, Lang CH (2007) Alcohol regulates eukaryotic elongation factor 2 phosphorylation via an AMP-activated protein kinase-dependent mechanism in C2C12 skeletal myocytes. J Biol Chem 282:3702-3712.

Hortnagl H, Tasan RO, Wieselthaler A, Kirchmair E, Sieghart W, Sperk G (2013) Patterns of mRNA and protein expression for 12 GABAA receptor subunits in the mouse brain. Neuroscience 236:345-372.

Houser CR, Zhang N, Peng Z (2012) Alterations in the Distribution of GABAA Receptors in Epilepsy.

Hsueh YP, Yang FC, Kharazia V, Naisbitt S, Cohen AR, Weinberg RJ, Sheng M (1998) Direct interaction of CASK/LIN-2 and syndecan heparan sulfate proteoglycan and their overlapping distribution in neuronal synapses. J Cell Biol 142:139-151.

Hung AY, Sung CC, Brito IL, Sheng M (2010) Degradation of postsynaptic scaffold GKAP and regulation of dendritic spine morphology by the TRIM3 ubiquitin ligase in rat hippocampal neurons. PLoS One 5:e9842.

Huttner WB, Schiebler W, Greengard P, De Camilli P (1983) Synapsin I (protein I), a nerve terminal-specific phosphoprotein. III. Its association with synaptic vesicles studied in a highly purified synaptic vesicle preparation. J Cell Biol 96:1374-1388.

Ibarrola N, Molina H, Iwahori A, Pandey A (2004) A novel proteomic approach for specific identification of tyrosine kinase substrates using [13C]tyrosine. J Biol Chem 279:15805-15813.

Ibarrola N, Kalume DE, Gronborg M, Iwahori A, Pandey A (2003) A proteomic approach for quantitation of phosphorylation using stable isotope labeling in cell culture. Anal Chem 75:6043-6049.

Iida J, Hirabayashi S, Sato Y, Hata Y (2004) Synaptic scaffolding molecule is involved in the synaptic clustering of neuroligin. Mol Cell Neurosci 27:497-508.

Im HI, Nakajima A, Gong B, Xiong X, Mamiya T, Gershon ES, Zhuo M, Tang YP (2009) Post-training dephosphorylation of eEF-2 promotes protein synthesis for memory consolidation. PLoS One 4:e7424.

Jelenkovic A, Jovanovic M, Ninkovic M, Maksimovic M, Bokonjic D, Boskovic B (2002) Nitric oxide (NO) and convulsions induced by pentylenetetrazol. Ann N Y Acad Sci 962:296-305.

Jin H, Wu H, Osterhaus G, Wei J, Davis K, Sha D, Floor E, Hsu CC, Kopke RD, Wu JY (2003) Demonstration of functional coupling between gamma -aminobutyric acid (GABA) synthesis and vesicular GABA transport into synaptic vesicles. Proc Natl Acad Sci U S A 100:4293-4298.

Joshi S, Kapur J (2012) GABAA Receptor Plasticity During Status Epilepticus.

Junge D (1981) Nerve and muscle excitation, 2d Edition. Sunderland, Mass.: Sinauer Associates.

Kanaani J, el-Husseini Ael D, Aguilera-Moreno A, Diacovo JM, Bredt DS, Baekkeskov S (2002) A combination of three distinct trafficking signals mediates axonal targeting and presynaptic clustering of GAD65. J Cell Biol 158:1229-1238.

Kandel ER, Schwartz JH, Jessell TM (2000) Principles of neural science, 4th Edition. New York: McGraw-Hill, Health Professions Division.

Kaul G, Pattan G, Rafeequi T (2011) Eukaryotic elongation factor-2 (eEF2): its regulation and peptide chain elongation. Cell Biochem Funct 29:227-234.

Kilman V, van Rossum MC, Turrigiano GG (2002) Activity deprivation reduces miniature IPSC amplitude by decreasing the number of postsynaptic GABA(A) receptors clustered at neocortical synapses. J Neurosci 22:1328-1337.

Kim HJ, Thayer SA (2009) Lithium increases synapse formation between hippocampal neurons by depleting phosphoinositides. Mol Pharmacol 75:1021-1030.

Klitgaard H (2005) Antiepileptic drug discovery: lessons from the past and future challenges. Acta Neurol Scand Suppl 181:68-72.

Kobayashi M, Buckmaster PS (2003) Reduced inhibition of dentate granule cells in a model of temporal lobe epilepsy. J Neurosci 23:2440-2452.

Kwon SE, Chapman ER (2011) Synaptophysin regulates the kinetics of synaptic vesicle endocytosis in central neurons. Neuron 70:847-854.

Labonte D, Thies E, Pechmann Y, Groffen AJ, Verhage M, Smit AB, van Kesteren RE, Kneussel M (2013) TRIM3 Regulates the Motility of the Kinesin Motor Protein KIF21B. PLoS One 8:e75603.

Laemmli UK (1970) Cleavage of structural proteins during the assembly of the head of bacteriophage T4. Nature 227:680-685.

Lee HK, Takamiya K, Han JS, Man H, Kim CH, Rumbaugh G, Yu S, Ding L, He C, Petralia RS, Wenthold RJ, Gallagher M, Huganir RL (2003) Phosphorylation of the AMPA receptor GluR1 subunit is required for synaptic plasticity and retention of spatial memory. Cell 112:631-643.

Leprivier G, Remke M, Rotblat B, Dubuc A, Mateo AR, Kool M, Agnihotri S, El-Naggar A, Yu B, Somasekharan SP, Faubert B, Bridon G, Tognon CE, Mathers J, Thomas R, Li A, Barokas A, Kwok B, Bowden M, Smith S, Wu X, Korshunov A, Hielscher T, Northcott PA, Galpin JD, Ahern CA, Wang Y, McCabe MG, Collins VP, Jones RG, Pollak M, Delattre O, Gleave ME, Jan E, Pfister SM, Proud CG, Derry WB, Taylor MD, Sorensen PH (2013) The eEF2 kinase confers resistance to nutrient deprivation by blocking translation elongation. Cell 153:1064-1079.

Li GL, Farooque M, Lewen A, Lennmyr F, Holtz A, Olsson Y (2000) MAP2 and neurogranin as markers for dendritic lesions in CNS injury. An immunohistochemical study in the rat. Apmis 108:98-106.

Li XJ, Sharp AH, Li SH, Dawson TM, Snyder SH, Ross CA (1996) Huntingtin-associated protein (HAP1): discrete neuronal localizations in the brain resemble those of neuronal nitric oxide synthase. Proc Natl Acad Sci U S A 93:4839-4844.

Liang J, Cagetti E, Olsen RW, Spigelman I (2004) Altered pharmacology of synaptic and extrasynaptic GABAA receptors on CA1 hippocampal neurons is consistent with subunit changes in a model of alcohol withdrawal and dependence. J Pharmacol Exp Ther 310:1234-1245.

Liang J, Suryanarayanan A, Chandra D, Homanics GE, Olsen RW, Spigelman I (2008) Functional consequences of GABAA receptor alpha 4 subunit deletion on synaptic and extrasynaptic currents in mouse dentate granule cells. Alcohol Clin Exp Res 32:19-26.

Liao L, Park SK, Xu T, Vanderklish P, Yates JR, 3rd (2008) Quantitative proteomic analysis of primary neurons reveals diverse changes in synaptic protein content in fmr1 knockout mice. Proc Natl Acad Sci U S A 105:15281-15286.

Lin AC, Holt CE (2007) Local translation and directional steering in axons. Embo J 26:3729-3736.

Lois C, Hong EJ, Pease S, Brown EJ, Baltimore D (2002) Germline transmission and tissue-specific expression of transgenes delivered by lentiviral vectors. Science 295:868-872.

Luo P, Li X, Fei Z, Poon W (2012) Scaffold protein Homer 1: implications for neurological diseases. Neurochem Int 61:731-738.

Manfredi I, Zani AD, Rampoldi L, Pegorini S, Bernascone I, Moretti M, Gotti C, Croci L, Consalez GG, Ferini-Strambi L, Sala M, Pattini L, Casari G (2009) Expression of mutant beta2 nicotinic receptors during development is crucial for epileptogenesis. Hum Mol Genet 18:1075-1088.

Mann M (2006) Functional and quantitative proteomics using SILAC. Nat Rev Mol Cell Biol 7:952-958.

Marin P, Nastiuk KL, Daniel N, Girault JA, Czernik AJ, Glowinski J, Nairn AC, Premont J (1997) Glutamate-dependent phosphorylation of elongation factor-2 and inhibition of protein synthesis in neurons. J Neurosci 17:3445-3454.

Medrihan L, Cesca F, Raimondi A, Lignani G, Baldelli P, Benfenati F (2013) Synapsin II desynchronizes neurotransmitter release at inhibitory synapses by interacting with presynaptic calcium channels. Nat Commun 4:1512.

Meldrum B, Horton R (1980) Effects of the bicyclic GABA agonist, THIP, on myoclonic and seizure responses in mice and baboons with reflex epilepsy. Eur J Pharmacol 61:231-237.

Mi R, Tang X, Sutter R, Xu D, Worley P, O'Brien RJ (2002) Differing mechanisms for glutamate receptor aggregation on dendritic spines and shafts in cultured hippocampal neurons. J Neurosci 22:7606-7616.

Minamoto Y, Itano T, Tokuda M, Matsui H, Janjua NA, Hosokawa K, Okada Y, Murakami TH, Negi T, Hatase O (1992) In vivo microdialysis of amino acid neurotransmitters in the hippocampus in amygdaloid kindled rat. Brain Res 573:345-348.

Mitsui K, Brady M, Palfrey HC, Nairn AC (1993) Purification and characterization of calmodulin-dependent protein kinase III from rabbit reticulocytes and rat pancreas. J Biol Chem 268:13422-13433.

Mody I, Kohr G, Otis TS, Staley KJ (1992) The electrophysiology of dentate gyrus granule cells in whole-cell recordings. Epilepsy Res Suppl 7:159-168.

Mohler H, Fritschy JM, Rudolph U (2002) A new benzodiazepine pharmacology. J Pharmacol Exp Ther 300:2-8.

Moreno JA, Radford H, Peretti D, Steinert JR, Verity N, Martin MG, Halliday M, Morgan J, Dinsdale D, Ortori CA, Barrett DA, Tsaytler P, Bertolotti A, Willis AE, Bushell M, Mallucci GR (2012) Sustained translational repression by eIF2alpha-P mediates prion neurodegeneration. Nature 485:507-511.

Murata Y, Constantine-Paton M (2013) Postsynaptic density scaffold SAP102 regulates cortical synapse development through EphB and PAK signaling pathway. J Neurosci 33:5040-5052.

Nairn AC, Bhagat B, Palfrey HC (1985) Identification of calmodulin-dependent protein kinase III and its major Mr 100,000 substrate in mammalian tissues. Proc Natl Acad Sci U S A 82:7939-7943.

Naldini L, Blomer U, Gallay P, Ory D, Mulligan R, Gage FH, Verma IM, Trono D (1996) In vivo gene delivery and stable transduction of nondividing cells by a lentiviral vector. Science 272:263-267.

Nosten-Bertrand M, Kappeler C, Dinocourt C, Denis C, Germain J, Phan Dinh Tuy F, Verstraeten S, Alvarez C, Metin C, Chelly J, Giros B, Miles R, Depaulis A, Francis F (2008) Epilepsy in Dcx knockout mice associated with discrete lamination defects and enhanced excitability in the hippocampus. PLoS One 3:e2473.

Nosyreva E, Szabla K, Autry AE, Ryazanov AG, Monteggia LM, Kavalali ET (2013) Acute suppression of spontaneous neurotransmission drives synaptic potentiation. J Neurosci 33:6990-7002.

Nusser Z, Mody I (2002) Selective modulation of tonic and phasic inhibitions in dentate gyrus granule cells. J Neurophysiol 87:2624-2628.

Ohno K, Koroll M, El Far O, Scholze P, Gomeza J, Betz H (2004) The neuronal glycine transporter 2 interacts with the PDZ domain protein syntenin-1. Mol Cell Neurosci 26:518-529.

Olsen JV, de Godoy LM, Li G, Macek B, Mortensen P, Pesch R, Makarov A, Lange O, Horning S, Mann M (2005) Parts per million mass accuracy on an Orbitrap mass spectrometer via lock mass injection into a C-trap. Mol Cell Proteomics 4:2010-2021.

Ong SE, Mann M (2006) A practical recipe for stable isotope labeling by amino acids in cell culture (SILAC). Nat Protoc 1:2650-2660.

Panatier A, Theodosis DT, Mothet JP, Touquet B, Pollegioni L, Poulain DA, Oliet SH (2006) Glia-derived D-serine controls NMDA receptor activity and synaptic memory. Cell 125:775-784.

Park S, Park JM, Kim S, Kim JA, Shepherd JD, Smith-Hicks CL, Chowdhury S, Kaufmann W, Kuhl D, Ryazanov AG, Huganir RL, Linden DJ, Worley PF (2008) Elongation factor 2 and fragile X mental retardation protein control the dynamic translation of Arc/Arg3.1 essential for mGluR-LTD. Neuron 59:70-83.

Pavur KS, Petrov AN, Ryazanov AG (2000) Mapping the functional domains of elongation factor-2 kinase. Biochemistry 39:12216-12224.

Perea G, Navarrete M, Araque A (2009) Tripartite synapses: astrocytes process and control synaptic information. Trends Neurosci 32:421-431.

Piccoli G, Verpelli C, Tonna N, Romorini S, Alessio M, Nairn AC, Bachi A, Sala C (2007) Proteomic analysis of activity-dependent synaptic plasticity in hippocampal neurons. J Proteome Res 6:3203-3215.

Pigott CR, Mikolajek H, Moore CE, Finn SJ, Phippen CW, Werner JM, Proud CG (2012) Insights into the regulation of eukaryotic elongation factor 2 kinase and the interplay between its domains. Biochem J 442:105-118.

Pinal CS, Tobin AJ (1998) Uniqueness and redundancy in GABA production. Perspect Dev Neurobiol 5:109-118.

Porter AG, Janicke RU (1999) Emerging roles of caspase-3 in apoptosis. Cell Death Differ 6:99-104.

Pyr Dit Ruys S, Wang X, Smith EM, Herinckx G, Hussain N, Rider MH, Vertommen D, Proud CG (2012) Identification of autophosphorylation sites in eukaryotic elongation factor-2 kinase. Biochem J 442:681-692.

Qi JS, Yao J, Fang C, Luscher B, Chen G (2006) Downregulation of tonic GABA currents following epileptogenic stimulation of rat hippocampal cultures. J Physiol 577:579-590.

Queenan BN, Lee KJ, Pak DT (2001) Wherefore art thou, homeo(stasis)? Functional diversity in homeostatic synaptic plasticity. Neural Plast 2012:718203.

Rappsilber J, Mann M, Ishihama Y (2007) Protocol for micro-purification, enrichment, pre-fractionation and storage of peptides for proteomics using StageTips. Nat Protoc 2:1896-1906.

Richardson BD, Ling LL, Uteshev VV, Caspary DM (2011) Extrasynaptic GABA(A) receptors and tonic inhibition in rat auditory thalamus. PLoS One 6:e16508.

Richerson GB (2004) Looking for GABA in all the wrong places: the relevance of extrasynaptic GABA(A) receptors to epilepsy. Epilepsy Curr 4:239-242.

Roffe M, Beraldo FH, Bester R, Nunziante M, Bach C, Mancini G, Gilch S, Vorberg I, Castilho BA, Martins VR, Hajj GN (2010) Prion protein interaction with stress-inducible protein 1 enhances neuronal protein synthesis via mTOR. Proc Natl Acad Sci U S A 107:13147-13152.

Ryazanov AG (2002) Elongation factor-2 kinase and its newly discovered relatives. FEBS Lett 514:26-29.

Ryazanov AG, Shestakova EA, Natapov PG (1988) Phosphorylation of elongation factor 2 by EF-2 kinase affects rate of translation. Nature 334:170-173.

Ryazanov AG, Ward MD, Mendola CE, Pavur KS, Dorovkov MV, Wiedmann M, Erdjument-Bromage H, Tempst P, Parmer TG, Prostko CR, Germino FJ, Hait WN (1997) Identification of a new class of protein kinases represented by eukaryotic elongation factor-2 kinase. Proc Natl Acad Sci U S A 94:4884-4889.

Saheki Y, De Camilli P (2012) Synaptic vesicle endocytosis. Cold Spring Harb Perspect Biol 4:a005645.

Sala C, Piech V, Wilson NR, Passafaro M, Liu G, Sheng M (2001) Regulation of dendritic spine morphology and synaptic function by Shank and Homer. Neuron 31:115-130.

Sala M, Braida D, Lentini D, Busnelli M, Bulgheroni E, Capurro V, Finardi A, Donzelli A, Pattini L, Rubino T, Parolaro D, Nishimori K, Parenti M, Chini B (2010) Pharmacologic rescue of impaired cognitive flexibility, social deficits, increased aggression, and seizure susceptibility in oxytocin receptor null mice: a neurobehavioral model of autism. Biol Psychiatry 69:875-882.

Sarto I, Wabnegger L, Dogl E, Sieghart W (2002) Homologous sites of GABA(A) receptor alpha(1), beta(3) and gamma(2) subunits are important for assembly. Neuropharmacology 43:482-491.

Scheetz AJ, Nairn AC, Constantine-Paton M (1997) N-methyl-D-aspartate receptor activation and visual activity induce elongation factor-2 phosphorylation in amphibian tecta: a role for N-methyl-D-aspartate receptors in controlling protein synthesis. Proc Natl Acad Sci U S A 94:14770-14775.

Scheetz AJ, Nairn AC, Constantine-Paton M (2000) NMDA receptor-mediated control of protein synthesis at developing synapses. Nat Neurosci 3:211-216.

Schratt GM, Nigh EA, Chen WG, Hu L, Greenberg ME (2004) BDNF regulates the translation of a select group of mRNAs by a mammalian target of rapamycin-phosphatidylinositol 3-kinase-dependent pathway during neuronal development. J Neurosci 24:7366-7377.

Scimemi A, Semyanov A, Sperk G, Kullmann DM, Walker MC (2005) Multiple and plastic receptors mediate tonic GABAA receptor currents in the hippocampus. J Neurosci 25:10016-10024.

Sheng M, Hoogenraad CC (2007) The postsynaptic architecture of excitatory synapses: a more quantitative view. Annu Rev Biochem 76:823-847.

Sheng M, Kim E (2011) The postsynaptic organization of synapses. Cold Spring Harb Perspect Biol 3.

Shevchenko A, Tomas H, Havlis J, Olsen JV, Mann M (2006) In-gel digestion for mass spectrometric characterization of proteins and proteomes. Nat Protoc 1:2856-2860.

Sihra TS, Wang JK, Gorelick FS, Greengard P (1989) Translocation of synapsin I in response to depolarization of isolated nerve terminals. Proc Natl Acad Sci U S A 86:8108-8112.

Simmons A, Whitehead RP, Kolokoltsov AA, Davey RA (2006) Use of recombinant lentivirus pseudotyped with vesicular stomatitis virus glycoprotein G for efficient generation of human anti-cancer chimeric T cells by transduction of human peripheral blood lymphocytes in vitro. Virol J 3:8.

Smolders I, Lindekens H, Clinckers R, Meurs A, O'Neill MJ, Lodge D, Ebinger G, Michotte Y (2004) In vivo modulation of extracellular hippocampal glutamate and GABA levels and limbic seizures by group I and II metabotropic glutamate receptor ligands. J Neurochem 88:1068-1077.

Sonenberg N, Hinnebusch AG (2009) Regulation of translation initiation in eukaryotes: mechanisms and biological targets. Cell 136:731-745.

Spellman DS, Deinhardt K, Darie CC, Chao MV, Neubert TA (2008) Stable isotopic labeling by amino acids in cultured primary neurons: application to brain-derived neurotrophic factor-dependent phosphotyrosine-associated signaling. Mol Cell Proteomics 7:1067-1076.

Staley KJ, Otis TS, Mody I (1992) Membrane properties of dentate gyrus granule cells: comparison of sharp microelectrode and whole-cell recordings. J Neurophysiol 67:1346-1358.

Sudhof TC (2004) The synaptic vesicle cycle. Annu Rev Neurosci 27:509-547.

Sudhof TC, Rizo J (2011) Synaptic vesicle exocytosis. Cold Spring Harb Perspect Biol 3.

Sutton MA, Taylor AM, Ito HT, Pham A, Schuman EM (2007) Postsynaptic decoding of neural activity: eEF2 as a biochemical sensor coupling miniature synaptic transmission to local protein synthesis. Neuron 55:648-661.

Tabuchi K, Biederer T, Butz S, Sudhof TC (2002) CASK participates in alternative tripartite complexes in which Mint 1 competes for binding with caskin 1, a novel CASK-binding protein. J Neurosci 22:4264-4273.

Tafoya LC, Mameli M, Miyashita T, Guzowski JF, Valenzuela CF, Wilson MC (2006) Expression and function of SNAP-25 as a universal SNARE component in GABAergic neurons. J Neurosci 26:7826-7838.

Taha E, Gildish I, Gal-Ben-Ari S, Rosenblum K (2013) The role of eEF2 pathway in learning and synaptic plasticity. Neurobiol Learn Mem 105:100-106.

Tavares CD, O'Brien JP, Abramczyk O, Devkota AK, Shores KS, Ferguson SB, Kaoud TS, Warthaka M, Marshall KD, Keller KM, Zhang Y, Brodbelt JS, Ozpolat B, Dalby KN (2012) Calcium/calmodulin stimulates the autophosphorylation of elongation factor 2 kinase on Thr-348 and Ser-500 to regulate its activity and calcium dependence. Biochemistry 51:2232-2245.

Teng J, Takei Y, Harada A, Nakata T, Chen J, Hirokawa N (2001) Synergistic effects of MAP2 and MAP1B knockout in neuronal migration, dendritic outgrowth, and microtubule organization. J Cell Biol 155:65-76.

Thyagarajan T, Totey S, Danton MJ, Kulkarni AB (2003) Genetically altered mouse models: the good, the bad, and the ugly. Crit Rev Oral Biol Med 14:154-174.

Tian N, Petersen C, Kash S, Baekkeskov S, Copenhagen D, Nicoll R (1999) The role of the synthetic enzyme GAD65 in the control of neuronal gamma-aminobutyric acid release. Proc Natl Acad Sci U S A 96:12911-12916.

Tyler WJ, Pozzo-Miller LD (2001) BDNF enhances quantal neurotransmitter release and increases the number of docked vesicles at the active zones of hippocampal excitatory synapses. J Neurosci 21:4249-4258.

Vaccaro P, Dente L, Onofri F, Zucconi A, Martinelli S, Valtorta F, Greengard P, Cesareni G, Benfenati F (1997) Anti-synapsin monoclonal antibodies: epitope mapping and inhibitory effects on phosphorylation and Grb2 binding. Brain Res Mol Brain Res 52:1-16.

Valtorta F, Benfenati F, Greengard P (1992) Structure and function of the synapsins. J Biol Chem 267:7195-7198.

Valtorta F, Pozzi D, Benfenati F, Fornasiero EF (2011) The synapsins: multitask modulators of neuronal development. Semin Cell Dev Biol 22:378-386.

van Amerongen R, Berns A (2006) Knockout mouse models to study Wnt signal transduction. Trends Genet 22:678-689.

Van der Kloot W (1991) The regulation of quantal size. Prog Neurobiol 36:93-130.

Verpelli C, Piccoli G, Zibetti C, Zanchi A, Gardoni F, Huang K, Brambilla D, Di Luca M, Battaglioli E, Sala C (2010) Synaptic activity controls dendritic spine morphology by modulating eEF2-dependent BDNF synthesis. J Neurosci 30:5830-5842.

Vezzani A (2009) Pilocarpine-induced seizures revisited: what does the model mimic? Epilepsy Curr 9:146-148.

Vogel C, Marcotte EM (2012) Insights into the regulation of protein abundance from proteomic and transcriptomic analyses. Nat Rev Genet 13:227-232.

Walls AB, Nilsen LH, Eyjolfsson EM, Vestergaard HT, Hansen SL, Schousboe A, Sonnewald U, Waagepetersen HS (2010) GAD65 is essential for synthesis of GABA destined for tonic inhibition regulating epileptiform activity. J Neurochem 115:1398-1408.

Wang X, Li W, Williams M, Terada N, Alessi DR, Proud CG (2001) Regulation of elongation factor 2 kinase by p90(RSK1) and p70 S6 kinase. Embo J 20:4370-4379.

Wei W, Zhang N, Peng Z, Houser CR, Mody I (2003) Perisynaptic localization of delta subunit-containing GABA(A) receptors and their activation by GABA spillover in the mouse dentate gyrus. J Neurosci 23:10650-10661.

Whittingstall K, Logothetis NK (2009) Frequency-band coupling in surface EEG reflects spiking activity in monkey visual cortex. Neuron 64:281-289.

Wiznerowicz M, Trono D (2003) Conditional suppression of cellular genes: lentivirus vector-mediated drug-inducible RNA interference. J Virol 77:8957-8961.

Wu Z, Moghaddas Gholami A, Kuster B (2012) Systematic identification of the HSP90 candidate regulated proteome. Mol Cell Proteomics 11:M111 016675.

Wysocki VH, Resing KA, Zhang Q, Cheng G (2005) Mass spectrometry of peptides and proteins. Methods 35:211-222.

Yizhar O, Fenno LE, Prigge M, Schneider F, Davidson TJ, O'Shea DJ, Sohal VS, Goshen I, Finkelstein J, Paz JT, Stehfest K, Fudim R, Ramakrishnan C, Huguenard JR, Hegemann P, Deisseroth K (2011) Neocortical excitation/inhibition balance in information processing and social dysfunction. Nature 477:171-178.

Yoon BC, Jung H, Dwivedy A, O'Hare CM, Zivraj KH, Holt CE Local translation of extranuclear lamin B promotes axon maintenance. Cell 148:752-764.

Zalfa F, Giorgi M, Primerano B, Moro A, Di Penta A, Reis S, Oostra B, Bagni C (2003) The fragile X syndrome protein FMRP associates with BC1 RNA and regulates the translation of specific mRNAs at synapses. Cell 112:317-327.

Zander JF, Munster-Wandowski A, Brunk I, Pahner I, Gomez-Lira G, Heinemann U, Gutierrez R, Laube G, Ahnert-Hilger G (2010) Synaptic and vesicular coexistence of VGLUT and VGAT in selected excitatory and inhibitory synapses. J Neurosci 30:7634-7645.

Zhang G, Neubert TA, Jordan BA (2012) RNA binding proteins accumulate at the postsynaptic density with synaptic activity. J Neurosci 32:599-609.

Zhang Y, Bhavnani BR (2006) Glutamate-induced apoptosis in neuronal cells is mediated via caspase-dependent and independent mechanisms involving calpain and caspase-3 proteases as well as apoptosis inducing factor (AIF) and this process is inhibited by equine estrogens. BMC Neurosci 7:49.